UNIVERSITY OF CRETE

University of Crete

School of Medicine

Graduate Program: Molecular Basis of Human Disease

Master's Thesis

Effects of BNN27 Microneurotrophin Delivery on Tissue Regeneration after Optic Nerve Injury

Xenofon Mallios

Supervisors
As. Prof. Charalampopoulos Ioannis
Prof. Gravanis Achilleas
Dr. Tzeranis Dimitrios

October 2020

ΠΑΝΕΠΙΣΤΗΜΙΟ ΚΡΗΤΗΣ

Πανεπιστήμιο Κρήτης

Ιατρική Σχολή

Μεταπτυχιακό Πρόγραμμα:
Μοριακή Βάση των Νοσημάτων του Ανθρώπου

Διπλωματική Εργασία

Η Επίδραση της Χορήγησης της Μικρονευροτροφίνης BNN27 στην Αναγέννηση Ιστού μετά από Τραύμα Οπτικού Νεύρου

Ξενοφών Μάλλιος

Επιβλέποντες
Αν. Καθηγητής Χαραλαμπόπουλος Ιωάννης
Καθηγητής Γραβάνης Αχιλλέας
Δρ. Τζεράνης Δημήτριος

Οκτώβριος 2020

Abstract

Traumatic Optic Neuropathy (TON) refers to a condition of optic nerve injury caused by direct or indirect head and/or facial trauma. Indirect TON is more common than direct, having as more usual causes road-traffic accidents (21.5%), falls (25.6%) and assaults (20.7%). Our vision depends on the successful and high-quality signal conduction from the retina to subcortical target areas of the brain via the optic nerve, which is formed by RGC axons. Taking into account that RGCs cannot regenerate their axons upon injury, as the majority of CNS neurons, TON could result in vision impairment or permanent vision loss. To this day there is no treatment available, able to prevent ONI-induced RGC loss or to stimulate efficient RGC axon elongation. Current clinical treatments include corticosteroid administration and surgical decompression of the optic canal, presenting limited results and a number of side-effects (hypertension, insomnia, hyperglycemia, etc.). Research TON treatments include the use of eye drops and intravitreal injections for the delivery of NTs and NTFs, drugs and peptides as well as biomaterial-based drug delivery strategies. Literature reports the use of grafts in combination with cells, NTs or other molecules; administration of micro- / nanospheres and liposomes containing NTs or drugs; the use of other delivery systems (e.g. reverse thermal gel). This study aims to quantify the effects of the microneurotrophin BNN27 on key cell phenotypes (RGC survival, astroglial activation) after ONC injury in mice, pursuing two BNN27 delivery strategies. The first strategy comprises administration of BNN27 via eye drops for 7 and 14 days after injury. The second strategy includes BNN27 delivery via biomaterials; BNN27 is entrapped in a peptide gel formed inside a porous collagen-GAG scaffold, placed directly at the injury site. Characterization of the developed ONC model revealed that ONC induced reduction in RGC survival, astroglial (GFAP) and microglial (IBA1) activation, as well as a trend for TrkC downregulation 7 and 14 days after injury. For the rest NT receptors studied ($p75^{NTR}$, TrkA, TrkB), no statistically significant alterations in their expression were observed 1 and 2 weeks after injury. Concerning the first strategy, BNN27 displayed a trend for RGCs protection from ONC-induced apoptosis 7 and 14 days post injury, whereas no effect was observed on astroglial activation (GFAP). Regarding the second strategy, BNN27 did not present any neuroprotective effects on RGC survival or astroglial activation 2 weeks after ONC, when delivered via a peptide gel formed in a collagen-GAG scaffold, possibly due to administration of insufficient BNN27 dose. Furthermore, BNN27 delivery via covalent conjugation on collagen-GAG scaffold using a novel linker (SPDP) was pursued through *in vitro* experiments. TC447 was successfully conjugated on collagen-GAG scaffold via covalent bond, although some amount of non-specific conjugation was observed. Finally, a significant finding of this study is that TC447 conjugation was highly enhanced on SPDP-activated scaffolds treated with DTT prior TC447, suggesting that chemical interactions among SPDP, collagen-GAG and DTT lead to the generation of a microenvironment that promotes TC447 conjugation on this scaffold more efficiently compared to TC447 conjugation on SPDP-activated scaffold alone.

Keywords: Optic Nerve Crush (ONC) ⋅ Drug Delivery ⋅ Biomaterials ⋅ Traumatic Optic Neuropathy (TON) ⋅ Retinal Ganglion Cells (RGCs) ⋅ Neuroprotection ⋅ Neurotrophins (NTs) ⋅ GFAP ⋅ IBA1 ⋅ Trk Receptors ⋅ $P75^{NTR}$

Περίληψη

Ο όρος Τραυματική Οπτική Νευροπάθεια (ΤΟΝ) αναφέρεται σε μια κατάσταση τραύματος οπτικού νεύρου η οποία έχει προκληθεί από άμεσο ή έμμεσο τραύμα στο κεφάλι ή/και στο πρόσωπο. Η πρόκληση ΤΟΝ από έμμεσα αίτια είναι πιο συχνή από ότι με άμεσα, με πιο συνηθισμένες αιτίες τα τροχαία ατυχήματα (21.5 %), πτώσεις (25.6%) και επιθέσεις (20.7%). Η όρασή μας εξαρτάται από την επιτυχή και υψηλής ποιότητας μετάδοση σήματος από τον αμφιβληστροειδή χιτώνα σε υποφλοιικές περιοχές του εγκεφάλου μέσω του οπτικού νεύρου, το οποίο αποτελείται από τους άξονες των γαγγλιακών κυττάρων του αμφιβληστροειδούς (RGCs). Λαμβάνοντας υπόψη ότι τα RGCs δεν μπορούν να αναγεννήσουν τους άξονές τους μετά από τραυματισμό, όπως η πλειοψηφία των νευρώνων του κεντρικού νευρικού συστήματος (ΚΝΣ), η ΤΟΝ μπορεί να οδηγήσει σε προβλήματα ή μόνιμη απώλεια όρασης. Μέχρι σήμερα, δεν υπάρχει κάποια διαθέσιμη θεραπεία που να μπορεί να εμποδίσει την απώλεια των RGCs λόγω τραύματος ή να επάγει επαρκή επιμήκυνση των αξόνων των RGCs. Οι τρέχουσες διαθέσιμες κλινικές θεραπείες περιλαμβάνουν την χορήγηση κορτικοστεροειδών και τη χειρουργική αποσυμπίεση του οπτικού καναλιού, παρέχοντας περιορισμένα αποτελέσματα όπως επίσης και παρενέργειες (υπερένταση, αυπνία, υπεργλυκαιμία κλπ.). Ερευνητικές θεραπείες της ΤΟΝ περιλαμβάνουν τη χρήση οφθαλμικών σταγόνων και ενδοϋαλοειδικών ενέσεων για παροχή νευροτροφινών (NTs) και νευροτροφικών παραγόντων (NTFs), φαρμάκων και πεπτιδίων, όπως επίσης περιλαμβάνουν στρατηγικές χορήγησης φαρμάκων με τη χρήση βιο-υλικών. Βιβλιογραφικές αναφορές κάνουν λόγο για χρήση μοσχευμάτων σε συνδυασμό με NTs ή άλλα μόρια, χορήγηση μίκρο- / νάνοσφαιρών και λιποσωμάτων που περιέχουν NTs ή άλλα φάρμακα, χρήση άλλων συστημάτων χορήγησης. Αυτή η μελέτη έχει ως στόχο να ποσοτικοποιήσει τα αποτελέσματα της μικρονευροτροφίνης BNN27 σε τύπους κυττάρων – κλειδιά (επιβίωση των RGCs, ενεργοποίηση της αστρογλοίας) έπειτα από τραύμα σύνθλιψης οπτικού νεύρου (ONC) σε ποντίκια, ακολουθώντας δύο στρατηγικές χορήγησης BNN27. Η πρώτη στρατηγική περιλαμβάνει τη χορήγηση BNN27 με τη χρήση οφθαλμικών σταγόνων για 7 και 14 ημέρες μετά το τραύμα. Η δεύτερη στρατηγική περιλαμβάνει τη χορήγηση BNN27 με τη χρήση βιο-υλικών: Παγίδευση BNN27 σε γέλη πεπτιδίου σχηματιζόμενη στο εσωτερικό ικριώματος κολλαγόνου-GAG, το οποίο τοποθετείται στο σημείο του τραύματος. Ο χαρακτηρισμός του μοντέλου τραύματος ONC που αναπτύξαμε αποκάλυψε ότι το ONC προκάλεσε μείωση της επιβίωσης των RGCs, αύξηση της ενεργοποίησης της αστρογλοίας (GFAP) και μικρογλοίας (IBA1) όπως επίσης και μια τάση για μείωση της έκφρασης του TrkC 7 και 14 ημέρες μετά το τραύμα. Για τους υπόλοιπους υποδοχείς νευροτροφινών που μελετήθηκαν ($p75^{NTR}$, TrkA, TrkB), δεν παρατηρήθηκε κάποια στατιστικά σημαντική αλλαγή στην έκφρασή τους 1 και 2 εβδομάδες μετά το τραύμα. Αναφορικά με την πρώτη στρατηγική, η BNN27 παρουσίασε μια τάση για προστασία των RGCs από την απόπτωση λόγω τραύματος 7 και 14 ημέρες μετά το τραύμα, ενώ δεν παρατηρήθηκε κάποια επίδραση στην αστρογλοιακή ενεργοποίηση (GFAP). Όσον αφορά τη δεύτερη στρατηγική, η BNN27 δεν παρουσίασε νευροπροστατευτική δράση στην επιβίωση των RGCs και την ενεργοποίηση της αστρογλοίας 2 εβδομάδες μετά το τραύμα, όταν χορηγήθηκε με τη χρήση γέλης πεπτιδίου σχηματιζόμενη στο εσωτερικό ικριώματος κολλαγόνου-GAG, πιθανότατα λόγω χορήγησης ανεπαρκούς δόσης BNN27. Επιπλέον, η

χορήγηση BNN27 μέσω ομοιοπολικής σύνδεσης σε ικρίωμα κολλαγόνου-GAG με τη χρήση καινοτόμου συνδετικού μορίου (SPDP) εξετάστηκε μέσω *in vitro* πειραμάτων. Η ουσία TC447 συνδέθηκε επιτυχώς σε ικρίωμα κολλαγόνου-GAG μέσω ομοιοπολικού δεσμού, ωστόσο παρατηρήθηκε και κάποιο ποσοστό μη ειδικής σύνδεσης. Τέλος, ένα σημαντικό εύρημα αυτής της μελέτης είναι ότι η σύνδεση του TC447 βρέθηκε σημαντικά ενισχυμένη σε ικριώματα ενεργοποιημένα με SPDP τα οποία επωάσθηκαν σε DTT πριν επωαστούν σε TC447, υποδεικνύοντας ότι χημικές αλληλεπιδράσεις μεταξύ των SPDP, κολλαγόνου-GAG και DTT οδηγούν στη δημιουργία μικρο-περιβάλλοντος το οποίο ευνοεί τη σύνδεση του TC447 στο παρών ικρίωμα με τρόπο πιο αποτελεσματικό από ότι σε ικρίωμα που έχει μόνο ενεργοποιηθεί με SPDP.

Acknowledgements

First of all, I would like to thank Associate Professor Ioannis Charalampopoulos and Professor Achilleas Gravanis of the School of Medicine at the University of Crete for giving me the opportunity to join their research groups and be involved in this study.

I am deeply grateful to Dr. Dimitrios Tzeranis of the Department of Mechanical and Manufacturing Engineering at the University of Cyprus, for the infinite amount of guidance and advising.

Furthermore, I would like to thank the PhD candidate Constantina Georgelou for sharing with me great amounts of knowledge concerning laboratory techniques as well as for her help, guidance and fruitful cooperation during the course of this study.

Moreover, I would like to thank the research groups of the Neural Tissue Engineering and the Regenerative Pharmacology Laboratories for the outstanding cooperation and help from all the members as well as for the warm and welcoming working environment.

I would like to thank all our collaborators for their contribution in this study.

I also want to acknowledge the University of Crete and specifically the Faculty of Medicine for providing me the chance first to study in the Biology department as a BSc student and then continue my studies as MSc student, in the "Molecular Basis of Human Disease" program.

Finally, I owe my deepest gratitude and a special thanks to my family and friends for their endless support in any way possible during my studies.

Xenofon Mallios

Table of Contents

Abbreviations

AAD: Acute Axonal Degeneration
ATF-3: Activating Transcription Factor 3
BBB: Blood Brain Barrier
BDNF: Brain-derived Neurotrophic Factor
BSA: Bovine Serum Albumin
CNTF: Ciliary Neurotrophin Factor
COI: Controlled Orbital Impact
CSPGs: Chondroitin Sulfate Proteoglycans
CTB: Cholera Toxin Subunit B
ChAT: Choline Acetyltransferase
DAG: Diacylglycerol
DARC: Detection of Apoptotic Retinal Cells
DB: Die Back
DDS: Drug Delivery System
DHEA: Dehydroepiandrosterone
DPX: Dibutylphthalate Polystyrene Xylene
DR: Diabetic Retinopathy
DRG: Dorsal Root Ganglia
DTT: Dithiothreitol
ECM: Extracellular Matrix
ELISA: Enzyme-Linked Immunosorbent Assay
ERG: Electroretinography
ERK: Extracellular signal-Regulated Kinases
Fmoc-FF: Fmoc-Phe-Phe-OH
GAP-43: Growth Associated Protein 43
GCL: Ganglion Cell Layer
GDNF: Glial cell line-Derived Neurotrophin Factor
GFAP: Glial fibrillary acidic protein
H&E: Hematoxylin-Eosin
HA: Hyaluronic Acid
IHC: Immunohistochemistry
INL: Inner Nuclear Layer
IP3: Inositol Trisphosphate
IVT: Intravitreal
Ig: Immunoglobulin
JNK: c-Jun N-terminal Kinase
LFB: Luxol Fast Blue
LGN: Lateral Geniculate Nucleus
MAG: Myelin-Associated Glycoprotein
MAIs: Myelin-Associated Inhibitors
MAPK: Mitogen-Activated Protein Kinases
MCs: Microglial Cells
MNPs: Magnetic Nanoparticles
MNTs: Microneurotrophins
NAION: Non-Arteritic Ischemic Optic Neuropathy
NFL: Nerve Fiber Layer
NGF: Nerve Growth Factor
NTs: Neurotrophins
NT-3: Neurotrophin 3
NT-4: Neurotrophin 4
NTRs: Neurotrophin Receptors
NTFs: Neurotrophic Factors
OBI: Ocular Blast Injury
OCT: Optimal Cutting Temperature
OMR: Optomotor Response
OMgp: Oligodendrocyte Myelin glycoprotein
ON: Optic Nerve
ONC: Optic Nerve Crush
ONI: Optic Nerve Injury
ONL: Outer Nuclear Layer
ONT: Optic Nerve Transection
PB: Phosphate Buffer
PBS: Phosphate Buffered Saline
PERG: Pattern-Electroretinography
PFA: Paraformaldehyde
PGA: Poly(glycolic acid)
PKC: Protein Kinase C
PLC: Phosphoinositide Phospholipase C
PLGA: Poly(lactic-co-glycolic acid)
PLR: Pupillary Light Reflex
PMCs: Phagocytic Microglial Cells
RAGs: Regeneration-Associated Genes
RGB: Red Green Blue
RGCs: Retinal Ganglion Cells
RGM: Repulsive Guidance Molecule
RNFL: Retinal Nerve Fiber Layer
RT: Room Temperature
SC: Superior Colliculus
SCs: Schwann cells
SCI: Spinal Cord Injury
SCS: Suprachoroidal Space
SI-TON: Sonication-Induced Traumatic Optic Neuropathy
SMCs: Surveying Microglial Cells
SPDP: 3-(2-Pyridyldithio)propionic acid N-hydroxysuccinimide ester
SPRR1A: Small Proline-Repeat Protein 1A
STRG: Sulfonated Reverse Thermal Gel
Sema 3A: Semaphorin 3A

Sema 4D: Semaphorin 4D
Sox11: SRY-box containing gene 11
TON: Traumatic Optic Neuropathy
TUNEL: Terminal deoxynucleotidyl transferase UTP Nick- End Labeling
Trk receptor: Tyrosine Kinase receptor
VF: Visual Field
VitE: Vitamin E
WD: Wallerian Degeneration
mTOR: mammalian Target of Rapamycin
pNH: Phosphorylated Neurophilament Heavy subunit
pONT: partial Optic Nerve Transection
rh-NGF: recombinant human Nerve Growth Factor
βME: 2-Mercaptoethanol

Chapter 1: Introduction

1.1 Traumatic Optic Neuropathy (TON)

1.1.1 Anatomy & Physiology of the Retina and the Optic Nerve

The visual pathway consists of the retina and the optic nerve (ON). Along the optic nerve while moving towards the brain, one observes the optic chiasm, optic tracts, lateral geniculate nucleus (LGN), optic radiations and the visual cortex *(Liorca 1972, Forrester et al. 2015, Friedman, Kaiser, and Trattler 2016, J. Salazar et al. 2019).*

The perceived visual field (VF) has an inverted and reversed relationship with the retina [*Figure 1-1*]. Specifically, the upper VF falls on the inferior retina (below the fovea), lower VF on the superior retina, nasal VF on the temporal retina and temporal VF on the nasal retina *(Kline and Bajandas 2008, J. Salazar et al. 2019).*

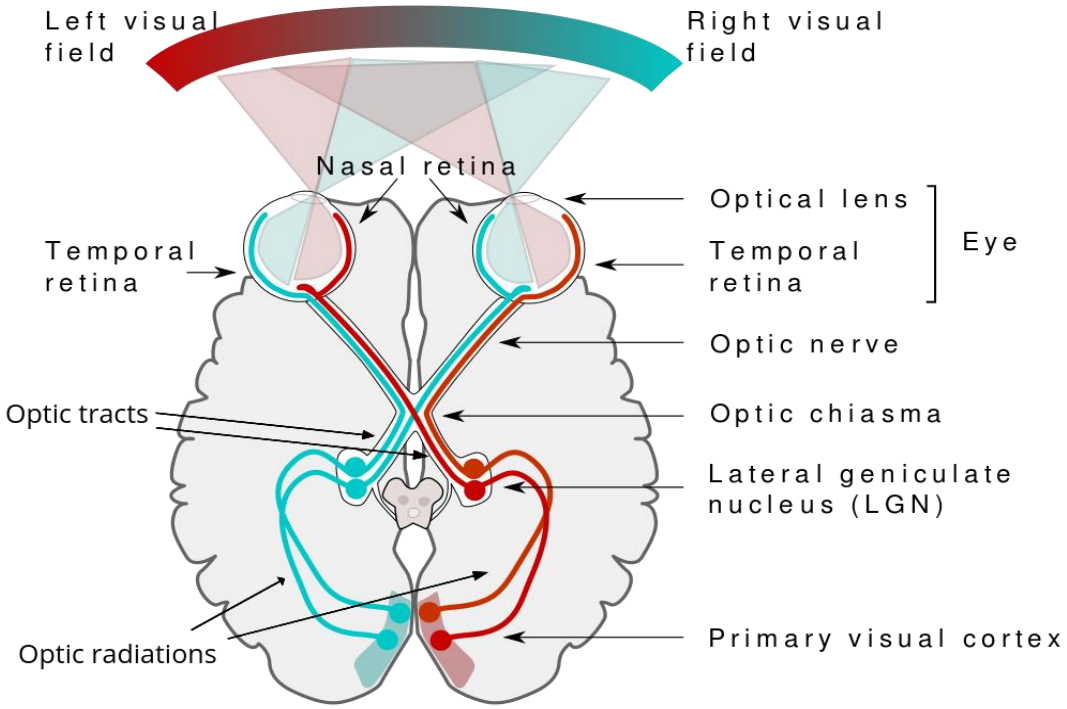

Figure 1-1: A simplified schema of the human visual pathway consisting of the eyes, the optic nerve and optic chiasma followed by the LGN and the primary visual cortex (Modified from (Nieto 2015)).

Retina is composed of various kinds of cells, which can be divided in three groups: cells of association, glial and neurons. Cells of association include horizontal and amacrine cells. Glial cells include Müller cells, astrocytes and microglia. Three kinds of retina neurons form three distinct layers [*Figure 1-2*] that connect with each other: photoreceptors (external neurons) in the outer nuclear layer (ONL), bipolar cells in the inner nuclear layer (INL), and **retina ganglion cells** (RGC; internal neurons) *(Liorca 1972, Kolb 2011b, J. Salazar et al. 2019).* Most RGC bodies are located in the ganglion cell layer (GCL), between the retinal nerve fiber layer (NFL) and the inner plexiform layer *(Forrester et al. 2015, J. Salazar et al. 2019).* RGC axons form the retinal NFL and form synapses with neurons in the LGN of the thalamus *(Liorca 1972, Forrester et al. 2015, J. Salazar et al. 2019).* Human retina contains 0.5 to 1.2 million RGCs *(J. Salazar et al. 2019, Liorca 1972, Friedman, Kaiser,*

and Trattler 2016), whereas in mice this number ranges from 32.000 to 87.000 cells *(May 2008)*. The central retina (fovea) is 60–80 μm thick and includes up to 7 layers of RGC bodies. The peripheral retina contains a single 10–20 μm thick layer of RGC *(Forrester et al. 2015, J. Salazar et al. 2019)*. RGC axons form cross-crossed bundles, which are separated and ensheathed by glial cells. Axon bundles pass through the lamina cribrosa where they become myelinated by oligodendrocytes, exit the eye and form the optic nerve (ON) *(J. Salazar et al. 2019, Liorca 1972, Forrester et al. 2015).*

Among the three distinct nerve layers (ONL, INL, GCL) there exist two neuropils (Outer Plexiform Layer (OPL); Inner Plexiform Layer (INL)) where synaptic contacts take place. In the first retina neuropil (OPL), rods and cones are connected with each other same as well as with vertically-oriented bipolar cells and horizontally oriented horizontal cells (Fain and Sampath 2018). In the second retina neuropil, known as the inner plexiform layer (IPL), vertical-information-carrying bipolar cells form synapses with RGCs. In IPL a variety of amacrine cells interact with the network to influence and integrate RGC signals that will eventually be transmitted to the brain *(Kolb 2011b).*

Photoreceptors (rods and cones) use glutamate to transmit signals to the next-order neurons in chain, bipolar and horizontal cells *(Mercer and Thoreson 2011)*, through metabotropic (mGluR6) and ionotropic (AMPA) glutamate receptors. Bipolar cells express mGluR6 and AMPA receptors at their dendrites along with GABA and glycine receptors at their axonal ending. All previous receptors (mGluR6, AMPA, GABA, glycine receptors) are also expressed by RGCs with the addition of acetylcholine receptors. Finally, dopamine 1 (D1) receptors are expressed by all three kinds of retina neurons (photoreceptors; bipolar, horizontal and amacrine cells; RGCs). Glutamate and acetylcholine are excitatory neurotransmitters. GABA and glycine are inhibitory neurotransmitters *(Kolb 2011a)*, while dopamine can act both ways *(Akaike et al. 1987)*.

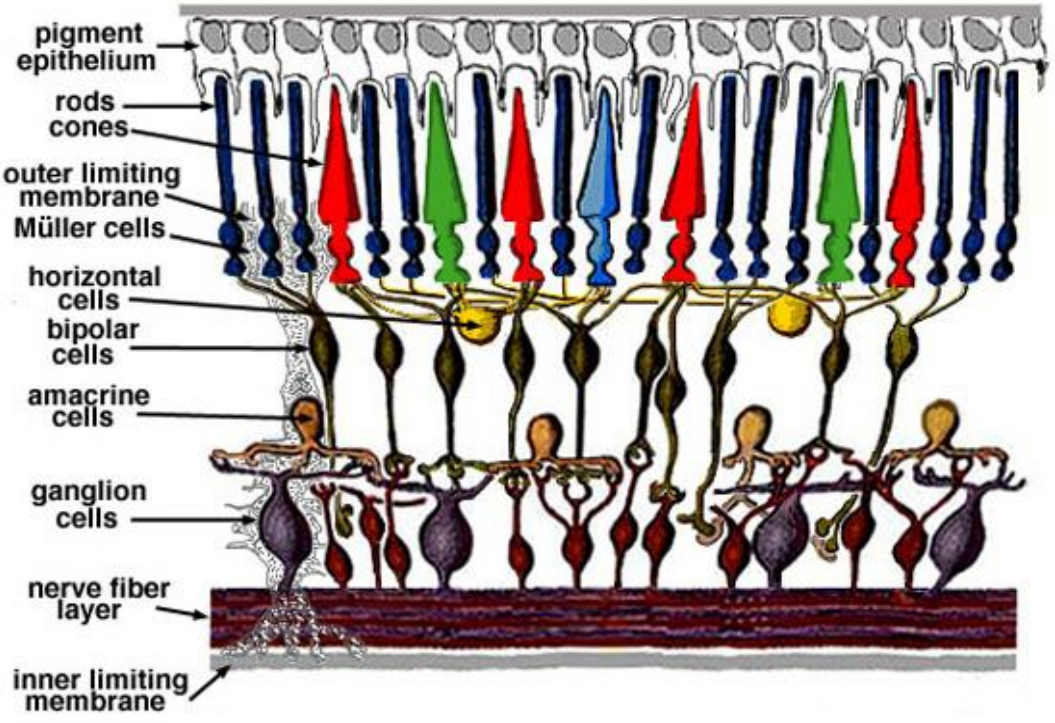

Figure 1-2: Schematic of retina structure. Retina includes 5 cell populations and 2 limiting membranes. Moving from the outer parts of the retina towards the inner layers we find the pigment epithelium, photoreceptors (rods and cones), the outer limiting membrane, Müller cells, bipolar cells

and cells of association (horizontal and amacrine cells), RGCs, the NFL and last the inner limiting membrane (Kolb 2011b).

The **optic nerve** (ON) is formed by the convergence of RGC axons at the optic disc, also known as papilla, which corresponds to the retina blind spot (retina spot that lacks photoreceptors; *(J. Salazar et al. 2019, Liorca 1972)*. Moreover, having a diameter of 2.6 – 4 mm in humans *(Benevento et al. 2004)* (approximately 0.2 mm in mice *(May 2008)*), the ON consists of four main sections: the intraocular nerve head, the intraorbital section, the intracanalicular section and the intracranial section [*Figure 1-3*]. The ON is composed of RGC axons, glial cells (astrocytes, oligodendrocytes, microglia), connective tissues (lamina cribosa, septa) that fasciculate the ON and blood vessels derived from both the central retinal artery (CRA) system and the ciliary system *(J. Salazar et al. 2019)*.

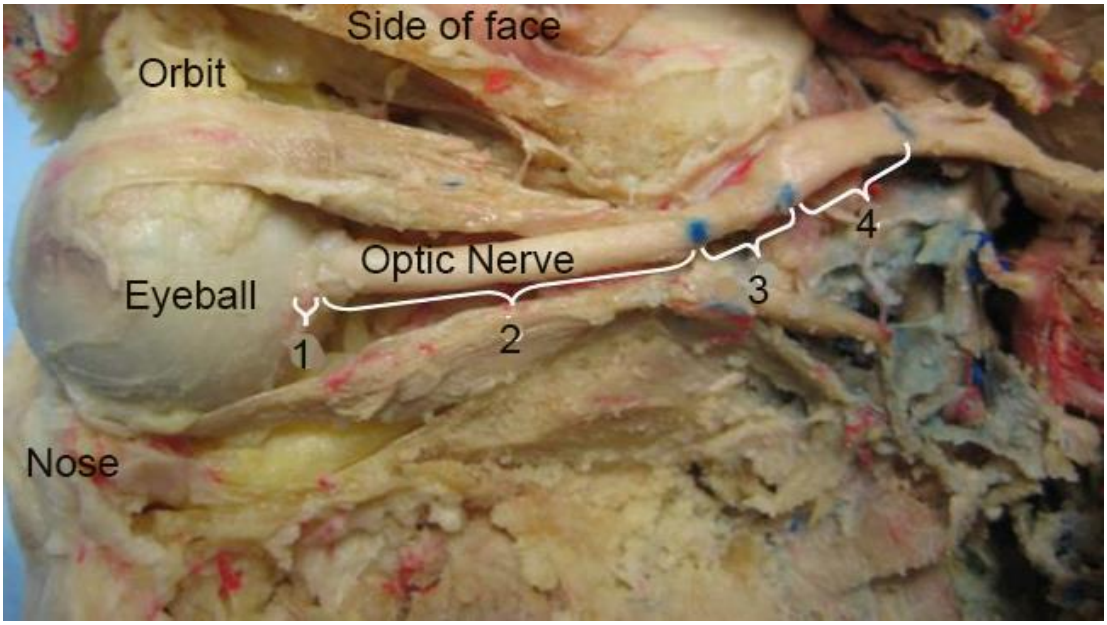

Figure 1-3: The four anatomical parts of the optic nerve. Intraocular nerve head (1), intraorbital part (2), intracanalicular part (3), intracranial part (4) (Anatomyczar).

In the optic nerve, **astrocytes** are located in the superficial NFL and are of two morphological types. One type has a thin cell body with processes running parallel to the RGC axons. The second astrocyte type has thick cell body and short processes *(J. Salazar et al. 2019, Triviño et al. 1998, Triviño et al. 1996)*. In retina, astrocyte morphology changes from a symmetrical stellate form *(Schnitzer 1988)* in peripheral retina to extremely elongated near the optic nerve *(Korb 2013)*. Under normal conditions, astrocytes establish contact with retinal neurons, providing stability to neural tissue *(Ramírez et al. 1996, J. Salazar et al. 2019)*. Various physiological studies have highlighted the important role of astrocytes functions in the ON and other parts of the CNS. Key astrocyte functions include glycogen storage and glucose delivery to neuronal cells, regulation and metabolism of neurotransmitters (e.g. GABA) *(Kumpulainen et al. 1983, Bringmann et al. 2006, J. Salazar et al. 2019, Nag 2011)*, fasciculation of axons *(Di Polo et al. 1998, Dreyer et al. 1996, J. Salazar et al. 2019)*. **Microglia**, a subtype of CNS glia, are activated in response to neuronal damage *(Perry et al. 1995, J. Salazar et al. 2019, Streit, Walter, and Pennell 1999)*. They are located in all retina layers. Retinal microglia have strange, multipolar forms with small cell bodies and irregular short processes. After retinal trauma, microglia are stimulated in a macrophagic function, exerting phagocytosis on degenerating retinal neurons *(Korb 2013)*. In the normal ON, microglia are quiescent and have a branched shape

with a small nucleus and a cell body with several processes. In the case of severe or moderate injury in the ON head, microglia are activated *(de Hoz et al. 2013, Gallego et al. 2012, J. Salazar et al. 2019)* and form accumulations of amoeboid microglia in the lamina cribrosa and surround blood vessels *(J. Salazar et al. 2019, Hernandez 2000, Neufeld 1999)*. **Müller cells,** the primary glial cells in retina, form architectural support structures spanning radially across the thickness of the retina. Their cell bodies are located in the inner nuclear layer and project irregularly thick and thin processes in either direction towards the inner and outer limiting membranes. Müller cell functions, being detrimental for the health of the retinal neurons, include control of retinal homeostasis, neuron protection from overexposure to neurotransmitters and involvement in phagocytosis of neural debris *(Korb 2013)*. In case of injury, Müller cells respond by changing their morphology, biochemistry and physiology *(Bringmann et al. 2009)*. Müller glia hypertrophy is often observed as part of the injury response, while depending on the severity of the trauma, Müller cell proliferation may be detected as well *(Goldman 2014)*. **Oligodendrocytes** are located among RGC axons in the ON and are responsible for the formation of the myelin sheaths around axons *(J. Salazar et al. 2019)*. Mature oligodendrocytes bear numerous processes (5-30 in rodents), with the terminal part of each one ensheathing an axon to form one internodal myelin segment *(Butt et al. 2004, Butt and Ransom 1989, 1993)*. Oligodendrocyte apoptosis leads to demyelination and impairs ON function *(Butt et al. 2004)*. Retinal cells of association (including **horizontal** and **amacrine cells**) have their bodies in the inner nuclear layer and are responsible for lateral interactions within the retina. Amacrine cell processes extend laterally in the inner plexiform layer, being post-synaptic to bipolar cell terminals and pre-synaptic to the RGC dendrites. Horizontal cell processes extend throughout the outer plexiform *(Purves et al. 2001)*.

1.1.2 TON Overview

"Traumatic Optic Neuropathy" (TON) refers to optic nerve injury caused by direct or indirect head and facial trauma *(Jang 2018)*. ON is vulnerable to indirect and direct trauma that can occur in the setting of head injury, often a consequence of road traffic accidents or falls *(Sarkies 2004)*. Optic nerve injury (ONI) can be classified according to the site or the mode of injury. The resulting damage to ON axons may occur in a direct or in an indirect way and can lead to partial or complete visual loss *(Steinsapir and Goldberg 1994, Yu-Wai-Man 2015, Jackson 2018).*

TON has reported incidence 0.7-2.5% *(Cockerham et al. 2009, Edmund and Godtfredsen 1963, Nau et al. 1987, Pirouzmand 2012)*, making this condition an infrequent cause of visual loss following blunt or penetrating head trauma *(Yu-Wai-Man 2015)*. Indirect TON is more common that direct *(Sarkies 2004)*. A national epidemiological survey of TON, conducted in the UK, found a minimum prevalence of 1 in 1.000.000 in the general population and showed that 79-85% of affected patients were adult males at their early 30s *(Yu-Wai-Man 2015, Lee et al. 2010)*. In this patient group the most common causes of TON injury are road-traffic accidents (21.5%), falls (25.6%) and assaults (20.7%) *(Lee et al. 2010)*. Another less frequent but equally important TON cause is the abusive injury which usually concerns infants *(Ford et al. 2012)*.

Direct TON arises from direct anatomical disruption of the ON fibers (direct ONI) due to penetrating trauma, especially orbital bone fragments entering within the optic canal, or nerve sheath hematomas. An example of direct ONI would be a high-velocity traveling projectile that penetrates the orbit and

causes significant damage to the ON *(Yu-Wai-Man 2015, Jackson 2018)*. Different varieties of direct ONI include optic nerve transection, avulsion, optic nerve sheath hemorrhage, orbital hemorrhage and orbital emphysema *(Sarkies 2004)*.

Indirect TON is developed due to the transmission of forces to the ON from a distant site (indirect ONI) through the oculofacial soft tissues and skeleton (indirect ONI), while no other damage is apparent to the ON surrounding tissue structures *(Yu-Wai-Man 2015, Sarkies 2004, Jackson 2018, Kumaran, Sundar, and Chye 2015)*. The consequent coup-countercoup forces injure the nerve transitions between mobile and fixed segments, most frequently occurring at the junction of the intraorbital and intracanalicular segments. This leads to limited vascular supply in the ON as a result of compression and destruction of pial vessels within the optic canal *(Kumaran, Sundar, and Chye 2015, Gross et al. 1981, Walsh 1966)*. Sites of head injury that usually cause blindness via indirect ONI are the forehead, the supraorbital ridge and (less frequently) the temporal region. In many cases of head injury, after the initial blow (which sometime results in consciousness loss but sometimes the resulting trauma may appear less severe), primary ocular examination appears normal, however various visual field defects along with ocular atrophy can occur after 4-6 weeks *(Sarkies 2004)*.

1.1.3 Molecular and Cellular Biology of TON

Human vision depends on the successful and high-quality signal conduction from the retina to subcortical target areas of the brain, via the optic nerve, which consists of RGC axon bundles. RGCs, as most neural cells in the central nervous system (CNS), are unable to regenerate injured axons. Therefore, head trauma, glaucoma, ischemia or optic nerve neurodegenerative diseases in general could result in permanent vision loss. The rodent ON has served as the key experimental model for understanding the underlying mechanisms for the inability of CNS mature neurons to regenerate their axons after injury *(Li, Schlamp, and Nickells 1999, McKinnon, Schlamp, and Nickells 2009, Yin et al. 2019)*.

Axonal injury in CNS neurons leads to primary and secondary degeneration, and eventually can lead to RGC death and spread of damage to neighboring cells. Interestingly, it has been shown that the manifestation of secondary degeneration happens in a very similar way in both acute injuries and chronic CNS diseases *(Bruno, Scapagnini, and Canonico 1993, Eitan et al. 1994, Schwartz 2004, Schwartz, Yoles, and Levin 1999)*. Secondary degeneration is carried out through various compounds that leak from degenerating fibers *(Schwartz 2004, Eitan et al. 1994)* including excitatory amino acids, opioids, free oxygen radicals and ions such as K^+ and Ca^{2+}. The release of these compounds leads to large changes in their extracellular concentration, which initiate several phenomena including phospholipid hydrolysis, inflammation, edema or induces alterations in metabolism and blood flow *(Schwartz 2004, Schwartz, Yoles, and Levin 1999)*. Several such mediator compounds are imperative for the correct function of neurons when found in their normal levels, however they become neurotoxic when they are present in abnormally elevated levels *(Schwartz 2004)*.

Inflammation

Apoptotic cells initiate a highly controlled cascade of events that ends up in the clearance of cell bodies by phagocytes *(Schwartz et al. 1993, Kerr, Wyllie, and Currie 1972, Nadal-Nicolás et al. 2017),* which in the CNS are microglial cells (MCs). Under normal conditions, microglia survey the tissue (SMCs) and are responsible for retinal homeostasis and synapse stabilization *(Nadal-Nicolás et al. 2017, Wang et al. 2016, Wong 2013)*. Microglia are located on four layers of the healthy retina: the retinal nerve fiber layer (NFL) containing RGC axons; in the GCL, containing RGC somatas and displaced amacrine cells; in the outer (OPL) and the inner plexiform layer (IPL), which besides neuropil also contains displaced RGCs. RGC death stimulates microglia activation *(Mac Nair et al. 2016)*. Activated microglia migrate to the damaged region *(Paques et al. 2010)* and participate in the clearance of cellular debris and local damage repair *(Wolf, Boddeke, and Kettenmann 2017, Nadal-Nicolás et al. 2017)*. After ONC or ONT, microglial morphology changes from ramified to fusiform (ameboid). Fusiform (or rod-like) microglia are, most commonly, found along RGC axons in the form of chains. On the other hand, ameboid MCs are found more often engulfing apoptotic RGCs. The clearance of dead RGCs by phagocytic microglia (PMCs) is initiated 3 days after RGC death and is similar in both lesion types (ONC / ONT). Moreover, RGC clearance appears to be linear in contrast with RGC death, which is described by a two-phase linear regression consisting of a quick and a slower phase. PMCs reach their highest number 14 days post-lesion, being approximately 10.000 more (including non-PMCs; in the GCL) compared to SMCs found in intact retinas. At the same time, the PMC population in IPL has decreased by 50% suggesting the migration between these two layers. 2 months post-lesion, RGC death has slowed down, microglia numbers in the GCL have returned to normal and the IPL seems to have been remodeled to its new status, indicating system restoration. After ON transection, microglia perform a cleansing role. There is no indication that microglia are involved in RGC death at least during the initial fast phase of RGC loss *(Galindo-Romero et al. 2013, Nadal-Nicolás et al. 2017).* Quiescent microglia are also found throughout the normal ON head on the walls of large blood vessels and surrounding capillaries in glial columns and cribriform plates. After moderate to severe injury, microglia are activated and appeared to form linear arrays near choriocapillaris vessels (Neufeld 1999). The density of microglia in ON under normal conditions is several times higher than the one in retina and this difference is increased 10 days post-ONC. 31 days post-ONC microglia population in the ON remains at high levels *(Heuss et al. 2018)*.

Axon Degeneration

Evidence suggests that axonal degeneration frequently precedes the loss of cell bodies *(Ribas et al. 2016, Knöferle et al. 2010)*. The degeneration of the axons occurs via three mechanisms: Wallerian Degeneration (WD), Acute Axonal Degeneration (AAD), and Die Back (DB).

Wallerian degeneration, that is degeneration of axons distal to an injury site, is more frequently observed in severely damaged axons, and results in atrophy and rapid loss of structure throughout the entire length of the axon. At the cellular level, initial segmentation of the myelin sheath is apparent, followed by swelling of the axolemma, disorganization of neurofilaments and microtubules, and mitochondrial swelling. The remaining axonal fragments then undergo phagocytosis by glial cells and macrophages. Concerning the cell body, it may live for a number of days, but ultimately undergoes apoptosis *(Saxena and Caroni 2007, Budak and Müberra 2010)*

AAD starts immediately following axonal lesion *(Ribas et al. 2016, Knöferle et al. 2010)* and, in contrast with WD, it results in sudden axonal disintegration extended for ~300 μm proximal and distal to the lesion *(Kerschensteiner et al. 2005)*. Time-course study of AAD after ONC showed that bulb-like axonal swellings begin to form within 30 min after lesion and continue to increase in size for about 240 min, while axons continued to disintegrate. At 60 min after ON lesion, the axonal integrity ratio both proximal and distal to the lesion site was significantly different from the intact axon. Regarding ultrastructure changes after lesion, condensation and misalignment of neurofilaments followed by microtubule fragmentation could be observed already at 30 min after crush. Although the mean axon diameter decreased significantly on both the distal and the proximal side of the crush compared to unlesioned axons, at 120 min and 360 min after crush the mean axon diameter showed a significant increase, which was faster on the proximal compared to the distal side of the crush. One of the main events in AAD is the intra-axonal influx of calcium *(Knöferle et al. 2010)*, which activates downstream calpain proteases, key mediators of cytoskeletal degradation *(Ribas et al. 2016, George, Glass, and Griffin 1995)*. In addition to calpain activation, autophagy is another important mechanism downstream of calcium that is increased in the course of axonal degeneration in the ON and the spinal cord *(Ribas et al. 2016, Ribas et al. 2015, Koch et al. 2010)*.

DB appears in axons that experience moderate injury. DB is characterized by slower retrograde degeneration with a distal-to-proximal progression (thus from the synapse to the soma) *(Seif, Nomura, and Tator 2007, Budak and Müberra 2010)*. Milder insults can permit greater functional connectivity between the soma, proximal and distal axonal segments and consequently die-back death can occur over several months *(Budak and Müberra 2010)*.

RGC Death

RGC death occurs in two phases with different kinetics, as shown in rat and mice ONC / ONT models. The initial quick phase takes place up to 14 days post-injury, leading to approximately 65% RGC loss for the first 7 days, which increases to 85% at 14 days after injury *(Feng et al. 2017, Takeuchi et al. 2018, Sánchez-Migallón et al. 2015, Sánchez-Migallón et al. 2018, Mesentier-louro et al. 2017, Mesentier-Louro et al. 2019, Grinblat et al. 2018, Guo et al. 2020, Kole et al. 2020, Laughter et al. 2018) (Levkovitch-Verbin et al. 2000, Agudo et al. 2009, Parrilla-Reverter et al. 2009, Nadal-Nicolás et al. 2017, Kim et al. 2015, Agudo et al. 2008)*. The second phase is characterized by slower steady rate of RGC apoptosis with one-half survival times ranging from1 month post-ONT and 6 months post-ONC in rats *(Villegas-Pérez et al. 1993)*. RGC death seems to be similar in ONT and ONC for the first 2 weeks. ONC leads to lower rates of RGC loss for the following period up to 3 months in comparison to ONT *(Villegas-Pérez et al. 1993, Nadal-Nicolás et al. 2017, Sánchez-Migallón et al. 2018)*. Aside from the type of ON injury (ONC; ONT), the distance of the injury site from the eye comprises a critical parameter for the severity of the injury and therefore for the rate of RGC death *(Sánchez-Migallón et al. 2018, Nadal-Nicolás et al. 2017, Villegas-Pérez et al. 1993, Agudo et al. 2009, Agudo et al. 2008)*. According to Berkelaar, during the period of massive RGC loss following ON transection close to the eye, a number of neurons in the GCL present morphologic changes correlated with apoptotic death such as nuclear fragmentation and DNA breakdown. 5 and 7 days post-injury, when RGC loss is intense, a small number of cells in the GCL presented clumped and fragmented nuclei. Such nuclei, indicating “apoptotic bodies”, were not present 1 or 3 days after

intraorbital axotomy or in intact retinas *(Berkelaar et al. 1994)*. Supporting evidence from mouse models indicate that at least half of RGCs die during the first 7 days post-ONT through caspase-depended apoptosis *(Sánchez-Migallón et al. 2015)*. Similarly, ONC in a rat model significantly increased retinal levels of activated caspase 3, STAT1, p38, SAPK/JNK and PARP, signaling molecules associated with cell stress and death *(Mesentier-louro et al. 2017)*. Taking the above into consideration, apoptotic cell death plays an important role in RGC loss after ON crush or transection.

Apoptosis is an active genetic process that triggers an organized series of events causing the cell to self-destruct, corresponding therefore to a form of "cell suicide". Apoptosis is active during development and neurodegeneration, facilitating controlled and clean cell death without affecting neighboring cells that are destined to survive. Apoptosis can be divided into three distinct phases: signaling, commitment and execution (occurring in the presented order). During the signaling phase, pro-apoptotic stimuli (e.g. ligand-induced activation of death receptors, cellular stress signals) initiate the sequence of events that will eventually lead to cell death. During the commitment phase, the cell either commits to apoptosis or activates mechanisms that block the signaling cascade initiated during the signaling phase in order to return in its normal state. The execution phase begins only after the cell is fully committed to die, passing the "point of no return". During the execution phase, enzyme systems become activated initiating the biochemical and morphological features of apoptosis. Such enzyme systems cleave proteins, externalize phosphatidylserine, degrade DNA, while cell membranes begin to bleb forming vesicles that contain high concentrations of cellular components that were formerly distributed in a more widespread manner with the cell *(Hengartner 2000, Mills 2001, Budak and Müberra 2010)*. At the end of the execution phase, vital cell structures and functions are destroyed. Phosphatidylserine becomes externalized, serving as an "eat-me" signal to phagocytosing cells, which ingest newly-dead cells without causing inflammation. Apoptosis can be initiated via extrinsic or intrinsic pathways, the activation of both of which are upregulated in rat RGCs after transection of the optic nerve *(Sánchez-Migallón et al. 2015, Agudo et al. 2009, Agudo et al. 2008)*. The extrinsic pathway is initiated by cell surface receptor activation upon binding to ligands. Activated death receptors, such as Fas, recruit adaptor proteins that activate caspase 8 by proteolytic cleavage. Active caspase 8, in turn, activates downstream executioner caspases 3 and 7. The intrinsic pathway is initiated by the permeabilization of the mitochondrial outer membrane. The resulting release of cytochrome C into the cytoplasm leads to the formation of the apoptosome complex and the activation of caspase 9 that activates effector caspases 3 and/or 7. After caspase 3, both pathways converge into the cleavage of specific substrates, destruction of cellular structures and consequent cell death *(McIlwain, Berger, and Mak 2013, Bähr 2000, D'Amelio, Sheng, and Cecconi 2012, Sánchez-Migallón et al. 2015)*.

Necrosis, on the other hand, is accidental in nature, and its purpose is to eliminate cells that have been severely damaged. Unlike apoptosis, necrosis is a passive process, during which the cell membrane is rapidly destroyed, and toxic cellular components spill into the extracellular space, potentially injuring nearby cells *(Dawson 2005, Budak and Müberra 2010)*. Low ATP levels or defective ATP production are factors predisposing cells towards necrosis *(Budak and Müberra 2010, Nicotera, Leist, and Ferrando-May)*. The cell membrane becomes permeable, organelles are dilated, ribosomes dissociate from the endoplasmic reticulum and the nucleus disintegrates. Proteases play major roles in cell degradation during necrosis. As a consequence, cellular contents are liberated into the intracellular space and evoke an inflammatory response *(Budak and Müberra 2010)*.

Axon Regeneration

Various animals, such as frog and fish, included in the category of cold-blooded vertebrates, can regenerate their optic nerve throughout their lives *(Yin et al. 2019, Grant and Keating 1989, Sperry 1948).* The foundation of this ability lies in i) the less inhibitory environment (less scar formation on injury site) inside the ON after transection *(Becker and Becker 2002, Lee-Liu et al. 2017)*, ii) the de-differentiation of many ON oligodendrocytes and Müller cells in order to become RGCs and replace the RGCs that were lost *(Ankerhold et al. 1998)* iii) the production of growth-promoting cues by retinal astrocytes *(Hirsch, Cahill, and Stuermer 1995)*, and iv) in a stronger cell-intrinsic capacity of growth *(Priscilla and Szaro 2019, Abdesselem et al. 2009, Becker and Becker 2014, Benowitz, Shashoua, and Yoon 1981).*

In mature mammal CNS, axon regeneration is extremely limited after injury. On the other hand, axons in the PNS can promptly regenerate after transection, allowing recovery of function. Milestone work has exhibited that adult mammalian CNS neurons, which under normal conditions have almost zero regenerative ability, are able to grow for long distances into the permissive environment of a peripheral nerve graft *(Richardson, McGuinness, and Aguayo 1980, Richardson, Issa, and Aguayo 1984, David and Aguayo 1981, Benfey and Aguayo 1982)*. This indicated that the PNS environment is stimulatory in contrast to the CNS environment which is inhibitory for axon growth *(Huebner and Strittmatter 2009).*

The two major classes of CNS regeneration inhibitors are myelin-associated inhibitors (MAIs) and chondroitin sulfate proteoglycans (CSPGs). These molecules limit axon regeneration, and, by interfering with their function, some degree of growth in the adult CNS is achieved. MAIs are proteins produced by oligodendrocytes as components of CNS myelin. MAIs have been shown to diminish neurite outgrowth *in vitro* and are thought to impair axon growth *in vivo* after CNS damage *(Huebner and Strittmatter 2009).* MAIs include Nogo-A *(Chen et al. 2000),* myelin-associated glycoprotein (MAG) *(McKerracher et al. 1994)*, oligodendrocyte myelin glycoprotein (OMgp) *(Kottis et al. 2002)*, ephrin-B3 *(Benson et al. 2005)* and Semaphorin 4D (Sema4D) *(Moreau-Fauvarque et al. 2003)*. CSPGs are the main inhibitory molecules found in the glial scar *(Asher et al. 2000, Morgenstern, Asher, and Fawcett)*, which constitutes a physical barrier to nerve regeneration after injury *(Huebner and Strittmatter 2009)*. After CNS damage, resulting reactive astrocytes induce upregulation of GSPGs, which are then excreted into the extracellular space. CSPG inhibitors include neurocan *(Asher et al. 2000)*, versican *(Schmalfeldt et al. 2000)*, brevican *(Yamada et al. 1997)*, phosphacan *(Inatani et al. 2001)*, aggrecan *(Huebner and Strittmatter 2009)* and NG2 *(Dou and Levine 1994)*.

Other kinds of axon regeneration inhibitors in the CNS (not present in myelin or the glial scar) include repulsive guidance molecule (RGM) and semaphorin 3A (Sema3A) *(Huebner and Strittmatter 2009).* Studies have demonstrated that administration of an anti-RGMa antibody *(Hata et al. 2006)* or a small-molecule inhibitor of Sema3A *(Kaneko et al. 2006)* increased functional recovery after spinal cord injury (SCI) in rats, suggesting involvement of RGM and Sema3A in limiting CNS regeneration. Additionally, slower axon debris clearance in the CNS compared to the PNS is another factor that may inhibit axonal re-growth.

Cell-autonomous factors are also important determinants of CNS regeneration failure. Neurons in the CNS fail to upregulate regeneration-associated genes (RAGs) to the same extent as do PNS neurons and therefore their regenerative ability is limited even in the absence of inhibitors *(Huebner and*

Strittmatter 2009, Bomze et al. 2001). Increasing RAG expression in CNS neurons permits improved axon regeneration within the CNS: simultaneous overexpression of GAP-43 and CAP-23 promoted sensory axon regeneration after SCI *(Bomze et al. 2001)*. RAGs include c-Jun *(Raivich et al. 2004)*, activating transcription factor-3 (ATF-3) *(Seijffers, Allchorne, and Woolf 2006)*, SRY-box containing gene 11 (Sox11) *(Huebner and Strittmatter 2009)*, small proline-repeat protein 1A (SPRR1A) *(Bonilla, Tanabe, and Strittmatter 2002)*, growth-associated protein-43 *(GAP-43)* and CAP-23 *(Bomze et al. 2001)*. Moreover, mammalian target of rapamycin (mTOR) has been found to be suppressed in injured RGCs in wild type mice. mTOR pathway activation promotes axon regeneration and neuroprotection while mTOR expression levels have been correlated with the extent and time course of ON regeneration *(Park et al. 2008)*. Activated mTOR signaling promotes axonal growth of axotomized RGCs over several millimeters, with some axons reaching the optic chiasm *(Pernet and Schwab 2014, Li et al. 2017)*.

The growth of RGC axons after ONI starts soon after injury and lasts over several months. Initially, ONI induces the formation of a dense neurite plexus at the inner surface of the retina due to massive axonal sprouting *(Pernet, Joly, Dalkara, et al. 2013)*. Axons undergo 'abortive regeneration', a phenomenon where axons present transient growth responses to injury. Injured axons begin to sprout as early as 14 h post-lesion with an average growth rate of 20 μm per day, and they continue until 10 days post injury at the lesion site in adult albino mice. Once regenerating axons begin to degenerate, the overall growth rate starts to decline over time *(Pernet and Schwab 2014).* Unfasciculated axons do not undergo abortive regeneration, as they continue to grow in a random pattern until at least 100 days post-lesion without presenting long-range growth *(McConnell and Berry 1982)*. At 1 month post-injury, less than 120 axons per ON reach the optic chiasm in mouse, representing only approximately 0.2% of all axons, assuming a total of 60,000 RGCs *(Luo et al. 2013)*. Small but nearly equal numbers of axons are observed at short distances beyond the chiasm ipsi- and contralaterally after 6 weeks *(Kurimoto et al. 2010)*, while regenerating fibers cross the midline of the chiasm within 10 weeks of ON injury *(De Lima et al. 2012)*. Almost 2 months after injury, regenerating axons converge onto suprachiasmatic nucleus neurons connected with existing brain circuitry. As a consequence, glutamatergic excitatory synapses are reformed *(Li et al. 2015)* while the growth pattern of the regenerating axons changes continuously for as long as 4 months after injury *(Pernet, Joly, Dalkara, et al. 2013)*. In order to achieve functional recovery of vision, damaged axons need to regenerate into the lateral geniculate nucleus and the superior colliculus, a distance longer than 8 mm from the ON lesion *(Pernet and Schwab 2014)*. During the process of axonal projection, axons fail to project correctly to the brain due to axonal misguidance and weak intrinsic growth capacity of adult RGCs *(Pernet, Joly, Jordi, et al. 2013)*. For successful regeneration, the cell bodies of injured RGCs must acquire accurate and timely information regarding the site and extent of the axonal damage and then initiate a transcription program to enhance their intrinsic growth ability *(Li et al. 2017, Yang and Yang 2012).*

1.2 Models of Traumatic Optic Neuropathy

1.2.1 Animal Models

RGC loss, one of the most common outcomes of TON, can lead to visual field loss or blindness. Even though such TON consequences have triggered considerable research, the underlying pathophysiology mechanisms of TON still remain partly elusive. In order to study the mechanisms that determine the cause and process of axon degeneration and RGC death after TON, as well as test the effectiveness of novel experimental treatments, the development and use of animal models is necessary *(Levkovitch-Verbin 2004)*.

The efficacy of an experimental animal model is closely related with its capability to imitate a human condition, primate animal models appear to be the best option. Monkeys are considered the most capable TON models since, apart from close phylogeny and high homology with humans, monkey eyes have almost identical retinal and ON anatomy with human eyes. Unfortunately, monkeys come at a high cost, are hard to acquire and require significant investment (highly-experienced personnel, housing facilities) *(Levkovitch-Verbin 2004)*. On the other hand, rodents (rats; mice) are easily available and handled, enable easy access to their superior colliculus, eyes, and optic nerves. Rodents require lower cost of purchase and housing, and are extensively used for research on human optic nerve disease due to the high degree of conservation between their and human genomes *(Paigen 1995, Levkovitch-Verbin 2004)*. Mouse models of optic nerve disease provide the ability to investigate RGC degeneration and test the efficiency of new therapeutic interventions. Finally, transgenic and knockout mice enable to probe the role of specific molecules or pathways *(John, Anderson, and Smith 1999) (Levkovitch-Verbin 2004)*.

1.2.2 TON Models

The generation of animal disease experimental models is crucial for understanding the biological mechanism of a disease as well as to test the efficacy of potential experimental treatments. Aiming to emulate the development of TON in humans different research groups have developed various rodent models [*Figure 1-4*]. Some models include a direct injury to the ON, mimicking direct TON. Others impose injury to the ON indirectly, mimicking indirect TON *(Levkovitch-Verbin 2004, Bastakis et al. 2019)*. Direct TON models include the established optic nerve transection (ONT) *(Magharious, D'Onofrio, and Koeberle 2011)* and optic nerve crush (ONC) *(Tang et al. 2011),* as well as the recently-developed and much less invasive controlled orbital impact (COI) model *(Ibrahim et al. 2018) (Bastakis et al. 2019)*. Indirect injury models include the Ocular Blast Injury (OBI) *(Hines-Beard et al. 2012)* and Sonication-induced traumatic optic neuropathy (SI-TON) *(Tao et al. 2017)*.

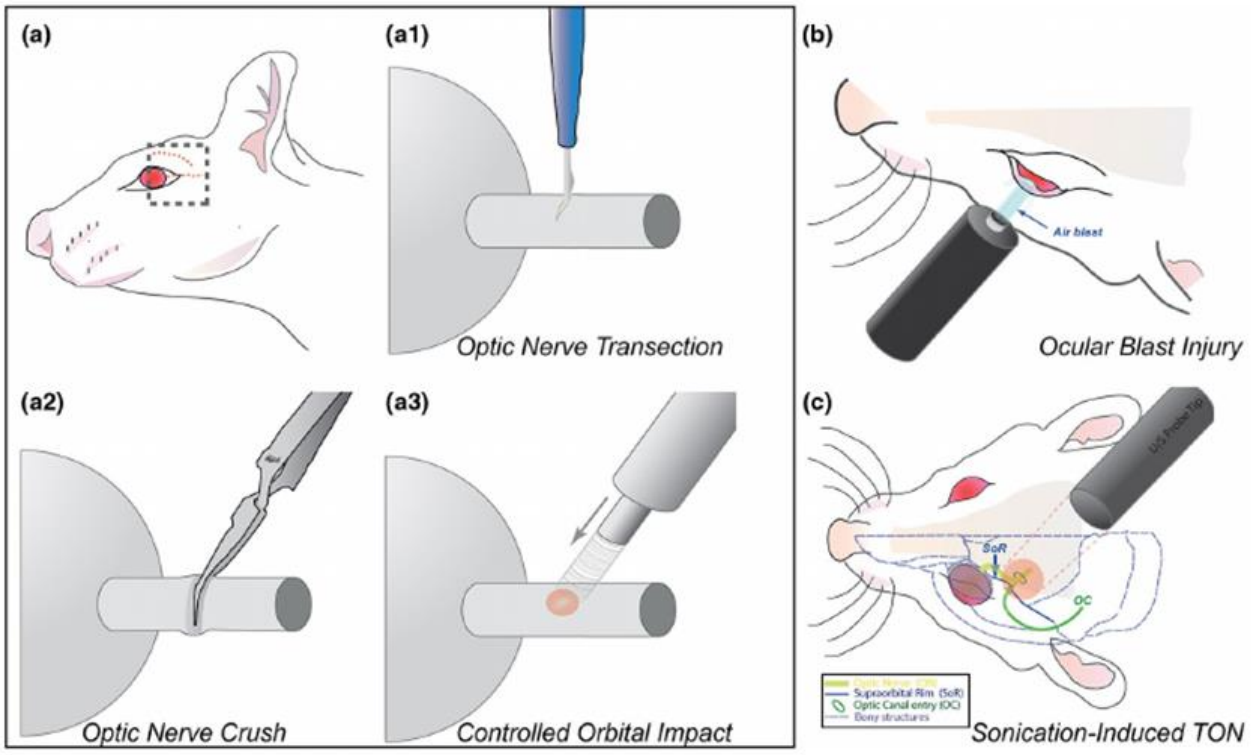

Figure 1-4: Rodent models of TON. (a) Invasive models. Orange dotted lines mark the incision required to reveal the ON. Invasive TON models include ON transection/axotomy (a1), ON crush (a2) and controlled orbital impact (a3). (b,c) Noninvasive TON animal models such as ocular blast (b) and sonication induced TON (c) (Bastakis et al. 2019).

Optic Nerve Transection

Optic nerve transection (ONT) is a widely-used TON model that provides reproducible results on the time course of ONT processes and RGC cell death. In ONT, the optic nerve is accessed within the orbit of the eye and then is completely transected. The transection of all RGC axons leads to significant RGC death: ONT leads to 90% loss of the injured RGCs within 2 weeks after transection. The primary cause of RGC death is apoptosis, which is delayed about 4 days after axotomy, providing a critical time window for experimental manipulations *(Villegas-Pérez et al. 1993, Berkelaar et al. 1994, Quigley et al. 1995, Magharious, D'Onofrio, and Koeberle 2011).*

In order to generate the ONT model, the superior conjunctiva is incised, the muscles and connective tissue are separated, and the intracranial optic nerve is exposed. Then a blade knife is used to transect the optic nerve behind the globe, taking care not to interfere with the blood supply and sparing meningeal sheaths. After ONT, the retina should be ophthalmoscopically examined to assure blood vessel patency *(Levkovitch-Verbin 2004)*.

ONT allows a large degree of experimental manipulation of the eye, enabling to target either the whole retina or directly injured RGCs using intraocular injections and several other techniques. ONT has been utilized to delineate the effects of possible treatments on ONT processes and RGC survival including studies of drug delivery in the retina and the ON *(Magharious, D'Onofrio, and Koeberle 2011, Bähr 2000, Weishaupt and Bähr 2001)*.

Optic Nerve Crush

The Optic Nerve Crush (ONC) model is suitable for studies on TON, glaucoma and other ON degeneration diseases. In ONC, the crush of the ON leads to axonal degeneration and gradual RGC apoptosis, leading to irreversible vision loss. These events make ideal for investigating the molecular processes behind RGC death and survival. Moreover, ONC permits the application of therapeutic substances for the treatment of different optic neuropathy types *(Tang et al. 2011).*

There are two possible ways for performing ONC injury: the intra-orbital approach and the intracranial approach *(Duvdevani et al. 1990, Chierzi et al. 1999, Levkovitch-Verbin 2004)*. The crush injury can be inflicted by various tools, including forceps, balloon, or other devices. However, the most common technique is using forceps to perform the intra-orbital approach *(Villegas-Pérez et al. 1993, Yoles, Wheeler, and Schwartz 1999, Levkovitch-Verbin 2004)*. In the intra-orbital approach, the crush injury is inflicted for 1 second by a cross-action forceps 2–3 mm from the eyeball, taking special care not to interfere with eye blood supply. This technique is fast and rather easy to perform, however the impotence of accurately imposing the proper amount of pressure via forceps required to inflict repeatable crush injury remains an obstacle *(Levkovitch-Verbin 2004)*. In the intra-orbital approach *(Levkovitch-Verbin 2004)*, the time of pressure application as well as the distance of the crush site from the eye varies between 1-10 seconds and from 0.5-3 mm (Laughter et al. 2018, Levkovitch-Verbin 2004, Nadal-Nicolás et al. 2017, Tang et al. 2011, Takeuchi et al. 2018).

Ocular Blast Injury

In order to delineate the effects of primary blast injury to the eye and prevent any confounding complications to parts of the mouse body exposed to the blast, the Ocular Blast Injury (OBI) mouse model utilizes a novel device to precisely direct a primary blast via an open-field waveform into the eye *(Hines-Beard et al. 2012)*. The nature of injury induced by ONI was assessed via optical coherence tomography, gross pathology, visual acuity and intraocular pressure *(Hines-Beard et al. 2012)*. Results demonstrated that OBI induced injuries (retinal damage, avulsion of the optic nerve, impaired visual acuity and corneal edema along with corneal abrasions) consistent with ones identified in Iraq war veterans who had suffered closed eye injuries as a result of blast exposure *(Hines-Beard et al. 2012, Thach et al. 2008, Cockerham et al. 2011, Hilber 2011).*

Sonication-Induced Traumatic Optic Neuropathy (SI-TON)

The Sonication-Induced Traumatic Optic Neuropathy (SI-TON) mouse model triggers TON via ultrasonic pulses. A microtip probe sonifier is placed on the supraorbital ridge directly above the entrance of the ON into the bony canal in order to deliver an ultrasonic pulse to the ON. As a result, pro-inflammatory markers in the ON increase within 6 h post-injury and then RGCs population and the visual function decline in a steady rate over a period of 2 weeks. The SI-TON model promises to deliver reproducible results, measurable reduction in RGC numbers, and no ocular morbidity if performed in a correct way. On the other side, ultrasound energy may scatter and affect neighboring

tissues, including the contralateral ON, rendering it non-trustworthy as a control tissue *(Tao et al. 2017)*.

Controlled Orbital Impact (COI)

Previously developed TON models suffer from various limitations: ONT and ONC suffer from large variability in the time and force applied to inflict the injury *(Tang et al. 2011)*, no opportunity to rescue or attenuate the inflammatory response *(Magharious, D'Onofrio, and Koeberle 2011)* and high mortality rates (~25-50%) *(Hines-Beard et al. 2012)*. OBI and SI-TON models suffer from the inability to focus sound waves on the desired site in a predictable way *(Tao et al. 2017)*.

The COI model promises to overcome such limitations. COI is a simple, minimally invasive experimental model, which allows the development of TON with varying levels of severity, along with the potential of precision control and reproducibility. COI delivers a controlled impact in the orbital area posterior to the globe, leading to the generation of a graded quantifiable deficit in the functions of retinal ganglion cells with zero presence of ocular fracture, morbidity, or mortality *(Ibrahim et al. 2018)*.

1.2.3 Behavioral Bioassays

Behavioral bioassays are used to assess an organism's behavior to detect and analyze external stimulus or as an indicator of an internal physiological or psychological state *(Brown and Bolivar 2018)*. Thus, behavioral bioassays use behavior to measure, in a qualitative or quantitative way, an animal's ability to detect environmental, physiological or neurological stimuli *(Winn 2001)*. Within neuroscience, there are a number of types of behavioral bioassays for drug action, brain lesions and neurological disorders *(Crawley 2007, Buccafusco 2009, Wahlsten 2011, Brown and Bolivar 2018)*.

Optomotor Response Assay

The Optomotor Response (OMR) is an innate behavior, exhibited by most vertebrates, that plays an important role in stabilizing the eye relative to the visual scene *(Emran, Rihel, and Dowling 2008)* and in compensating for whole visual field movements *(De Lima et al. 2012)*. OMR is evaluated using an OptoMotor cylinder apparatus (Cerebral Mechanics), where a mouse is placed on a small elevated platform surrounded by a banked array of four liquid-crystal monitors. The monitor displays simulate high-contrast stripes of variable spatial frequency, rotating in either a clockwise or counterclockwise direction *(Prusky et al. 2004)*. Mirrors are placed on the floor and ceiling of the apparatus in order to create a 3D appearance. The speed of rotation, spatial frequency, and contrast of the stimuli are controlled by the system software. Video recordings of the mouse are taken over 5-minute intervals. The videos are analyzed in to determine the maximum spatial frequency at which mice show a reliable tracking response *(De Lima et al. 2012)*. OMR has also been performed in zebrafish in order to assess the functionality of their visual pathway. The drum is rotated in clockwise and counter-clockwise directions, and eye movements are analyzed using a dissecting scope equipped with camera *(Brockerhoff 2006)*.

Visual Cliff Assay

Using mice's innate aversion to depth, depth perception/avoidance is assessed using the visual cliff apparatus *(Glynn, Bortnick, and Morton 2003)*. One side of a transparent plexiglas box, ("shallow end") is positioned 18 cm above a checkerboard pattern with black and white squares (2x2 cm). The other side ("deep end") is suspended 70 cm above a similar pattern with larger square dimensions (60x60 cm). The animal is placed at the back of the shallow end and its behavior is recorded for 2 minutes. Mice depend on visual cues to distinguish the shallow end from the deep end. Video analysis is utilized to quantify the latency to step off the shallow end and the total time spent on the shallow end *(De Lima et al. 2012)*.

Circadian Activity Assay

Mice are maintained on a continuous 12:12 hour light-dark cycle before being placed individually in a cage of InfraMot Activity System (TSE Systems). Infrared sensors are used to monitor animals' locomotor activity in 20-minute bins during the 5-day interval period. On day 3, the light-dark cycle is changed (set back 6 hours) and mice are evaluated for entrainment of their circadian activity patterns *(De Lima et al. 2012)*.

Pupillary Light Reflex (PLR)

Awake, alert mice are hand-held under the lamp of a surgical microscope and the pupillary response is video-recorded in ambient and increased light conditions. PLR is evaluated via quantifying the change of the animal's pupillary diameter over a 40-second period *(De Lima et al. 2012).*

1.2.4 Tissue Assays Utilized in TON Response Studies

Besides behavioral assays, which focus on the vision system functional level, researchers also use various tissue-based assays to investigate TON effects in the tissue and molecular level. Most such assays quantify markers related to cell (nuclei) number, RGC number and survival, axon degeneration and regeneration, neuron functionality, inflammation, cell apoptosis, cell morphology and localization within the tissue.

Histology and Immunohistochemistry

Histological analysis is the gold standard for tissue examination for research and diagnostic purposes, qualitative or quantitative measurements. In TON studies, histology is routinely utilized to determine the inflammation and healing stage of a tissue. Various histology stains are used to identify certain kinds of structures and cells *(Paramitha et al. 2017).* In Hematoxylin-Eosin (H&E) staining, hematoxylin deep blue-purple color stains nucleic acids, whereas Eosin pink stains proteins in the extracellular matrix *(Chlipala et al. 2020, Fischer et al. 2008)*. H&E stain has been utilized in TON

studies for morphological evaluation of the ON, verification of the injury site *(Tao et al. 2017)* and the assessment of neuron survival via neuron nuclei counting in retinal sections *(Li, Fang, and Jiang 2010)*.

Immunohistochemistry (IHC) permits the identification and localization of specific antigens in tissue preparations using antigen-specific antibodies. IHC permits morphologic evaluation by light microscopy. IHC utilize monoclonal and polyclonal antibodies to determine the tissue distribution of antigens of interest in healthy and diseased tissues *(Ahmed 2006, Drew and Shieh 2015, Kaliyappan et al. 2012).*The distribution and abundance of such antigens can be utilized to study key processes of interest in the retina or the ON including RGC survival, tissue inflammation axon degeneration and regeneration.

Assays of RGC Survival and Apoptosis

RGC survival can be evaluated using IHC by staining RGCs in order to compare RGC density before and after TON. Most common RGC markers are Brn3A, NeuN and RBPMS *(Hajdú et al. 2019)*. Brn3A is a transcription factor expressed by most RGCs in GCL *(Nadal-Nicolas et al. 2009, Badea et al. 2009, Hajdú et al. 2019).* NeuN protein is found in the nucleus and perinuclear cytoplasm of most CNS neurons in mammals, therefore is used to label RGCs bodies in GCL *(Hajdú et al. 2019, Rodriguez, de Sevilla Müller, and Brecha 2014, Gusel'nikova and Korzhevskiy 2015)*. RBPMS is an RNA-binding protein specific for RGCs *(Rodriguez, de Sevilla Müller, and Brecha 2014, Hajdú et al. 2019).*

Quantification of RGC apoptosis can be performed using the TUNEL assay in whole retina mounts or radial retina sections. The TUNEL (Terminal deoxynucleotidyl transferase UTP Nick-End Labeling) assay detects apoptotic cells by labeling the extensive DNA degradation that takes place during late apoptosis. TUNEL relies on template-independent identification of blunt ends of dsDNA breaks by TdT, which catalyzes the addition of fluorescently-labeled dUTPs to 3'-termini of DNA ends. Fluorescently-labeled dUTPs are subsequently visualized using fluorescence imaging *(Kyrylkova et al. 2012)*.

Assays of Astrogliosis and Inflammation

Glial fibrillary acidic protein (GFAP) comprises a protein biomarker for astrocytes and activated Müller cells *(Petzold 2015, Jünemann et al. 2015)*. Müller cells activation is a key response to retinal injury, involving increased expression of GFAP and scar formation *(Jünemann et al. 2015, Wickham et al. 2012)*. Increased GFAP expression is also a critical marker for astrocyte activation both in retina and ON *(Pekny and Pekna 2004, Zhang et al. 2017)*, and therefore for glial scarring, since astrocytes form glial scars through activation and proliferation *(Sofroniew 2009, Zhang et al. 2017)*. According to the literature ONC induces significant GFAP upregulation as well as $GFAP^+$ astroglial and Müller cell processes spanning across retinal layers *(Wang et al. 2016, Mesentier-louro et al. 2017, Mesentier-Louro et al. 2019, Tang et al. 2020, Huang et al. 2018, Nascimento-Dos-Santos et al. 2020)*.

Additionally, tissue inflammation is evaluated by assessing the number and the morphology of microglia. Microglia constitute the primary immune cells in the CNS *(Eggen et al. 2013, Hovens, Nyakas, and Schoemaker 2014)*. When a danger signal is detected, microglia are submitted to a rapid change in morphology and function, a process also known as activation *(Hovens, Nyakas, and Schoemaker 2014, Kreutzberg 1996)*. The number and state of microglia can be studied via IHC using antibodies for ionized calcium-binding adaptor protein-1 (IBA1), a specific marker of all microglia *(Hovens, Nyakas, and Schoemaker 2014)*. Although related literature is limited, almost all reports agree that the number of $IBA1^+$ cells was increased in injured retinas 7 and 14 days after ONC, suggesting that ONC induces microglial activation *(Bohm et al. 2012, Huang et al. 2018, Nascimento-Dos-Santos et al. 2020, Tang et al. 2020, Wang et al. 2016)*. However, one study reports no significant differences in retinal microglia (IBA1) between healthy and injured retinas *(Morzaev et al. 2015)*.

Assays of Axonal Degeneration and Regeneration

Neural degeneration and subsequent regeneration after TON can be monitored via IHC using antibodies that mark neuronal axons, including antibodies against neurofilaments, neuronal-specific tubulin isoforms and axonal-specific proteins. Neural degeneration can be assessed by staining against the phosphorylated neurofilament heavy subunit (pNFH), a principal constituent of the neuronal cytoskeleton *(Vorobyeva et al. 2014).* Additionally, antibodies against neuron-specific class beta III tubulin (such as the TuJ1 antibody) can stain RGC axons in the ON. Furthermore, growth-associated protein 43 (GAP-43) is highly expressed in neuronal growth cones during development and regeneration, and therefore is used in order to assess the axonal regeneration after injury *(Holahan 2015)*. Other IHC studies stain against the neural cell adhesion molecule L1, a transmembrane protein involved in numerous processes during nervous system development, including neurite growth *(Lagenaur and Lemmon 1987, Kamiguchi, Tateno, and Mikamo 1990)*. L1 is expressed on the surface of axonal shafts and growth cones of developing neurons and as a consequence is used as a marker for axon regeneration *(Kamiguchi, Tateno, and Mikamo 1990)*.

Apart from antibodies that target axons, another useful tool for monitoring axonal elongation is the use of retrograde tracers. FluoroGold (FG) is a widely-used retrograde fluorescent tracer used to assess the number and function of RGCs *(Yao et al. 2018)*. FG is endocytosed by damaged neurons or at nerve terminals and then is transported along the axon cytoskeleton towards the soma *(Bilsland and Schiavo 2009, Mead and Tomarev 2016)*. In TON research FG is usually injected in the superior colliculus (SC) of intact or injured ON in order to stain RGCs. FG injection in the SC prior to injury, or FG injection proximal to the lesion site will stain all RGC. FG injection distal to the lesion site will stain those spared or regenerating RGCs whose axons extended past the lesion site *(Mead and Tomarev 2016)*. Another commonly used tracer for evaluating RGC survival and axonal elongation is Cholera toxin subunit B (CTB). CTB is a nontoxic subunit of the cholera toxin protein complex that binds cellular surfaces via the pentasaccharide chain of monosialotetrahexosylganglioside *(Yao et al. 2018)*. CTB enters the cytoplasm by adsorptive endocytosis and can be used both as retrograde or anterograde tracer *(Lai et al. 2015).*

Assays of Demyelination and Remyelination

Luxol Fast Blue (LFB) is an alcohol-soluble amine salt of sulfonated copper phthalocyanine used to stain myelin in paraffin processed tissue *(Klüver and Barrera 1953, Bruce-Gregorios 2006)*. LFB stains myelin blue-green while neurons are stained purple *(ClinSciences)*. LFB has been used to evaluate demyelination in the ON using a 0-3 point relative scale (0: no demyelination; 1: scattered foci of demyelination; 2: prominent foci of demyelination; 3: large (confluent) areas of demyelination *(Khan et al. 2018, Grinblat et al. 2018)*.

1.2.5 Monitoring TON Response *in vivo*

Over the past years several methods have been developed in order to determine the effects of TON *in vivo*.

Electrophysiology

RGC function can be assessed non-invasively by monitoring variations in Electroretinography (ERG) electrical responses of various cell types in retina. These variations are modified in order to emphasize the activity of inner retina neurons. The most specific technique for electrophysiological assessment of RGC function appears to be pattern-ERG (PERG), which is dominated by inner retina activity *(Porciatti, Saleh, and Nagaraju 2007, Porciatti 2015)*.

Detection of Apoptotic Retinal Cells (DARC)

Annexin V is a Ca^{2+}-dependent phospholipid-binding protein that has high affinity for phosphotidylserines localized on the outer leaflet of cell membranes. Annexin V bound to phosphotidylserine has been utilized as a probe for the identification of cells undergoing apoptosis. In the DARC technique, fluorescently-labeled Annexin V is administered via an intravitreal injection to the retina of animal TON models. This enabled imaging apoptotic annexin V- labeled RGC in live rodents via confocal scanning laser ophthalmoscopy, enabling quantifying RGC apoptosis *in vivo (Ahmad 2017)*.

1.3 Neurotrophins in Traumatic Optic Neuropathy

1.3.1 Neurotrophins and Neurotrophin Receptors

Neurotrophins

The neurotrophin family consists of nerve growth factor (NGF), brain-derived neurotrophic factor (BDNF), neurotrophin-3 (NT-3) and neurotrophin-4 (NT-4) *(Huang and Reichardt 2001, Houlton et al. 2019)*. Neurotrophins (NTs) are major regulators of neural survival and regeneration. They play key roles in the development, function, and plasticity of neural cells, they regulate normal daily function, while at the same time exert protection and recovery effects *(Houlton et al. 2019, Huang and Reichardt 2001)*.

Neurotrophins are produced in their precursor form, pro-neurotrophins, which are later cleaved either intracellularly by enzymes (by furin or pro-convertases), or extracellularly (by metalloproteases and plasmin) in order to become mature neurotrophins. Mature neurotrophins bind with high selectivity to their specific Trk (tropomyosin-related kinase) receptors so as to exert their neurotrophic effects. Mature neurotrophins also bind to the $p75^{NTR}$ receptor albeit with lower affinity. Pro-neurotrophins exert pro-apoptotic effects through binding to the $p75^{NTR}$/sortilin receptor complex *(Houlton et al. 2019)*.

Neurotrophins in damaged nerves are thought to be essential for survival and regeneration of injured neurons *(Huang and Reichardt 2001, Korsching 1993, Levi-Montalcini et al. 1996)*. During development, in regions being invaded by sensory axons en route to their final targets, NTs are expressed in order to provide trophic support to neurons that have not reached their targets yet. Moreover, neurotrophins are synthesized by neurons, where they can either provide support for neural axons in their vicinity alone or they can travel through intracellular transport and support more distant neurons *(Anthony Altar et al. 1997, Brady et al. 1999, Fariñas et al. 1998, Huang et al. 1999, Huang and Reichardt 2001)*.

Neurotrophin Receptors

Every neurotrophin binds specifically to a Trk receptor with high affinity. All NTs bind to the $p75^{NTR}$ receptor with lower affinity. Namely, NGF binds specifically to TrkA receptor, BDNF and NT-4 bind specifically to TrkB receptor. NT-3 binds with high affinity to the TrkC receptor and with lower affinity the other Trk receptors *(Huang and Reichardt 2001, Bothwell 1995)*.

Neurotrophins binding to Trk receptors, cause them to form dimers, leading to their phosphorylation and activation of tyrosine kinases on their cytoplasmatic domains. This promotes the docking of adaptor proteins that activate various intracellular signaling pathways *(Houlton et al. 2019)*. The site where Trk receptors interact with neurotrophins lies at the most proximal immunoglobulin (Ig) domain of each receptor *(Huang and Reichardt 2001, Ultsch et al. 1999, Urfer et al. 1998, Wlesmann et al. 1999)*. Trk-induced activation of PLC-γ1 and its second messengers IP3 and DAG leads to elevated intracellular Ca^{2+}. Subsequent Ca^{2+}-triggered PKC-mediated signaling can enhance neuronal and synaptic plasticity *(Chao 2003, Yoshii and Constantine-Paton 2010, Houlton et al. 2019)*. Activated Trk receptors can also activate Ras small GTPase and its downstream signaling pathways including the MAPK-ERK signaling pathway. Activated ERK phosphorylates a number of factors,

including CREB, which regulate genes associated with neurite growth and neural differentiation *(Houlton et al. 2019, Kaplan and Miller 2000)*. Trk receptors also activate the PI3K/AKT signaling pathway that promotes NFkB-mediated neuronal survival, and regulates cell proliferation, survival and growth under normal or pathological conditions *(Houlton et al. 2019, Cantley 2002, Reichardt 2006)*.

$P75^{NTR}$ can enhance Trk function upon mature neurotrophin binding. In the absence of Trk, $p75^{NTR}$ forms a complex with sortilin, a co-receptor for pro-neurotrophin binding, promoting apoptotic signaling *(Houlton et al. 2019, Nykjaer et al. 2004, Reichardt 2006, Teng et al. 2005)*. Following pro-neurotrophin binding to a $p75^{NTR}$/sortilin complex, activated Ras triggers the JNK pathway, which results in apoptotic cell death via the activation of pro-apoptotic genes *(Harrington, Kim, and Yoon 2002, Reichardt 2006, Houlton et al. 2019)*. $P75^{NTR}$ has also been shown to interact with Lingo-1 and Nogo-66 (NgR1) receptors, forming a signaling complex that activates RhoA small GTPase, inhibiting oligodendrocyte myelination and differentiation as well as cellular growth in CNS *(Houlton et al. 2019, Tang et al. 2014)*. The $p75^{NTR}$/NgR1/Lingo1 receptor complex has the ability to interact with mature neurotrophins as well as with pro-neurotrophins, exerting contrasting effects on neurite growth: Binding to mature neurotrophins NGF and BDNF prevents RhoA activation and promotes neurite growth. Binding to pro-NGF and pro-BDNF, induces growth cone collapse in neural cell cultures, inhibiting further neurite extension *(Houlton et al. 2019, Yamashita, Tucker, and Barde 1999, Lehmann et al. 1999, Deinhardt et al. 2011, Sun et al. 2012)*.

1.3.2 NTs and NTRs Expression in the CNS and ON

Neurotrophins are differentially distributed throughout the Central Nervous System (CNS) and the Peripheral Nervous System (PNS). In the CNS, NGF mRNA is present at high levels in the hippocampus, cerebral cortex, thalamus and hypothalamus, at medium levels in the striatum and brainstem, while lower levels were found in the cerebellum and the spinal cord. In adult mouse brain, mRNAs of BDNF and NT-3 present the highest concentration in the area of hippocampus, reaching 50 times more compared to NGF mRNA *(Hofer et al. 1990, Pediaditakis 2015)*. In the PNS, high levels of NGF mRNA were measured in the sciatic nerve and in sympathetic and sensory ganglia. Lower NGF mRNA levels were measured in the trigeminal ganglion. NGF mRNA was also detected in non-neuronal tissues including the liver, skin, adrenal gland and heart *(Goedert et al. 1986)*. NGF and its receptors are expressed in various cell types, such as neurons, glia (including Schwann cells and oligodendrocytes), immune cells (including microglia and macrophages) and also in smooth muscle cells, epithelial cells and fibroblasts *(Lee, Everitt, and Thomas 2004)*.

Under normal conditions, NGF is produced primarily during development and declines in adulthood whereas in pathological conditions NGF production is reactivated, acting as a protective mechanism *(Lee, Everitt, and Thomas 2004)*. In retinal tissue, neurotrophins are either transported to RGC somata from the superior colliculus via retrograde transport through the ON. Alternatively, neurotrophins are locally produced by retinal neurons and glia, which is the case for NGF. Mature and pro-NGF are mainly expressed by RGCs and glial cells (Müller cells, microglia) in adult rodent retina *(Von Bartheld 1998, Garcia, Hollborn, and Bringmann 2017)*. Moreover, studies have proposed that stratified RGCs regulate the size of their population in chick retina via NGF secretion, which kills incoming migrating RGCs by interacting with $p75^{NTR}$ on their cell membrane *(Frade, Rodriguez-*

Tebar, and Barde 1996, González-Hoyuela, Barbas, and Rodríguez-Tébar 2001). NT-3 has the highest expression in immature CNS, compared to other neurotrophins such as BDNF, the expression of which is very low. On the other hand, in mature CNS, BDNF is expressed in higher levels than NT-3 *(Maisonpierre et al. 1990)*. Both BDNF and NT-3 are expressed during development and differentiation in the mouse retina, presenting different expression patterns which overlap in some areas such as the retinal pigment epithelium *(Bennett, Zeiler, and Jones 1999)*. In addition to BDNF and NT-3, protein and mRNA of NT-4 and NT-5 have been detected in the neonatal rat retina and in target sites such as the superficial layers of superior colliculus *(Spalding, Rush, and Harvey 2004)*. NGF expression during development follows region-dependent patterns *(Maisonpierre et al. 1990)*.

Studies about TrkA protein and mRNA distribution conducted in the rat and human CNS showed TrkA expression in basal forebrain cholinergic neurons *(Steininger et al. 1993, Sobreviela et al. 1994)*, and the presence of $TrkA^{+}p75^{NTR+}$ neurons in the striatum *(Allen et al. 1989, Dawbarn, Allen, and Semenenko 1988b)*. TrkB and TrkC are more widely distributed *(Chao and Bothwell 2002)*. In the case of PNS, TrkA expression is limited in sympathetic and sensory neurons. TrkB and TrkC receptors are not essential for correct sympathetic or sensory development *in vivo.* On the other hand, TrkA receptors are of detrimental value for the survival of sympathetic and sensory neurons during late embryogenesis and early postnatal development *(Pediaditakis 2015, Fagan et al. 1996)*. TrkA, TrkB and $p75^{NTR}$ expression in the developing rat retina (post-natal days 0 to 10) follows the temporal pattern of differentiation and the initiation of programmed cell death throughout retinal layers indicating involvement of neurotrophins in these processes *(Ugolini.G.1995)*. TrkC expression in normal rat retina is weak *(Cui.Q.2002)*. Based on co-localization studies of choline acetyltransferase (ChAT) and $p75^{NTR}$ *(Dawbarn, Allen, and Semenenko 1988a, Kordower et al. 1988, Pediaditakis 2015)* along with immunohistochemical and *in situ* analysis of $p75^{NTR}$ distribution in the rat and primate brain *(Allen et al. 1989, Dawbarn, Allen, and Semenenko 1988b, Kordower et al. 1988, Riopelle, Richardson, and Verge 1987, Pediaditakis 2015)*, $p75^{NTR}$ is limited in basal forebrain cholinergic neurons. However, $p75^{NTR}$ is expressed in the nervous system during development and after injury *(Pediaditakis 2015, Chao 2003)* while research has been conducted in order to determine its role as a regulator of survival and apoptosis in neurons and glia cells *(Dechant and Barde 2002, Pediaditakis 2015)*.

In the optic nerve, glial cells can produce neurotrophins either for other glial cells or in order to support RGC axons. Neurotrophins can also be delivered to glial cells via anterograde transport from the retina or retrograde transport from RGC targets in the brain. Glial cells in the ON express NGF, NT-3 and NT-4 mRNAs *(Elkabes 1995, Ceccatelli et al. 1991, Condorelli et al. 1995)* and possibly BDNF mRNAs *(Elkabes 1995)*. Moreover, glial cells in the ON also express TrkA *(Elkabes 1995),* full length TrkB and TrkC as well as their truncated forms that lack the intracellular tyrosine kinase domain *(Elkabes 1995, Ceccatelli et al. 1991, Condorelli et al. 1995, Jelsma et al. 1993, Barres et al. 1994, Robinson and Miller 1996, Von Bartheld 1998)*. Indeed, in the optic nerve the amount of truncated TrkB is significantly more compared to full-length TrkB *(Jelsma et al. 1993)*. Furthermore, evidence show reduction of TrkB and TrkC expression during development in the same area *(Elkabes 1995)*.

1.3.3 NTs and NTRs Expression Alterations after ONT

Degeneration of RGCs after ONI results from processes where numerous growth factors are involved, including NGF *(Lewin and Carter 2014, Mesentier-louro et al. 2017)*. NGF has been shown to affect the survival and growth of retinal neural cells in all stages of life (development, adult life, aging) *(Mesentier-louro et al. 2017, Frade, Rodriguez-Tebar, and Barde 1996, Cui 2006, Jansen et al. 2007, Lebrun-Julien et al. 2009)*. TrkA activation via NGF promotes neural survival *(Cui 2006, Mesentier-louro et al. 2017, Reichardt 2006)* whereas $p75^{NTR}$ activation triggers signaling pathways associated with cell death during early retinal development *(Frade, Rodriguez-Tebar, and Barde 1996, Jansen et al. 2007, Mesentier-louro et al. 2017, Harada et al. 2006)* and adulthood *(Lebrun-Julien et al. 2009, Lebrun-Julien et al. 2010, Mesentier-louro et al. 2017)*. Pro-NGF is known to interact with $p75^{NTR}$, thus elevated pro-NGF in combination with unbalanced levels of TrkA and $p75^{NTR}$ are believed to be part of a pathological cycle that induces neuronal degeneration *(Mesentier-louro et al. 2017)*.

Mesentier-Louro et al. studied the effects of ONC on NGF expression and signaling in adult rat retina in a time-depended manner. A significant increase of pro-NGF and mature NGF was detected 7 and 14 days after crush, along with an immediate increase of $p75^{NTR}$ that started on day 1 and peaked 14 days after crush. No significant changes were observed for TrkA expression 7 days after crush, whereas a slight decrease was observed 14 days post-ONC in comparison with healthy control rats *(Mesentier-louro et al. 2017)*. This decrease in TrkA expression was not reported, under the same conditions, in a following study published from the same research group, suggesting that literature reports for TrkA expression are unclear *(Mesentier-Louro et al. 2019)*. Concerning the expression of TrkB, no significant alterations were observed 7 days after ONC *(Chen and Weber 2004, Zhang et al. 2012)*, however a significant 40% decrease was reported 14 days post-ONC in rats *(Zhang et al. 2012)*. Regarding TrkC, no reports for its expression after ONC were found in the literature. Furthermore, BDNF expression has been shown to increase transiently in rat GCL after ONC. Specifically, 24 hours post lesion BDNF expression was significantly elevated, along with the number of $BDNF^{+}$ cells in the GCL which was doubled (10%) in comparison with the control group (5-6%). 48 hours after ONC, the fraction of $BDNF^{+}$ cells in the GCL peaked at 28%. At this time, more $BDNF^{+}$ cells were in the central than peripheral retina. After 48 hours, the fraction of $BDNF^{+}$ cells in GCL started to decline reaching 23% at 72 hours (5-6% in control group), 12% by the end of the first week (7% in control group), finally reaching a basal level of 3.4% two weeks post-ONC, similar to the control group (3.3%) *(Gao et al. 1997)*.

1.3.4 Neurotrophins As Optic Nerve Injury Treatments

Since growth factors can regulate neural growth and survival, their exogenous administration has been proposed as a way to promote CNS regeneration *(Connor and Dragunow 1998, Sofroniew, Howe, and Mobley 2001, Houlton et al. 2019)*. Feng et al. found that axon loss after ONC was delayed by 7 days in BDNF-overexpressing mice compared to wild type mice *(Feng et al. 2017)*. Large-soma RGC survival was also delayed by 1 week in BDNF-overexpressing mice after ONC *(Feng et al. 2017)*. Under normal conditions, neurotrophic factors (NTFs) are transferred to the RGC body via axon-mediated transport *(Raff et al. 1993)*. After ONI, damaged axons are unable to conduct this process, leaving RGCs susceptible to apoptotic signals and subsequent death *(Almasieh et al. 2012,*

Calkins 2012, Laughter et al. 2018). Significant research has focused on developing neuroprotection strategies by direct NTF delivery to RGCs *(Laughter et al. 2018, Flachsbarth et al. 2014, Agudo et al. 2009, Parrilla-Reverter et al. 2009, Sobrado-Calvo, Vidal-Sanz, and Villegas-Pérez 2007)*.

Despite the important effects of neurotrophins (NTs) on the regeneration, survival, development and plasticity of neural cells, their therapeutic applications suffer from major limitations that makes less than ideal for clinical use *(Gravanis, Pediaditakis, and Charalampopoulos 2017)*. Specifically, NTs cannot pass through the blood brain barrier (BBB), have poor serum pharmacokinetics and bioavailability.

Microneurotrophins (MNTs) constitute a novel class of chemical compounds synthesized as 17-carbon derivatives of Dehydroepiandrosterone (DHEA), an endogenous BBB-permeable neurosteroid with the ability to bind and activate all Trk and $p75^{NTR}$ neurotrophin receptors and protect neurons against apoptosis *(Gravanis, Pediaditakis, and Charalampopoulos 2017, Glajch et al. 2016)*. BNN27 is a small C17-spiroepoxy BBB-permeable MNT that can specifically bind and activate the TrkA receptor promoting neuronal survival whereas it cannot interact with TrkB, TrkC or any steroid hormone receptors. Additionally, BNN27 enhanced NGF binding to TrkA receptors while differentially inducing the fast return of internalized TrkA receptors into neuronal cell membranes. Furthermore, BNN27 has the ability to synergize with low levels of NGF resulting in the promotion of axonal outgrowth and rescue of NGF-dependent and TrkA positive sympathetic and sensory neurons from apoptosis, *in vitro*, ex vivo and *in vivo* in NGF-null mice. Interestingly, BNN27 completely lacks the hyperalgesic effects of NGF *(Gravanis, Pediaditakis, and Charalampopoulos 2017, Pediaditakis et al. 2016)* and has minimal toxicity in mice and rats. Last but not least, BNN27 interacts with the $p75^{NTR}$ receptor, in specific amino-residues of its extracellular domain, inducing the recruitment of $p75^{NTR}$ receptor to its effector proteins RIP2 and TRAF6 and the simultaneous release of Rho GDI in primary neuronal cells *(Gravanis, Pediaditakis, and Charalampopoulos 2017, Pediaditakis et al. 2016)*. What is more, literature also reports that BNN27 synergized with low levels of NGF in promoting axonal outgrowth, resulting in increased maximum neurite length both in PC12 cells and dorsal root ganglia (DRG) sensory neurons *(Pediaditakis et al. 2016)*.

1.4 Drug Treatments for Traumatic Optic Neuropathy

Traumatic Optic Neuropathy (TON) is the result of an acute direct or indirect optic nerve injury (ONI). To this day, due to the inability of the optic nerve to regenerate, there is no available treatment that can prevent the devastating effects of ONI, namely vision impairment or loss. Similarly, if ONI induces RGC loss, there is no way to restore the patient's sight by replacing lost RGCs or induce efficient RGC axonal elongation. Available treatments rely on corticosteroid administration and surgical decompression and have very limited effects *(Chaon and Lee 2015)*. Furthermore, systemic administration of steroids suffers from low efficiency compound delivery to the ON and side effects including hypertension, insomnia and hyperglycemia *(Pula and MacDonald 2012, Lee et al. 2018).*

Frequently-used techniques for local drug delivery to the eyes are eye drops and intravitreal injections. Due to the short retention time of the injected compounds into the eye, multiple injections of highly-concentrated drugs are necessary. This can be potentially dangerous for the patient: large local drug concentrations can lead to toxic effects. Frequent injections can also induce severe complications including endophalmitis, retinal detachment, cataract or glaucoma *(Lee et al. 2018, Honda et al. 2011)*.

1.4.1 Drug Delivery via Drops or Injection

Drug Delivery via Drops

Several studies delivered compounds in TON models using drops. These studies differed on the compound used, compound concentration, drop composition administrated, see *Table 1*. Most studies used drops where the drug concentration ranged from 2.5 µg/ml to 540 µg/ml. Several studies administered much higher compound concentrations, ranging from 6.3 mg/ml to 156 mg/ml.

Most studies delivered drops to the eye. Kitamura et al. administered TUDCA (49.9 mg/ml), Citicoline (48.8 mg/ml) or NT-4 (0.01 µg/ml) via eye drops in a rat model of ONC. Compounds were diluted in PBS. Rats were treated twice per day for 2 weeks by compounds alone or in combinations *(Kitamura et al. 2019)*.

A rat model of diabetic retinopathy was used to delineate the effects of the microneurotrophin BNN27 in three concentrations (6.3 mg/ml; 31.2 mg/ml; 156.2 mg/ml). BNN27 was diluted in 80 µl DMSO per drop and was administered once per day for 1 week *(Ibán-Arias et al. 2019).* Two recent studies used eye drops of rh-NGF in the same concentrations (140 µg/ml, 580 µg/ml) after ONI in rats. One study administered 10 µl rh-NGF in PBS per drop immediately after ONC and then twice per day for 1 or 2 weeks *(Mesentier-Louro et al. 2019)*. The second study treated rats after partial ONT (pONT) twice per day for 3 weeks. This study does not report the volume and composition of drops *(Guo et al. 2020)*. Grinblat et al. administered ST226, an amnion-cell derived cellular cytokine solution, in 20 µl drops intranasally once per day for 5 to 10 days in mice after ONC *(Grinblat et al. 2018)*.

A single study delivered drops directly on the ON rather than the eye. Specifically, 4 µl drops of amiloride (22.5 µg/ml), amlodipine (2.5 µg/ml) or NBQX (335 µg/ml) diluted in PBS were administered directly on rat ON 30 min before ONC. This drop treatment was intended to supplement to the main treatment, which administrated larger amounts of the aforementioned compounds via intravitreal injection *(Ribas et al. 2016)*.

All abovementioned treatments that delivered drugs via drops reported neuroprotective results including increased RGC and axon survival as well as increased axon regeneration *(Ribas et al. 2016, Grinblat et al. 2018, Guo et al. 2020, Mesentier-Louro et al. 2019, Kitamura et al. 2019)*. In some cases, there was evidence of visual function preservation, reduced demyelination *(Grinblat et al. 2018)* or reduced glial activation *(Guo et al. 2020)*. Interestingly, one study that administrated a high dose of BNN27 resulted in neuroprotection and restoration of the diabetic damage caused on RGCs and amacrine cells in a rat model of diabetic retinopathy *(Ibán-Arias et al. 2019)*.

***Table 1-1:** Detailed description of studies performed drug delivery via eye drops*

		Model		Compound			Drop		
#	**Pub.**	**Animal**	**Injury**	**Name**	**Mass [µg]**	**Conc. [µg/ml]**	**Vol. [µl]**	**Admin. Freq.**	**Result**
1	Ribas et al. 2016	Rat	ONC	Amiloride	0.09	22.5	4	30 min before crush	Increased RGC survival & axon regeneration
				Amlodipine	0.01	2.5			
				NBQX	1.34	335			
2	Grinblat et al. 2018	Mouse	ONC	ST226	-	-	20	Daily for 5-10 days	Increased RGC survival
3	Kitamura et al. 2019	Rat	ONC	TUDCA	-	4.99E+04	-	Twice daily for 14 days	Increased RGC survival & axon regeneration
				Citicoline	-	4.88E+04			
				NT-4	-	0.01			
4	Arias et al. 2019	Rat	DR	BNN27	505.36	6.30E+03	80	Daily for 7 days	Neuroprotection & restoration of diabetic damage on RGCs
					2500.24	3.12E+04			
					12501.24	1.56E+05			
5	Mesentier-Louro et al. 2019	Rat	ONC	rhNGF	1.8	180	10	1 at 0h; Twice daily for 14 days	Increased RGC survival & axon regeneration
					5.4	540			
6		Rat	pONT	rhNGF	-	180	-		

	Guo et al. 2020				-	540-	-	Twice daily for 3 weeks	Increased RGC & survival; Reduced glial activation

Drug Delivery via Intravitreal Injection

Another popular approach for the delivery of therapeutic compounds for TON is intravitreal injection [*Table 1-2*].

Sánchez-Migallón et al. treated mice with BDNF and Z-DEV_fmk (caspase 3 inhibitor) in order to investigate RGC survival and caspase 3 activation after ONT. Compounds were administered immediately after injury via intravitreal injection, which contained either 2.5 μg BDNF in PBS or 0.125 μg Z-DEV_fmk in DMSO/Saline *(Sánchez-Migallón et al. 2015)*. Wang et al. studied the neuroprotective effect of NgR1(310)-FC, a NogoReceptor1 blocking decoy, in rats following ONC and in a microbead glaucoma model. Following ONC, a single injection of 5 μg NgR1(310)-FC in PBS was administered intravitreally (day 0). In the case of glaucoma model, injections where administered at day 0 and 7 *(Wang et al. 2015)*. In another study, a mix of calcium inhibitors, Amiloride (1.37 μg), Amlodipine (0.2 μg) and NBQX (200 μg), were used in ONC rat model. Compounds were diluted in PBS and were injected intravitreally 2 h and 30 min before ONC *(Ribas et al. 2016)*. Another study delineated the effects of AQEE-30, a VGF peptide, after ONC in mice. 367.5 μg AQEE-30 diluted in PBS were administered via intravitreal injection immediately after ONC as well as at days 2 and 5 *(Takeuchi et al. 2018)*. Last year, Mesentier-Louro et al. investigated the neuroprotective effects of human recombinant NGF after ON injury. Injections of rh-NGF (1-1.5 μg) diluted in PBS, were administered in the vitreous humor of rats 0 and 3 after ONC *(Mesentier-Louro et al. 2019).*

Based on the amount of the administered compound, previous studies can be classified into two groups. The first group includes studies that administered 0.1μg to 2.5μg of compound *(Sánchez-Migallón et al. 2015, Wang et al. 2015, Ribas et al. 2016, Mesentier-Louro et al. 2019)*. The second group includes studies that administered 200 μg and 367.5 μg *(Ribas et al. 2016, Takeuchi et al. 2018).*

Interestingly all the above treatments report that the delivered compounds resulted in neuroprotective action, including suppressed loss of RGCs, increased axon regeneration and attenuated axon degeneration *(Sánchez-Migallón et al. 2015, Wang et al. 2015, Ribas et al. 2016, Mesentier-Louro et al. 2019)*. These results were presented either individually or in combination depending on the treatment and the animal model.

Table 1-2: Detailed description of studies performed drug delivery via injection

		Model		Compound			Injection		
#	**Pub.**	**Animal**	**Injury**	**Name**	**Mass [µg]**	**Conc. [µg/ml]**	**Vol. [µl]**	**Admin. Freq.**	**Result**
1	Sánchez-Migallón et al. 2015	Mouse	ONT	BDNF	2.5	-	-	Day 0	Delayed RGC loss by 24 h
				Casp3 Inhib.	1.25E-01	-	-		
2	Wang et al. 2015	Rat	ONC	NgR1(310)-FC	5	1000	5	Day 0, 7	Increased regenerating RGCs
3	Ribas et al. 2016	Rat	ONC	Amiloride	1.37	342.5	4	2 h 30 min before ONC	Increased RGC survival & axon regeneration
				Amlodipine	0.2	50			
				NBQX	200	5E+04			
4	Takeuchi et al. 2018	Mouse	ONC	AQEE-30	367.5	1.84E+05	2	Day 0, 2 & 5	Slightly suppressed RGC loss
5	Mesentier-Louro et al. 2019	Rat	ONC	Rh-NGF	1-1.5	-	-	Day 0, 3	Increased RGC survival, axon growth and regeneration

Drug Delivery Characterization

Characterization of the drug delivery aims to delineate if an administered compound has successfully reached the desired target as well as the amount of the compound that was delivered. Most of the studies mentioned in this thesis infer the successful delivery of administered compounds based on the results yielded by the provided treatment. Only a small number of studies utilize biochemical assays to provide evidence on compound delivery in the desired tissue. The pharmacokinetics of human NgR1(310)-Fc delivery in rat retina after intravitreal delivery (5 µg), was quantified via sandwich ELISA in rat retina vitreal liquid samples *(Wang et al. 2015)*. In another study, the presence of rh-NGF in the retina and the ON after eye drop administration in rats, was also quantified via ELISA *(Guo et al. 2020)*.

1.4.2 Drug Delivery via Biomaterials

Although conventional eye drops may be an easy way for drug delivery to the eye, the intraocular bioavailability of the drug is rather poor due to various factors such as nasolachrymal drainage, drug dilution with tears, conjunctival absorption. Therefore, only small amounts of the drug (1-3%) eventually penetrate cornea and manage to reach the intraocular tissue *(Urtti 2006, Kulkarni et al. 2016)*. In order to overcome these limitations [*Table 1-3*], Kulkarni et al. developed controlled-release ocular films, using a natural hydrogel that can release the drug in a controlled way over a period of 8 hours *(Kulkarni et al. 2016)*. Ocular iontophoresis is another safe and non-invasive technique used in driving drugs (medicine ions, charged macromolecules) into the anterior and posterior segments of the eye via penetrating the ocular tissues with poor permeability, such as the corneal epidermis *(Zhang et al. 2016, Souza et al. 2015)*. Zhang et al. used ocular iontophoresis on rabbits and achieved 5 to 7 times greater drug concentration in the eyeball, compared to delivery via eye drops *(Zhang et al. 2016).* In the same model animal, Garcia-Caballero et al. achieved sustained drug delivery for up to six months, using a single intravitreal injection of GDNF-loaded PLGA/VitE micorspheres *(García-Caballero et al. 2017)*. Jung et al. achieved targeted drug delivery to the posterior region of the suprachoroidal space (SCS) of the eye using drug particles injected along a hyaluronic acid (HA) hydrogel formulation in the SCS *(Jung, Desit, and Prausnitz 2018)*.

In order to investigate whether an artificial graft can provide the environment for the regeneration of RGC axons in adult rats, Negishi et al. transplanted grafts (consisting of Schwann cells (SCs), extracellular matrix (ECM) and trophic factors) in rats after ONT and evaluated their effects on RGC axons regeneration. Five types of grafts were used, namely ECM, ECM and SCs, ECM with SCs and NGF (100 ng/ml) / BDNF (100 ng/ml) / NT-4 (100 ng/ml), ECM with SCs and both BDNF (100 ng/ml) and NT-4 (100 ng/ml) combined with intravitreal injection of BDNF (100 ng/ml) in PBS. Grafts were connected to the retinal segment of the ON throughout the sclera and dura mater using nylon sutures *(Negishi 2001)*. Using the same animal model, a similar study used PGA-Chitosan conduits coated with recombinant L1-FC to bridge the stumps of transected ON rats *(Xu et al. 2004)*. Fang et al. developed a PGA-Chitosan conduit seeded with CNTF-transfected SCs in order to promote axonal growth in rats after ONT. In this study, the one end of graft was sutured directly on the sclera and dura mater while the other end was secured to connective tissue on the skull *(Fang et al. 2010)*. Another study evaluated PLGA microspheres and nanospheres containing GDNF-Vitamin E (5 μg) and epidermal growth factor receptor inhibitors (2.17 μg) as possible treatments for ONC and glaucoma in rats. Both micro- and nanospheres were injected in the vitreous humor of the animal's eye *(Checa-Casalengua et al. 2011, Robinson et al. 2011)*.

Giannaccini et al. performed intravitreal delivery of magnetic nanoparticles (MNPs) conjugated with NGF (0.5 μg) or BDNF (2 μg) in a zebrafish model of RGC loss induced by oxidative stress *(Giannaccini et al. 2018)*. Using a mouse model of non-arteritic ischemic optic neuropathy, Lee et al. developed liposomes to improve the treatment efficiency for optic nerve diseases by delivering therapeutic materials directly to the ON. Liposomes were filled with dexamethasone and were delivered via intravitreal injection *(Lee et al. 2018)*. Laughter et al. engineered an injectable sulfonated reverse thermal gel (STRG) as a delivery system for CNTF (0.5-2.5 μg). SRTG-CNTF was intravitreally injected in mice after ONC in order to determine the neuroprotective capacity this delivery system *(Laughter et al. 2018)*. In the same context, a new drug delivery system (DDS) constituted from Tafluprost, Benzyl Benzoate and Glycol 400 developed to enable controlled release

of Tafluprost was tested in a rat ONT model. The DDS was administered in rats via intravitreal injection and delivered Tafluprost in three doses of 0.8 µg, 4 µg and 20 µg *(Sato et al. 2020)*.

The aforementioned studies can be classified in two groups based on the means of biomaterial administration. The first group consists of studies where "large" biomaterial grafts were administered via surgical methods *(Negishi 2001, Fang et al. 2010, Xu et al. 2004)*. The second group consists of studies where "small" biomaterial constructs were administered via intravitreal injections *(Laughter et al. 2018, Sato et al. 2020, Lee et al. 2018, Checa-Casalengua et al. 2011, Robinson et al. 2011, Giannaccini et al. 2018)*.

Several biomaterial-based means for drug delivery claim successfully results by demonstrating neuroprotective capabilities including promotion of RGC survival, increased axon regeneration and growth *(Negishi 2001, Fang et al. 2010, Robinson et al. 2011, Checa-Casalengua et al. 2011, Lee et al. 2018, Laughter et al. 2018, Sato et al. 2020, Xu et al. 2004, Giannaccini et al. 2018)* as well as increased axon remyelination *(Xu et al. 2004)*. Of note, is the study of Giannaccini et al. which presented total prevention of RGCs loss *(Giannaccini et al. 2018)*.

***Table 1-3:* Detailed description of studies performed drug delivery via biomaterials**

		Model		Compound		Biomaterial		
#	**Pub.**	**Animal**	**Injury**	**Name**	**Mass [µg]**	**Description**	**Admin.**	**Result**
1	Negishi et al. 2001	Rat	ONT	NGF	-	ECM+SCs+ NGF (100 ng/ml)	Sewed on ON tissue	Increased RGC survival & axon regeneration
				BDNF	-	ECM+SCs+ BDNF (100 ng/ml)		
				NT-4	-	ECM+SCs+ NT-4 (100 ng/ml)		
				BDNF + NT-4	-	ECM+SCs+ BDNF+NT-4 +IVT BDNF (100 ng/ml)		
2	Xu et al. 2004	Rat	ONT	Recomb. L1-FC	-	PGA-Chitosan conduit coated with L1-FC	Sewed on ON tissue	Promoted axonal regeneration

3	Robinson et al. 2011	Rat	ONC	EGFR TKI	2.17	PLGA micro-/ nanospheres containing EGFR TKI	IVT injection	Increased axon regeneration
4	Checa et al. 2011	Rat	Glauc.	GDNF	5	PLGA microspheres containing GDNF/VitE	IVT injection	Increased RGC survival
5	Fang et al. 2010	Rat	ONT	CNTF	-	Grafts seeded with SCs overexpressing CNTF	Sewed on ON tissue	Increased axon regeneration and growth
6	Giannaccini et al. 2018	Zebra-fish	Oxidative Stress	NGF	0.5	MNPs conjugated to NGF/BDNF	IVT injection	Totally prevented RGC loss
				BDNF	2			
7	Laughter et al. 2018	Mouse	ONC	CNTF	0.5-2.5	SRTG	IVT injection	Increased RGC survival, axon regeneration & growth
8	Lee et al. 2018	Mouse	NAION	Dexamethasone	3.30E-02	Liposomes	IVT injection	Reduced RGC loss
9	Sato et al. 2020	Rat	ONT	Tafluprost	0.8	DDS: Tafluprost, Benzyl Benzoate, Glycol 400	IVT injection	Improved RGC survival
					4			
					20			

1.5 Thesis Scope

This study focuses on quantifying the effects of microneurotrophin BNN27 on key cell phenotypes after optic nerve crush (ONC) injury in mice. BNN27 was delivered by two strategies: i) BNN27 administration via eye drops and ii) BNN27 delivery using biomaterials. Biomaterial delivery of BNN27 was pursued via two approaches. In the first approach, BNN27 is entrapped in a gel formed by self-assembled peptides inside a porous collagen-GAG scaffold, which afterwards was placed directly around a crushed ON injury site. In the second approach, BNN27 is covalently conjugated on porous collagen-GAG scaffolds.

This study initially characterizes a mouse ONC model by IHC-based quantification of RGC survival, astroglial and microglial activation as well as the expression of NT receptors ($p75^{NTR}$, TrkA, TrkB, TrkC). Then, two animal studies focus on evaluating the effects of BNN27 delivery via drops for 7 and 14 days after injury on RGC survival and astroglial activation. Then, an animal study focuses on evaluating the effects of BNN27 delivery via biomaterials (entrapped in a peptide gel formed inside a porous graft) on RGC survival and astroglial activation

The results of this study can shed light in the field of tissue regeneration after optic nerve injury producing valuable information about BNN27 effects on retinal tissue regeneration in mice. Lastly, this study generates new knowledge on the field of research treatments for TON, providing data on novel drug delivery strategies, facilitating the development of innovative TON treatments.

Chapter 2: Materials & Methods

Optic Nerve Crush Model

A standard mouse ONC model *(Tehrani et al. 2018)* was adapted in order to place a biomaterial graft around the injury site or administrate eye drops as treatment [*Figure 2-1*]. Specifically, 2-month old C57BL/6 mice (20-30 g) underwent systemic anesthesia with intraperitoneal injection of ketamine/xylazine. The conjunctiva of one eye was incised and the optic nerve (ON) was exposed at its exit from the eye globe by gently putting aside the orbital muscles. The ON was crushed approximately 1 mm away from the eyeball using a pair of Dumont #5 fine forceps for 6 sec. Great care was taken in order not to damage the ophthalmic artery. In the control animal group, the ON was left to heal spontaneously. In experiments where BNN27 was delivered via eye drops, one day after the surgery, the mice were administered with 5 μl BNN27 (10mM or 50mM diluted in DMSO) or only DMSO in each eye daily for 6 days or every second day for 13 days.

In grafted animal groups, a 4x3x1.5 mm porous collagen-GAG scaffold (CGS; 0.5% mass fraction, 95 μm mean pore diameter) was placed around the crushed nerve site. Prior to grafting, grafts were soaked by adding 6 μl of i) Fmoc-FF peptide solution (20 μg/ml Fmoc-FF (Bachem, B-2150) diluted in ethanol and mixed with H_2O (see below)) or ii) BNN27 solution (50 μM BNN27 in DMSO) or iii) BNN27 Fmoc-FF peptide solution (50 μM BNN27 and 20 μg/ml Fmoc-FF). Fmoc-FF and BNN27, were initially diluted in ethanol, and then were mixed with H_2O (see below). For better dilution, the Fmoc-FF solutions were placed in water bath for 9 min at 50°C and then was sonicated briefly (5 sec).

The dissolved Fmoc-FF peptide was polymerized (self-assembly) by mixing with water according to a 1:3 ratio of ethanol:water volume. Once water was added to the dissolved peptide solution, it was briefly pipetted 3 times and then was fully polymerized over 30-40 sec. In order to get the peptide to polymerize inside the scaffold, a 6 μl drop of the resulting peptide solution (in 1:3 ethanol:water) was immediately pipetted on a glass coverslip and the scaffold was quickly placed on top of the drop. Due to capillary action, the scaffold absorbed the peptide solution and was left for up to 7 min until placed to the injury.

In all experiments, mice were sacrificed 7 or 14 days post-injury (dpi). Subsequently tissues (eye and optic nerve) were harvested for further processing.

All surgical procedures (infliction of ONC, scaffold / graft placement etc.), preparation of BNN27 solutions for eye drop treatment and administration of eye drops to mice were performed by Constantina Georgelou (IMBB Neural Tissue Engineering Lab). Animal sacrifices and tissue harvesting (eye enucleation) were performed in cooperation with Constantina Georgelou. Preparation of Fmoc-FF peptide solutions and preparation of grafts soaked in Fmoc-FF peptide solutions were conducted in cooperation with Chrysanthi-Pinelopi Apostolidou (Mitraki research group, Department of Materials Science, University of Crete).

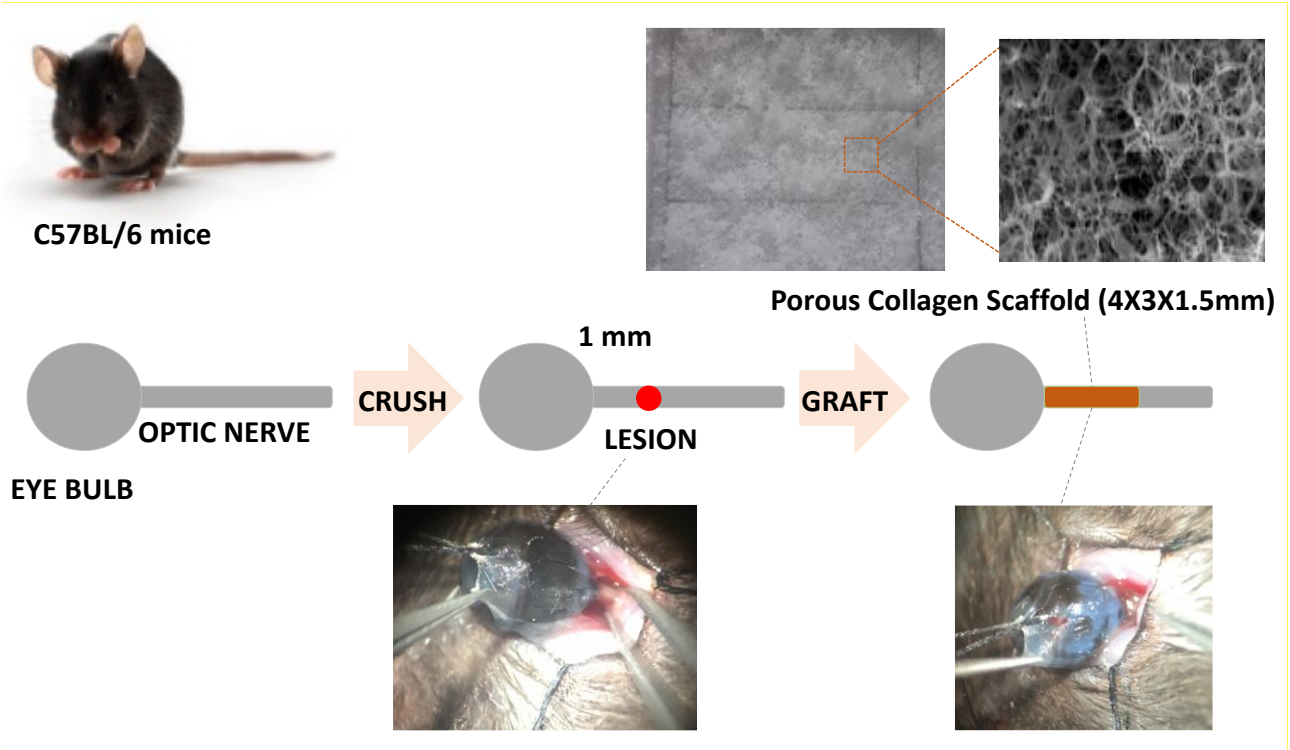

Figure 2-1: Optic nerve injury mouse model. Schematic representation of the procedure followed for the creation of the ONC mouse model. (A) A 4 mm x 3 mm x 1.5 mm porous collagen-GAG scaffold graft. (B, C, D) Main steps during surgical procedure: (B) intact optic nerve | C) crushed optic nerve 1 mm from eye bulb | D) porous collagen-GAG scaffold placed around the ON crush site. (E) Picture from the moment the crush is inflicted and (F) from the moment the porous collagen-GAG scaffold is placed at the injury site. Images and schematic prepared by Constantina Georgelou.

Tissue Preparation

After mice were sacrificed via cervical dislocation, the eyes were carefully removed by using a pair of forceps. Specifically, the two parts of the forceps were maintained apart, in a small distance, in order to avoid damaging the ON but also to be able to push against the eyeball and efficiently pull out the eye and ON from the eye socket. Removed eyes were placed in 4% paraformaldehyde (PFA) solution at 4°C for 24 h, briefly washed once with PBS (phosphate buffered saline) at RT and placed in 30% sucrose solution in PB (phosphate buffer) at 4°C for 24 h. ON was carefully separated from the retina using scissors and then cut in sections using a cryostat microtome. Retinas were immersed in handmade moulds filled with OCT (Optimal Cutting Temperature) compound (VWR Chemicals, 361603E) and then snap frozen at -70°C using isopentane and dry ice. Cryo-sectioning was performed at -25°C, ON was placed directly on frozen OCT and sectioned longitudinally in 10 μm thick sections. Frozen retina samples were sectioned vertically in 20 μm thick sections at the same temperature. For both ON and retina, serial sections were placed on 5 slides (6 sections per sample). After cryo-sectioning all samples were stored at -80°C.

Immunohistochemistry (IHC)

All manipulations were performed at room temperature (RT) unless stated otherwise.

Sections were immersed in cold acetone at -20°C for 5 min, air-dried in laminar flow for 10 min, washed twice in PBS for 10 min, washed in 0.1% PBST (Triton X-100, 0.1% in PBS) for 15 min, washed in 0.3% PBST (Triton X-100, 0.3% in PBS) for 30 min, blocked in 0.1% PBST (0.1% Triton X-100 in PBS) supplemented with 10% horse / goat serum and 0,1% Bovine Serum Albumin (BSA) for 1 h. Then, they were incubated in the desired primary antibodies (Neun Millipore MAB377, 1:200; GFAP Millipore AB5541, 1:2000; IBA1 Wako 019-19741, 1:1000; TrkA Millipore 06-574, 1:100; TrkB Abcam AB33655, 1:200; TrkC Cell Signaling C44HS, 1:200; $p75^{NTR}$ Promega G3231, 1:100) diluted in the aforementioned blocking solution at 4°C overnight, washed 3 times in 0.1% PBST for 15 min, incubated in fluorophore-conjugated secondary antibodies diluted 1:1000 in 0.1% PBST for 1h, washed in 0.1% PBST for 15 min, washed in PBS for 15 min, counterstained with Hoechst 1:10000 in PBS for 15 min, washed in PBS for 15 min, washed in PB for 15 min, mounted and stored at 4°C. Stained sections were imaged in a Leica TCS SP8 inverted confocal microscope.

A number of sections were also stained with NeuroTrace™ Fluorescent Nissl Stain (Molecular Probes, N-21470), following a different procedure. Sections were placed in 0.1 M PBS for 40 min, washed in 0.1% PBST for 10 min, washed twice in PBS for 5 min, incubated in NeuroTrace™ diluted 1:100 in PBS for 20 min, washed in 0.1% PBST for 10 min, washed twice in PBS for 5 min, washed in PBS for 2 h at 4°C, counterstained with Hoechst 1:10000 in PBS for 15 min, washed in PBS for 15 min, washed in PB for 15 min, mounted and stored at 4°C.

Imaging and Histological Evaluation

Fluorescently labeled samples were imaged in a Leica TCS SP8 inverted confocal microscope using a x40 oil-immersion objective lens (Leica Microsystems, Wetzlar, Germany) in cooperation with Constantina Georgelou. 2-8 z-stack images (1-4 z-stacks from 1-2 sections) per sample were taken from the area of peripheral retina close to each side of the iris [*Figure 2-2*] under identical parameters using a z-step of 1.5 μm.

Image analysis was performed using ImageJ (Fiji) software. Initially each z-stack was converted to a maximum intensity z-projection image including the appropriate channels for each analysis. RGC survival in mouse retina was evaluated by manually counting $Hoechst^{+}NeuN^{+}$ cells in the GCL and calculating the number of $Hoechst^{+}NeuN^{+}$ cells per mm^2 and per 100 μm GCL length. The level of astrogliosis in mouse retina was evaluated by manually counting $GFAP^{+}$ astroglial and Müller cell processes throughout the retinal section and calculating the number of processes per 100 μm. To assess TrkA, TrkB, TrkC and $p75^{NTR}$ levels in the GCL of mouse retina, fluorescent intensity quantification was performed. To quantify fluorescence intensity the area of the GCL was outlined in each z-stack image in the desired channel, background signal (noise) was estimated (by calculating the mean grey value in a region where no signal is expected), image threshold was set in close range above the noise signal, and the percentage (%) of positive pixels in the designated area was determined.

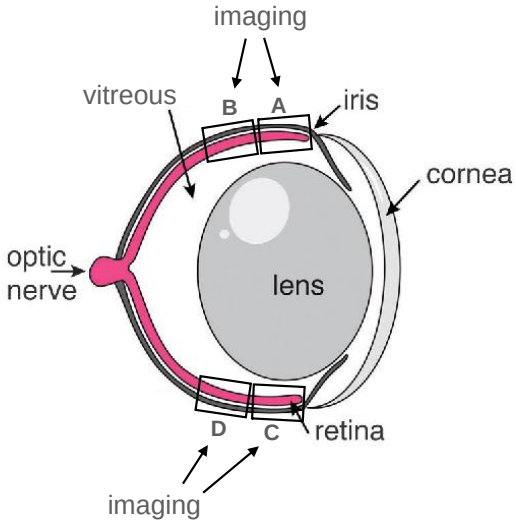

Figure 2-2: Conceptual illustration of mouse retina. (A), (B), (C), (D) represent the positions in the peripheral mouse retina from where images were acquired for histological evaluation. (Modified from (Milde et al. 2013))

Quantification of RGC Survival

RGC survival was calculated by manually measuring the Hoechst$^+$NeuN$^+$ cells in mouse retinal sections. Images acquired by a Leica TCS SP8 inverted confocal microscope *(.lif extension file)* were accessed using ImageJ software *(Import options: view stack with Hyperstack; color mode set to 'composite')*. After opening the desired series, the channels 1 (Hoechst) and 3 (NeuN) were selected via *'Channels Tool'*, the stack was converted to RGB. Then a max-intensity z-projection was created, the GCL was outlined using *'polygon selections'* tool and the area was calculated in square microns (µm^2) using the option *'measure'*. Next the *'segmented-line'* tool was used to measure the GCL length in µm using again the *'measure'* option. The z-projection image was duplicated and channels were split in the one copy of z-projection image generating one image for each of the three (3) channels (red, green, blue). Hoechst$^+$NeuN$^+$ cells were measured using *'cell counter'* in combination in the image of the i) green and ii) blue channels as well as iii) in the z-projection image [*Figure 2-3*]. The fraction of the Hoechst$^+$NeuN$^+$ cell number per mm^2 and per 100 µm GCL length was calculated for every z-stack and the average was found for every sample (mouse).

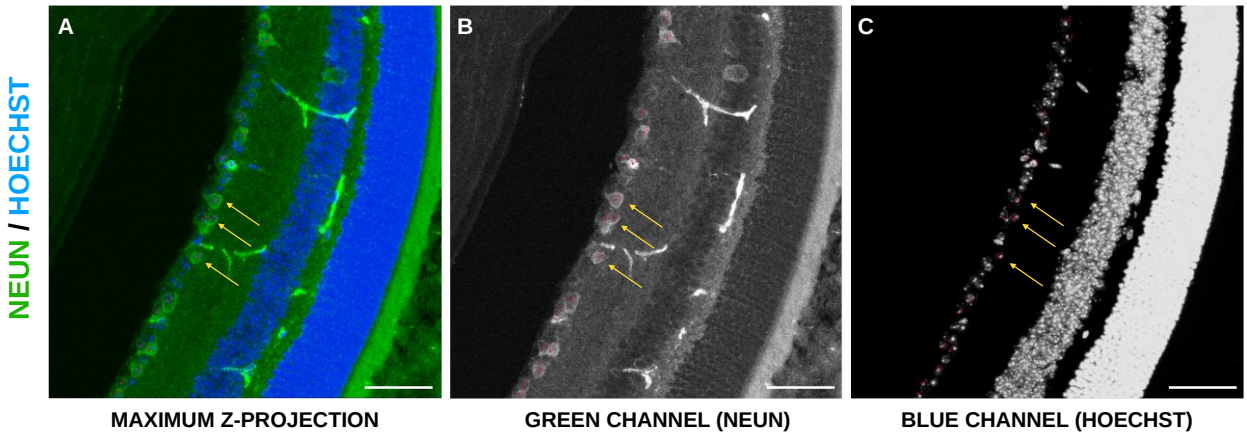

Figure 2-3: Representative quantification of RGC survival in immunostained mouse retinal sections by image analysis. (A) Maximum z-projection of acquired confocal image stack. Blue: Hoechst. Green: NeuN. (B) Represents the green and (C) represents the blue channel after the channels are split. For accurate counting of RGCs 'cell counter' (red dots) is used to count cells on all three images (A; B; C) at the same time. The arrows highlight RGCs (Hoechst$^+$NeuN$^+$ cells) in all channels to facilitate detection. Scale Bars: 50 µm

Quantification of Astroglial Activation

The activation of astroglial cells was evaluated by manually counting GFAP$^+$ astrocyte and Müller cell processes spanning retinal layers. Images acquired by a Leica TCS SP8 inverted confocal microscope *(.lif extension file)* were accessed using ImageJ software *(Import options: view stack with Hyperstack; color mode set to 'composite')*. After opening the desired series, the first (Hoechst) and second channel (GFAP) were selected using *'Channels Tool'*, the stack was converted to RGB and then a max-intensity z-projection was created. Next, channels were split, the second channel (red) was selected, a line approximately 100 µm long was drawn on the retinal section using the *'segmented line'* tool and the GFAP$^+$ processes included in that distance were manually counted [*Figure 2-4*]. The number of GFAP$^+$ processes per 100 µm was calculated following this procedure for every z-stack and the average was calculated for every sample (mouse).

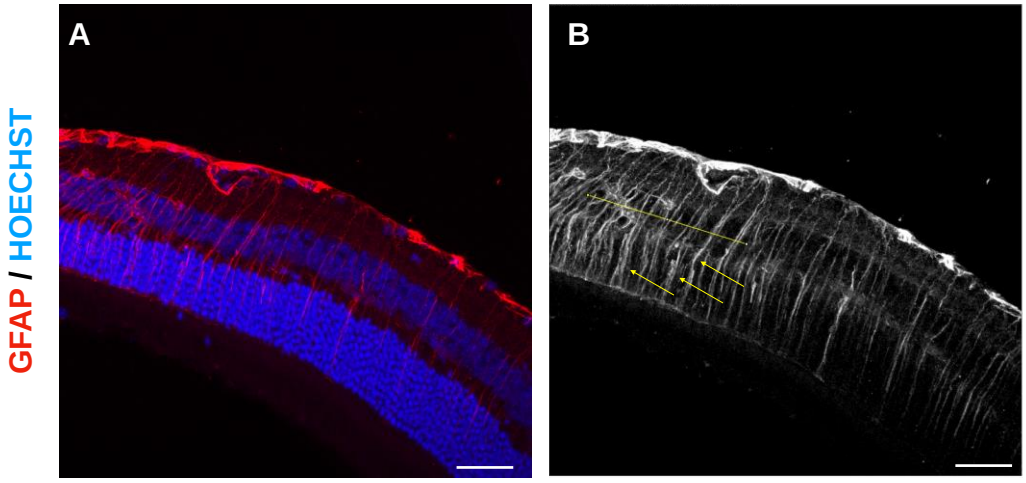

Figure 2-4: Representative quantification of GFAP expression in immunostained mouse retinal sections by image analysis. (A) Maximum z-projection of acquired confocal image stack. Blue:

Hoechst. Red: GFAP. (B) Represents the red channel after the channels are split. The yellow line represents the length (approximately 100 μm) in which cells processes are counted and the arrows highlight GFAP$^+$ cell processes to facilitate detection. Scale Bars: 50 μm.

Quantification of p75^{NTR}, TrkA, TrkB, TrkC Expression

The amount of p75^{NTR} neurotrophin receptor and tyrosine kinase receptors TrkA, TrkB and TrkC was calculated in the GCL of mouse retinal sections by performing fluorescence intensity quantification on the images acquired from the Leica TCS SP8 inverted confocal microscope [*Figure 2-5*]. The images *(.lif extension file)* were accessed using ImageJ software *(Import options: view stack with Hyperstack; color mode set to 'composite')*. After opening the desired series, the channels 1 (Hoechst) and 2 (p75^{NTR}; TrkA; TrkB; TrkC) were selected using *'Channels Tool'*, the stack was converted to RGB and then a max-intensity z-projection was created. The GCL was outlined using the *'polygon selection'* tool and the selection was added to the *'Manager'*. The z-projection was duplicated, one of the duplicates was selected and channels were split for that z-projection. Using the appropriate channel for the receptor (channel 2), background signal (noise) was estimated (by calculating the mean grey value in a region where no signal is expected, using 'straight lines' tool) and image threshold was set in close range above the noise signal. After threshold adjustment, the GCL selection previously added in 'Manager' was applied in the current image and the percentage (%) of positive pixels in the selected area (% Area) was measured. % Area was calculated for every z-stack and the average was found for every sample (mouse). Every receptor (p75^{NTR}, TrkA, TrkB, TrkC) was quantified separately from the others following this procedure.

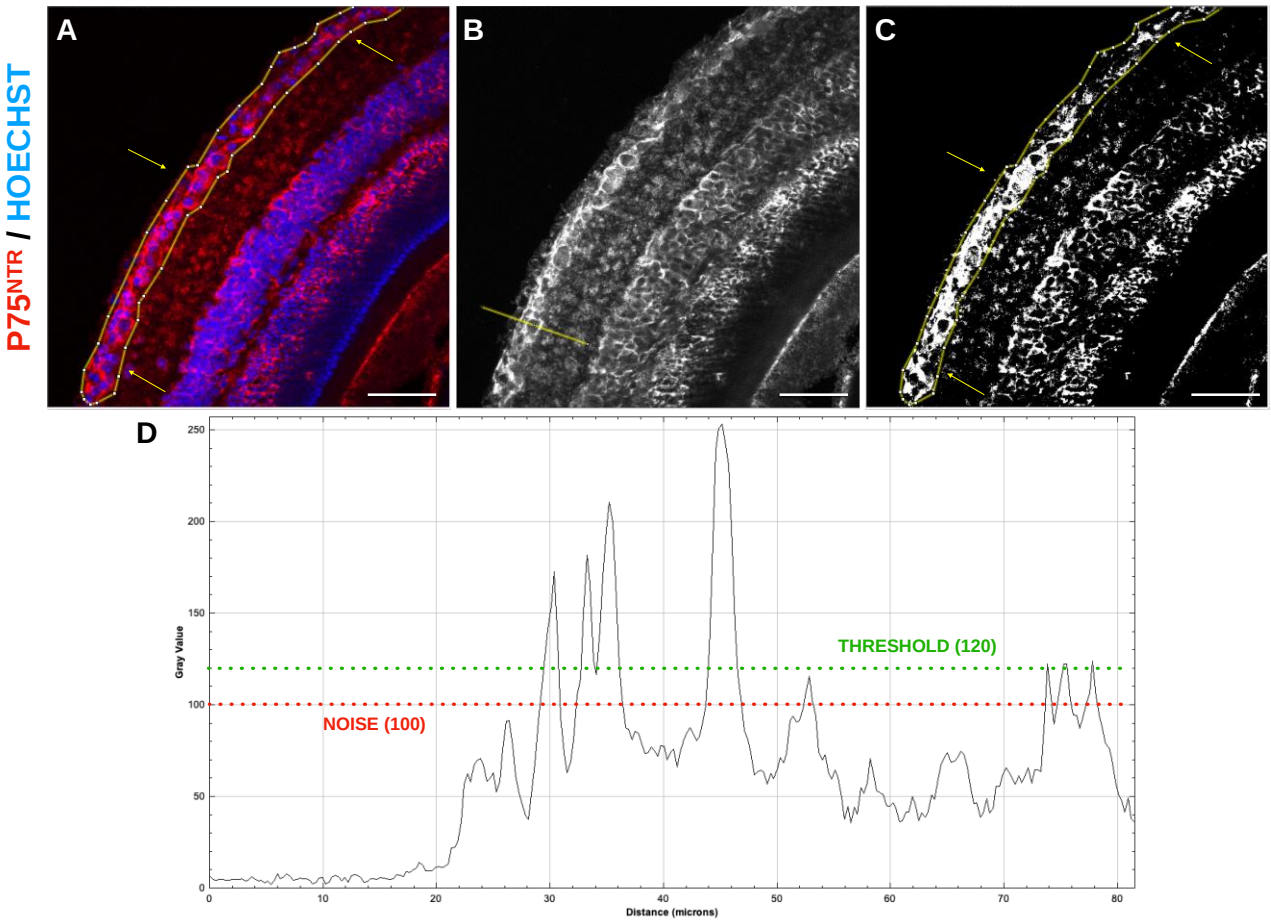

Figure 2-5: Representative image processing pipeline for the quantification of p75^{NTR} receptor expression in immunostained mouse retinal sections. (A) Maximum z-projection of the acquired confocal image stack. Blue: Hoechst. Red: P75^{NTR}. (B) Maximum z-projection of the p75^{NTR} channel after channel splitting. Yellow line represents 'straight line' tool used to estimate the background noise. (C) The corresponding p75^{NTR} channel after background noise estimation and image threshold. The yellow line outlines GCL and is manually selected for quantification purposes (A; C). Yellow arrows highlight the outlined area to facilitate detection (A; C). (D) Profile plot of the p75^{NTR} channel along the yellow line shown in (B) (y-axis: Gray value; x-axis: Distance in microns (μm) used to estimate noise signal. The same procedure is utilized for the quantification of Trk receptors. Scale Bars: 50 μm

Histology (Hematoxylin - Eosin staining)

Sections were retrieved from -80°C, washed with running water for 5 min, washed in 100% ethanol for 5 min, in 90% ethanol for 2 min, in 70% ethanol for 2 min and placed in Hematoxylin for 2-3 min. Slides were briefly washed in running water, momentarily immersed in 1% acid alcohol, briefly washed in running water and placed in Scott's tap water substitute (1 L distilled water, 29 g MgSO4, 3.5 g NaHCO3) until tissue sections turned blue. Then the slides were washed in running water for 2 min, instantly immersed 15 times in Eosin solution, briefly washed in running water, washed in 70% alcohol for 2 min, in 90% alcohol for 2 min, in 100% alcohol for 5 min, in Xylene for 5 min and finally were mounted in DPX. All manipulations were done in RT unless stated otherwise.

Stained sections were imaged using a Leica DFC310 FX optical microscope. Three (3) sections were imaged per animal tissue, three (3) images per section. Images were acquired randomly from all over the GCL length, however only images from peripheral retina where used for RGC quantification [*Figure 2-6*]. RGCs were manually counted in the GCL. RGC density was expressed as RGC number per 100 μm GCL length.

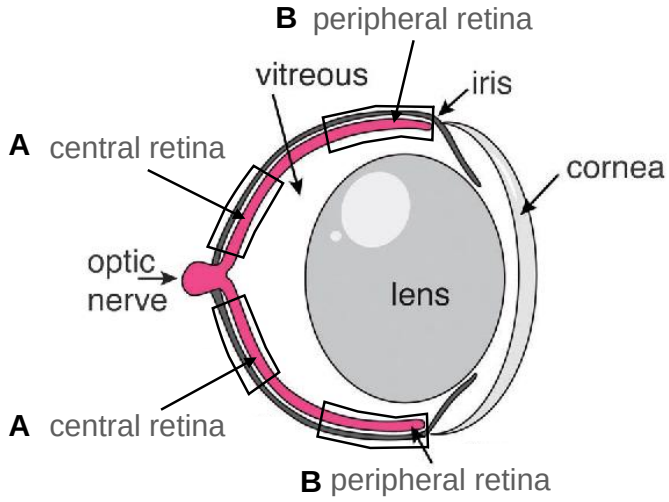

Figure 2-6: Conceptual illustration of mouse retina. Central (A) and peripheral (B) retina are highlighted to facilitate detection. (Modified from (Milde et al. 2013)).

The following three protocols were based on methods described in the Bachelor's Thesis of Marileta Tsakanika *(Tsakanika 2019)*. Experiments utilized 1x1x1.5 mm porous collagen-GAG scaffolds precisely laser cut by Fereniki Moschogiannaki (Department of Physics, University of Crete). All scaffold manipulations were performed using a pair of fine forceps, taking great care not to damage scaffolds.

Porous Collagen Scaffold Fabrication

Porous collagen-GAG scaffold sheets were fabricated as described previously *(Kourgiantaki et al. 2020, O'Brien et al.),* by lyophilizing a 5 mg/ml microfibrillar collagen I suspensions supplemented with 0.44 mg/ml Ch6Sin 50 mM acetic acid. The resulting scaffold sheets were cross-linked via dehydro-thermal treatment (105 °C, 50 mTorr, 24 h). 1x1x1.5 mm scaffold samples were cut using precision laser ablation by F. Moschogiannaki at IESL-FORTH. Cylindrical scaffold samples (3 mm diameter, 2.5 mm-thick) utilized for *in vitro* experiments were cut using a biopsy punch.

Peptide Polymer Preparation

Fmoc-FF (Fmoc-Phe-Phe-OH) (Bachem, B-2150) was dissolved in 100% ethanol at 20 μg/ml concentration. For better dilution, the solution was placed in water bath for 9 min at 50°C and submitted to a brief sonication period (5 sec) during that time. Fmoc-FF spontaneously formed a gel (referred to here as "polymerize") when the dissolved peptide was mixed with water to achieve 1:3 ratio of ethanol:water solution. Once the water was added to the dissolved peptide solution, it was briefly pipetted three (3) times. Peptide polymerization was completed within 30-40 sec. In order to

achieve peptide polymerization inside a porous-GAG scaffold, immediately after mixing water with the dissolved peptide solution, a 6 µl drop of the resulting peptide solution was placed on a glass coverslip. Then, a 1x1x1.5 µm scaffold was quickly placed on top of the drop. Due to capillary action, the scaffold absorbed the drop and was incubated for 7 min before being grafted around the ONC injury site.

Drug Release *In Vitro* Assay

In order to quantify the release rate of BNN27 when entrapped in a Fmoc-FF gel inside a porous-GAG scaffold, fluorescein (Sigma Aldrich; F6377) was used instead of BNN27 as it can be easily quantified using standard lab equipment via its fluorescence emission [*Figure 2-7*]. Fluorescein sodium was used in a concentration of 5 µM in three different conditions. In the first group, scaffolds were soaked in 5 µM fluorescein sodium salt dissolved in water. In the second group, fluorescein sodium was dissolved in the water used to polymerize the Fmoc-FF peptide as described in the above paragraph, maintaining a final concentration of 5 µM entrapped in the peptide polymerized inside the scaffold. The expected steady-state condition (after fluorescein diffuses out of the scaffold into the surrounding solution) was modeled by adding a fluorescein solution of 5 µM directly inside the well. Diffusion experiments were conducted in a 24-well-plate (Costar, 38017) by placing porous-GAG scaffolds in cell inserts (Sarstedt, 833932041) and then (t=0) placing these inserts inside wells that contained 800 µl water. [*Figure 2-7*]. The concentration of fluorescein released into the solution was estimated by quantifying the fluorescent intensity of solution samples. Fluorescence intensity measurements acquired using a Synergy™ HTX Multi-Mode Reader (Biotek) at 11 time-points after placing the scaffold into the water solution (0 h; 2 h; 4 h; 6 h; 8 h; 24 h; 30 h; 48 h; 52 h; 100 h; 124 h). During measurements, gain was set to 65, temperature was set at 37°C and optics were set to measure from the bottom.

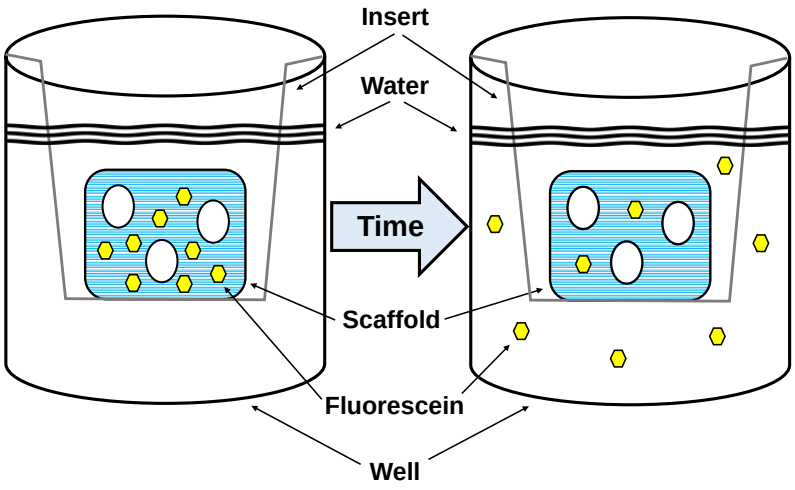

Figure 2-7: Representation of the in vitro drug release assay. A scaffold soaked in fluorescein solution was placed on a porous insert inside the well of a 24-well-plate. The fluorescence of fluorescein released into the surrounding solution was used to quantify drug release rate.

SPDP Functionalization of Porous Scaffold

In order to activate collagen-GAG scaffolds by SPDP, 1x1x1.5 mm collagen-GAG scaffolds were carefully immersed in 50 µl 500 µM SPDP in 1 mM PBS-EDTA for 1h at RT. In order to enhance the diffusion of SPDP molecules inside scaffold pores, the solution was pipetted (20 µl pipetting volume) every 15 min during the 1h incubation, taking great care not to aspirate and damage the scaffold with the tip. After 1h SPDP incubation, the solution was removed and SPDP-activated scaffolds were washed three times in 1 ml 1 mM PBS-EDTA for 10 min at RT. During the washes again the solution around the scaffold was carefully pipetted (400 µl pipetting volume) every 5 min. Then, the scaffold was placed in 1ml PBS, overnight in a rotator at 4°C. Finally, the scaffold was stored in 1 ml PBS at 4°C. The final protocol ("A1. SPDP Functionalization of a Porous Collagen Scaffold Sample") can be found in *Appendix* (page 80).

SPDP-activated Amine Group Quantification

In order to evaluate the level of activation achieved on collagen-GAG scaffolds by SPDP incubation, the amount of SPDP-activated amine groups contained in the collagen scaffolds was measured. SDPD-activated scaffolds were incubated in 100 µl 25 mM DTT (Minotech, K09-1) in PBS for 1h at RT. In order to enhance the diffusion of DTT molecules inside scaffold pores the solution was pipetted (40 µl pipetting volume) every 15 min taking great care not to draw or damage the scaffold with the tip. 100 µl supernatant was transferred in a 96-well plate and the absorbance of pyridine 2-thione was measured at 343 nm using Synergy™ HTX Multi-Mode Reader (Biotek). The quantity (moles) of activated amine groups are equal to the moles of pyridine 2-thione released by DTT, which are calculated using the following procedure:

Based on Beer-Lampert Law:

$$A = \varepsilon \cdot c \cdot l$$

the absorbance A of the released pyridine 2-thione solution depends on the molar attenuation coefficient ε (in M^{-1} cm^{-1}) of pyridine 2-thione, the concentration c of pyridine 2-thione, and the optical path length l (unit: cm) where absorbance takes place. The concentration c can be expressed as $c = n/V$ (where n is the moles of pyridine 2-thione and V is solution volume) therefore:

$$A = \varepsilon \cdot \frac{n}{V} \cdot l$$

The optical length l (in cm) in a 96-well plate can be expressed as a function of the solution volume V (in L) and the well radium r (in mm) as:

$$V = 10^{-5} \pi r^2 l$$

Combining the previous three equations, and utilizing appropriate units, pyridine 2-thione moles n can be estimated based on absorbance A measurements as:

$$n = 10^{-5} \pi \frac{A}{\varepsilon} r^2$$

Where ε is in units M^{-1} cm^{-1} and r is in units mm. In the case of pyridine 2-thione (ε = 8080 $M^{-1}cm^{-1}$) measurements in a 96-well plate (r = 3 mm), the quantity n_{P2T} of released pyridine 2-thione can be estimated as:

$$n_{P2T} = 10^{-5}\pi\frac{A}{8080}3^2 = 3.5 \cdot 10^{-8} \cdot A$$

Since the quantity n_{P2T} of released pyridine 2-thione equals the quantity n_{SPDP} of SPDP-activated-NH2 in the scaffold, the fraction of SPDP-activated-NH2 in the scaffold equals:

$$f_{activated} = \frac{n_{SPDP}}{n_{NH2,collagen}}$$

Additionally, $n_{NH2,collagen}$ equals:

$$n_{NH2,collagen} = C_{NH2,collagen} \cdot V_{scaffold}$$

Where $C_{NH2,collagen}$ is the concentration of the amine groups contained in the collagen scaffold expressed in M and $V_{scaffold}$ is the total volume of the scaffold expressed in μl.

$$C_{NH2,collagen} = C_{collagen} \cdot 282$$

Where $C_{collagen}$ is the concentration of collagen included in the scaffold and the number 282 is the number of amine groups contained in a collagen molecule.

Combining the two previous equations,

$$n_{NH2,collagen} = C_{collagen} \cdot 282 \cdot V_{scaffold}$$

For this scaffold $C_{collagen} = 1.66 \cdot 10^{-5}\ M$ and $V_{scaffold} = 1 \cdot 1 \cdot 1.5 = 1.5\ mm^3 = 1.5\ \mu l$

Therefore,

$$n_{NH2,collagen} = 1.66 \cdot 10^{-5} \cdot 282 \cdot 1.5 = 7.02 \cdot 10^{-9} = 7.02\ nmol$$

The protocol utilized ("A3. Quantification of SPDP-Activated Amine Groups in Porous Collagen Scaffold") can be found in *Appendix* (page 83-84). During the development of the aforementioned protocol β-Mercaptoethanol was also assessed as reducing agent but DTT was preferred. Moreover, NanoDropND-1000 (Thermo Scientific) was used in a trial run for pyridine 2-thione absorbance measurements but was not selected due to low measurement sensitivity.

TC447 Conjugation on a SPDP-Activated Porous Scaffold

SPDP-activated scaffolds were immersed in 50 µl TC447 solution of the desired concentration (0.5 µM; 5 µM; 50 µM) at 4°C overnight, covered with aluminium foil to protect from light due to the light-sensitive nature of TC447. TC447 conjugated scaffolds were washed three (3) times in 1ml PBS for 10 min at RT and placed in 1 ml PBS overnight in rotation at 4°C. In order to enhance the diffusion

of PBS inside scaffold pores, the solution was pipetted (400 µl pipetting volume) every 5 min during the washing periods, taking great care not to damage the scaffold with the tip. The protocol utilized ("A2. TC447 Conjugation With an SPDP-Activated Porous Collagen Scaffold") can be found in *Appendix* (page 81-82).

Porous Collagen Scaffold Imaging and TC447 Quantification

Fluorescently labeled scaffolds were imaged in a Leica TCS SP8 inverted confocal microscope using a 40x water-immersion objective lens (Leica Microsystems, Wetzlar, Germany) [*Figure 2-8*]. Each scaffold hydrated by a drop of PBS was sandwiched between two coverslips. Three z-stacks per scaffold were acquired using a z-step of 1.5 µm. The struts of the porous collagen-GAG scaffold were visualized by collagen autofluorescence which was excited using a 405 nm laser. The attached TC447 was visualized by its BODIPY group, which was excited by a 488 nm laser line.

TC447 was quantified based on the fluorescence emitted by its BODIPY group. The images *(.lif extension file)* were accessed using ImageJ software *(Import options: view stack with Hyperstack; color mode set to 'composite')*. The z-stack was converted to RGB, black z-planes were excluded and 1/3 of the z-stack was selected using 'Slice Keeper' tool (increment = 3). The stack was duplicated and channels were spit for the one copy of the duplicates. The collagen channel (blue) was selected and the threshold was adjusted by choosing *'Image > Adjust > Threshold > Auto'*. The thresholded z-plane was compared with the corresponding z-plane of the remaining copy of the original z-stack and further threshold adjustment was made if deemed necessary. After threshold adjustment, *'Median'* filter (Median Radius = 1 pixel) was applied to the z-plane by choosing *'Image > Process > Filter > Median > Radius = 1 pixel'*. The area of the collagen material (positive pixels) was selected using *'polygon selections'* tool and added to the *'Manager'*. The area was applied on the BODIPY (green) channel of the selected z-plane and the mean gray value was calculated by using the option *'Measure'*. 3 z-stacks per scaffold were acquired, 1/3 of the total number of z-planes per stack were analyzed and the average mean gray value per scaffold was calculated.

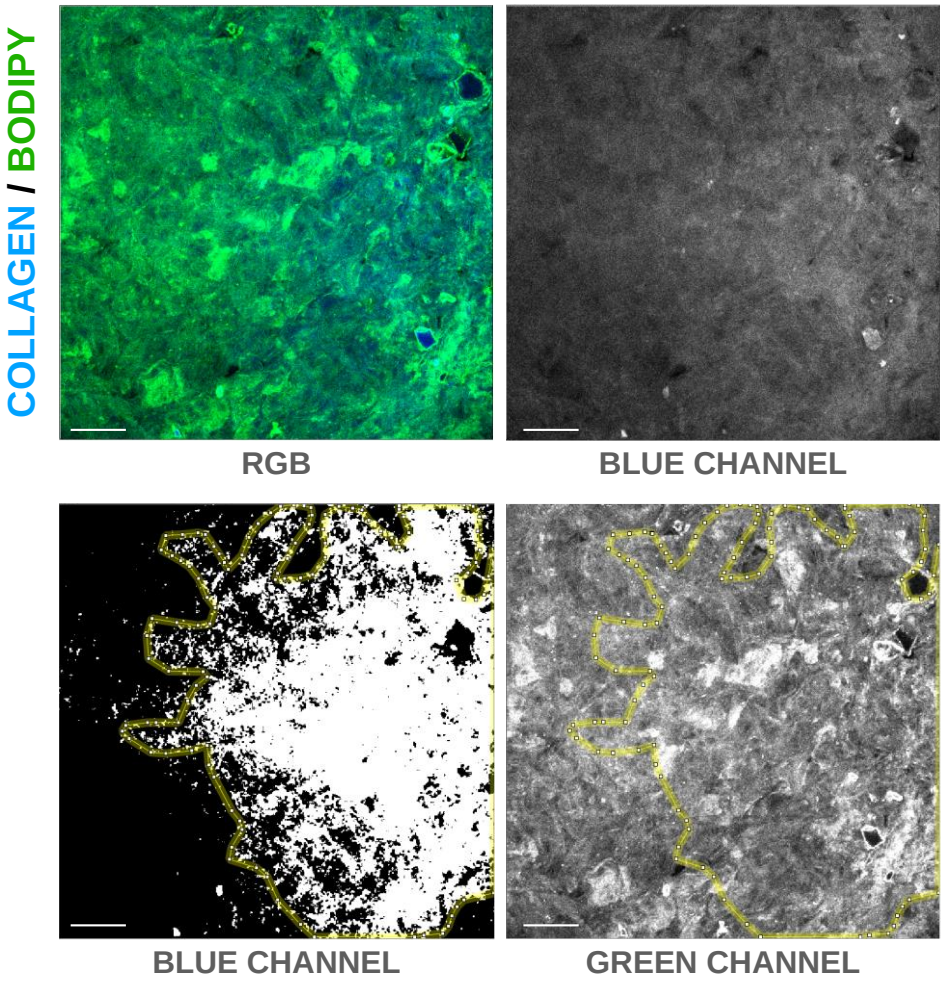

Figure 2-8: Representative image processing pipeline for the quantification of TC447 in TC447-conjugated porous collagen-GAG scaffold. A) Original RGB z-plane. B) Collagen (blue) channel of selected z-plane. C) Collagen (blue) channel of selected z-plane after threshold adjustment and 'Median' filter application. Highlighted area represents the area containing collagen material (positive pixels). D) TC447 (green) channel of selected z-plane after application of the previously selected area (highlighted area). Scale Bars: 50 μm.

Statistical Analysis

All data were analyzed using the Prism 8.0 (GraphPad Software, Inc., San Diego, CA, USA) software. Evaluation of statistical significance was performed using one-way ANOVA followed by Tukey post hoc analysis. Concerning *in vivo* experiments, a separate data pool was created for i) intact; ii) ONC 1 week; iii) ONC 2 weeks animal groups in order to increase the number of animals (n value) in each experimental group. Differences are considered statistically significant when $p < 0.05$. Data are plotted as the mean ±SEM. The number of animals used in each experimental group (n values) is shown in the legend of relevant figures.

Chapter 3: Results

3.1 Characterization of the ONC Model

In order to characterize the Optic Nerve Crush (ONC) model used it was necessary to verify that the ON crush injury was successful and reproducible during the operation as well as to delineate the effects of the ONC on the mouse. Attempting to answer these questions fourteen (14) C57BL/6 mice were selected and surgically submitted to ONC injury. Five (5) of them were sacrificed seven (7) days post-ONC, nine (9) of them were sacrificed fourteen (14) days post-ONC and two (2) were excluded due to technical problems regarding the injury. Pursuing to evaluate the degree of success of the surgical procedure aiming to inflict the ONC injury in mice, RGC survival rates in retina was the first parameter to be analyzed. In order to do so, a decision was made to evaluate the specificity of two different RGC markers, NeuN and Neurotrace, and utilize the most reliable for the RGC survival analysis.

As seen in *Figure 3-1* & *Figure 3-2* when NeuN (A) is used as a marker for RGCs, RGC survival is reduced by 50% seven (7) days and 70% fourteen (14) days post-injury. On the contrary, when Neurotrace (B) is used as an RGC marker, no significant differences are observed in the number of RGCs among intact or injured eyes during the first or second week post-ONC, indicating that Neurotrace is not a specific marker for RGCs. Under the light of these events, NeuN was considered as a reliable RGC maker and was used for the estimation of RGC survival in mouse retina. Furthermore, the fact that ONC induced 50% RGCs loss within the first and 65% within the second week post-injury, in combination with the fact that twelve (12) out of fourteen (14) mice were included in the study, clearly demonstrates that ONC is performed in an accurate and repeatable manner.

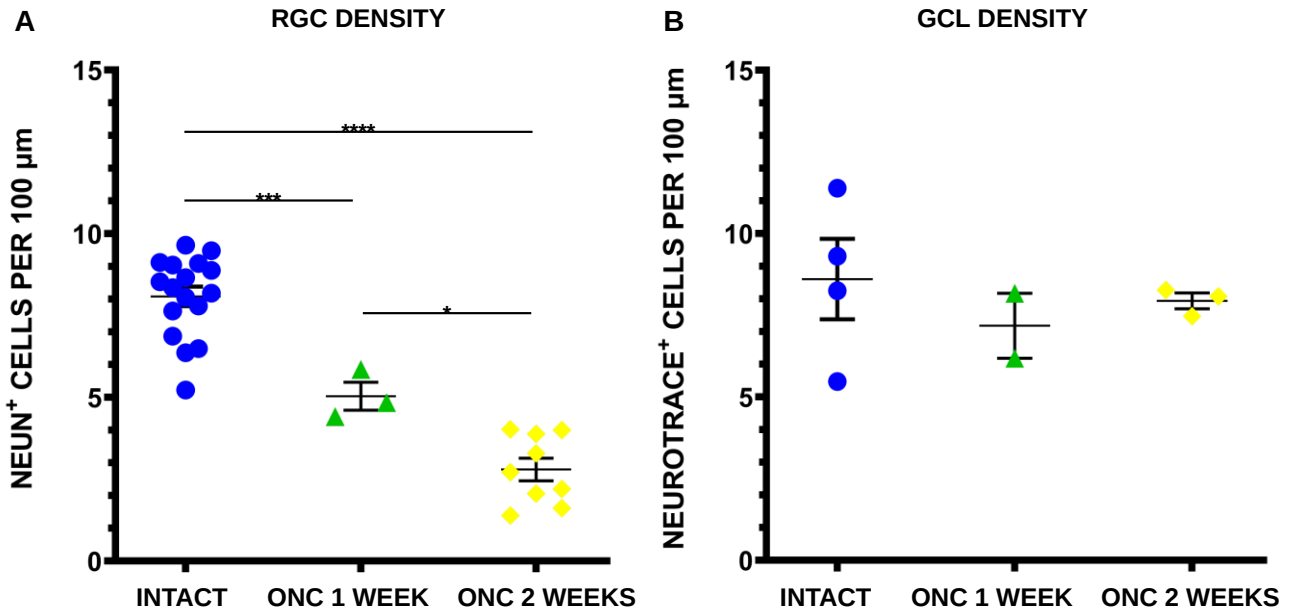

*Figure 3-1: Quantification of RGC survival in immunostained mouse retinal sections by image analysis. (A) NeuN$^+$ cells (RGCs) in per 100 µm. (B) Neurotrace$^+$ cells in per 100 µm. Data are presented as mean ± SEM; (A) "INTACT" n=17; "ONC 1 WEEK" n=3; "ONC 2 WEEKS n=9 | (B) "INTACT" n=4; "ONC 1 WEEK" n=2; "ONC 2 WEEKS n=3; *P < 0.05; ***P < 0.001; ****P < 0.0001; Tukey's post-hoc pairwise test assuming $P_{1\text{-way-Anova}} < 0.05$.*

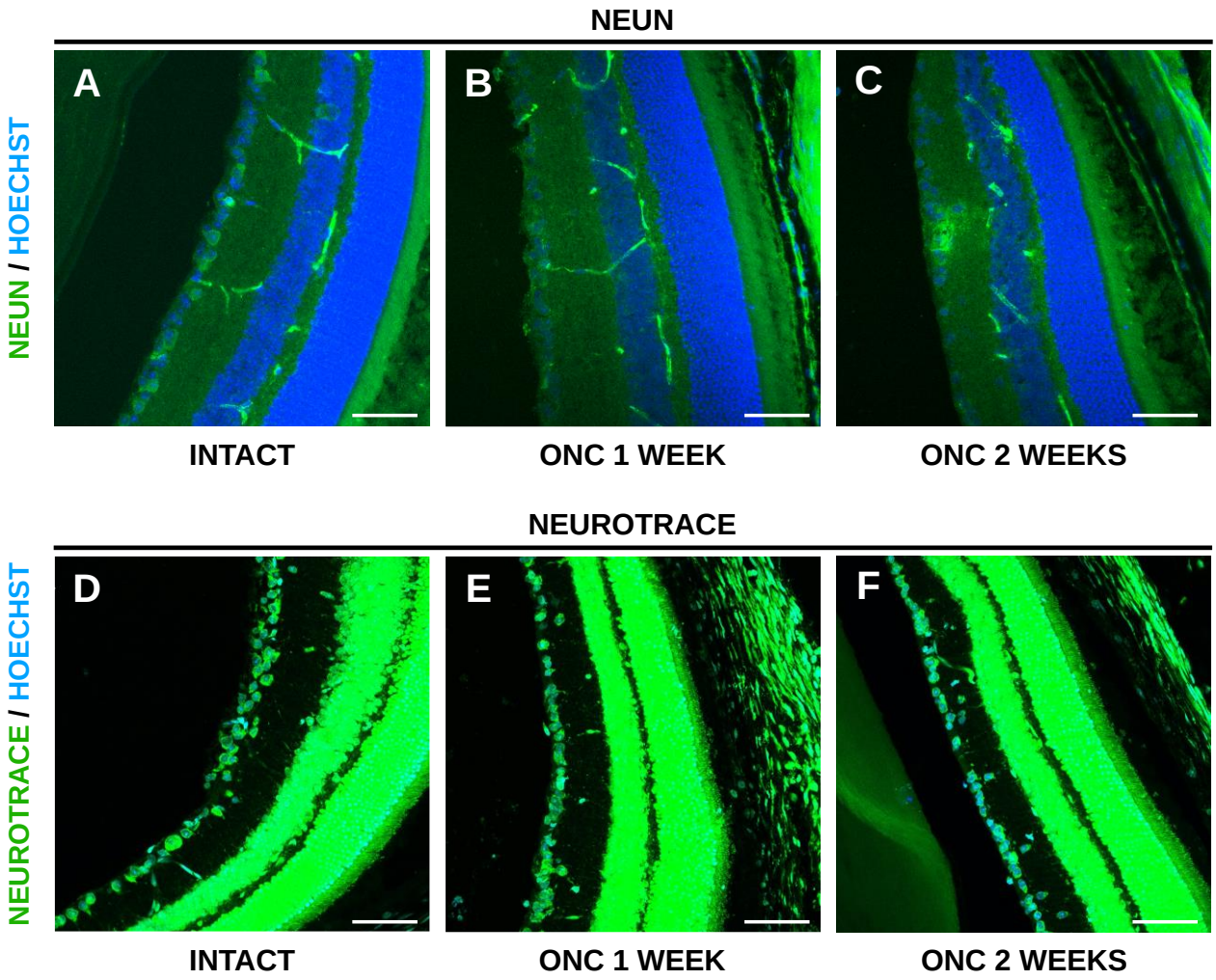

Figure 3-2: Representative confocal fluorescence images of intact (A; D) and injured eyes 7 (B; E) and 14 days (C; F) post-ONC, acquired from mouse retinal sections immunostained for NeuN. (A; B; C) Blue: Hoechst; Green: NeuN. (D; E; F) Blue: Hoechst; Green: Neurotrace. Scale bar: 50 μm.

Furthermore, in order to be more accurate and find the more appropriate metric for counting RGCs in mouse retinal sections, both the number of RGCs per GCL length (per 100 μm) as well as per area (per mm^2) were calculated [*Figure 3-3*]. No significant differences were detected among the two ways of visualization. According to bibliography, when counting RGCs from retinal sections a calculation of RGCs per length units seems more preferable *(Takeuchi et al. 2018, Mead et al. 2014)*, whereas in the case of retinal whole-mounts the RGCs number is calculated per area units *(Parrilla-Reverter et al. 2009, Kole et al. 2020, Mead et al. 2014)*. Since there were no significant differences between the two metrics, taking into consideration current bibliography it was decided to proceed with expressing the number of RGCs in the GCL per length units, and more specifically per 100 μm.

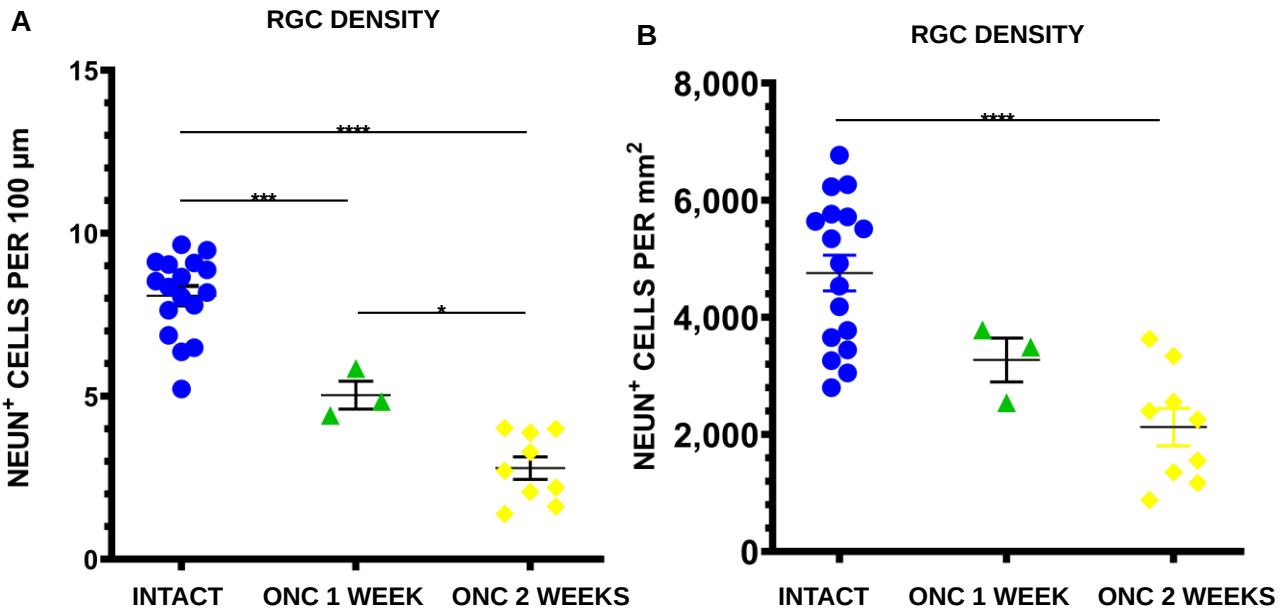

*Figure 3-3: Quantification of RGC survival in immunostained mouse retinal sections by image analysis. (A) NeuN$^+$ cells (RGCs) per 100 µm. (B) NeuN$^+$ cells (RGCs) per mm^2. Data are presented as mean ± SEM; "INTACT" n=17; "ONC 1 WEEK" n=3; "ONC 2 WEEKS n=9; *P < 0.05; ***P < 0.001; ****P < 0.0001; Tukey's post-hoc pairwise test assuming $P_{1\text{-way-Anova}} < 0.05$.*

Taking the investigation of the ONC impact one step further, the activation of astroglial cells was evaluated next. In order to assess astroglial activation in mouse retina, the number of GFAP$^+$ processes was manually counted in all retinal layers. Given that GFAP expression is upregulated in activated astrocytes and Müller cells after injury *(Chang et al. 2007)*, GFAP was used as an astroglial marker and GFAP$^+$ cell processes were calculated per 100 µm. As visualized in *Figure 3-4* the number of GFAP$^+$ processes were increased in injured eyes both one (1) and two (2) weeks after ONC by approximately eleven times compared to intact eyes. Therefore, it can be concluded that ONC does induce astroglial activation, supporting that ONC is successfully inflicted during the surgical procedure.

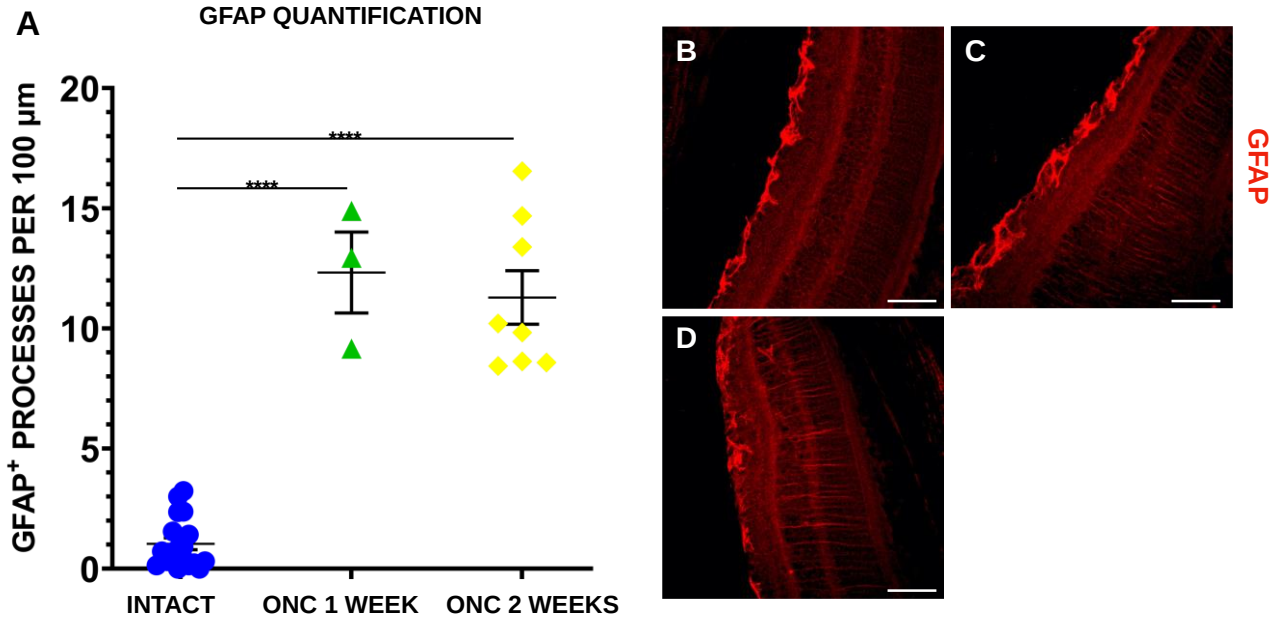

*Figure 3-4: Quantification of GFAP expression in immunostained mouse retinal sections by image analysis. (A) GFAP$^+$ (astroglial) cell processes per 100 µm. Data are presented as mean ± SEM; "INTACT" n=18; "ONC 1 WEEK" n=3; "ONC 2 WEEKS n=8; ****P < 0.0001; Tukey's post-hoc pairwise test assuming $P_{1\text{-way-Anova}} < 0.05$. (B; C; D) Representative confocal fluorescence images of intact (B) and injured eyes 7 (C) and 14 days (D) post-ONC, acquired from mouse retinal sections immunostained for GFAP; Red: GFAP. Scale bar: 50 µm.*

Microglia activation was also evaluated based on images of mouse retinal sections immunostained for IBA1 [*Figure 3-5*]. Although quantification of IBA1 was not performed, no clear effect of ONC on IBA1 staining is shown by the images.

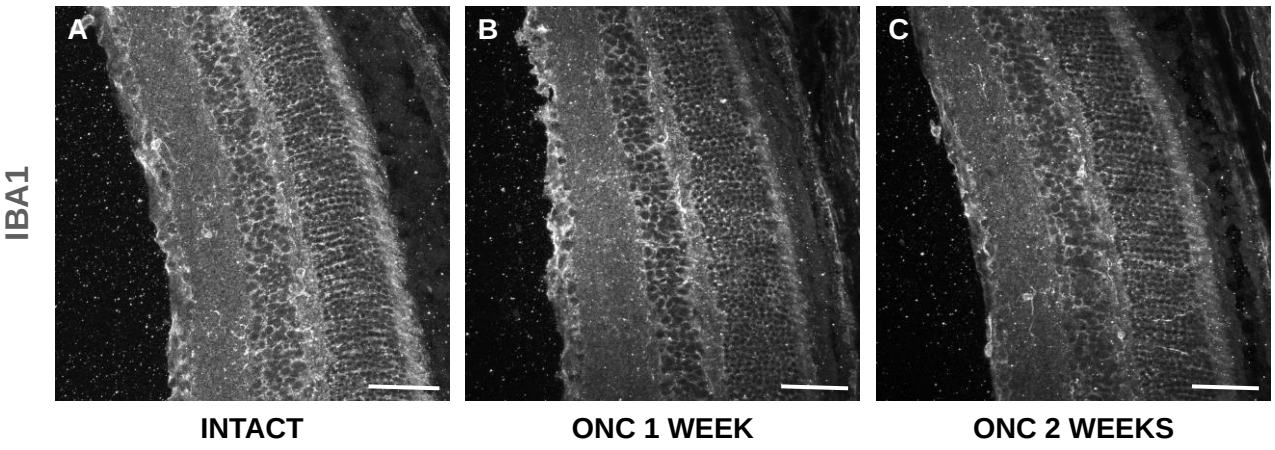

Figure 3-5: Representative confocal fluorescence images of IBA1 in intact (A) and injured eyes 7 (B) and 14 days (C) post-ONC, acquired from immunostained mouse retinal sections. Scale bars: 50 µm.

To further characterize the impact of ONC in mouse retina, the amount of neurotrophic receptor p75^{NTR} as well as the amount of tyrosine kinase receptors TrkA, TrkB, and TrkC was calculated [*Figure 3-6 & Figure 3-7*]. *Figure 3-6 & Figure 3-7* show that all receptors continue to be expressed 7 and 14 days post injury. Specifically, no statistically significant alterations are observed in the expression of p75^{NTR}, TrkA and TrkB, whereas a trend for TrkC downregulation is detected 7 (P = 0.15) and 14 days (P = 0.11) post-ONC. At this point it should be noted that the number of animals used to quantify the expression of the aforementioned receptors is small (7 days: n=2; 14 days: n=3).

Therefore, if more animals were to be analyzed, the TrkC reduction would reach statistical significance.

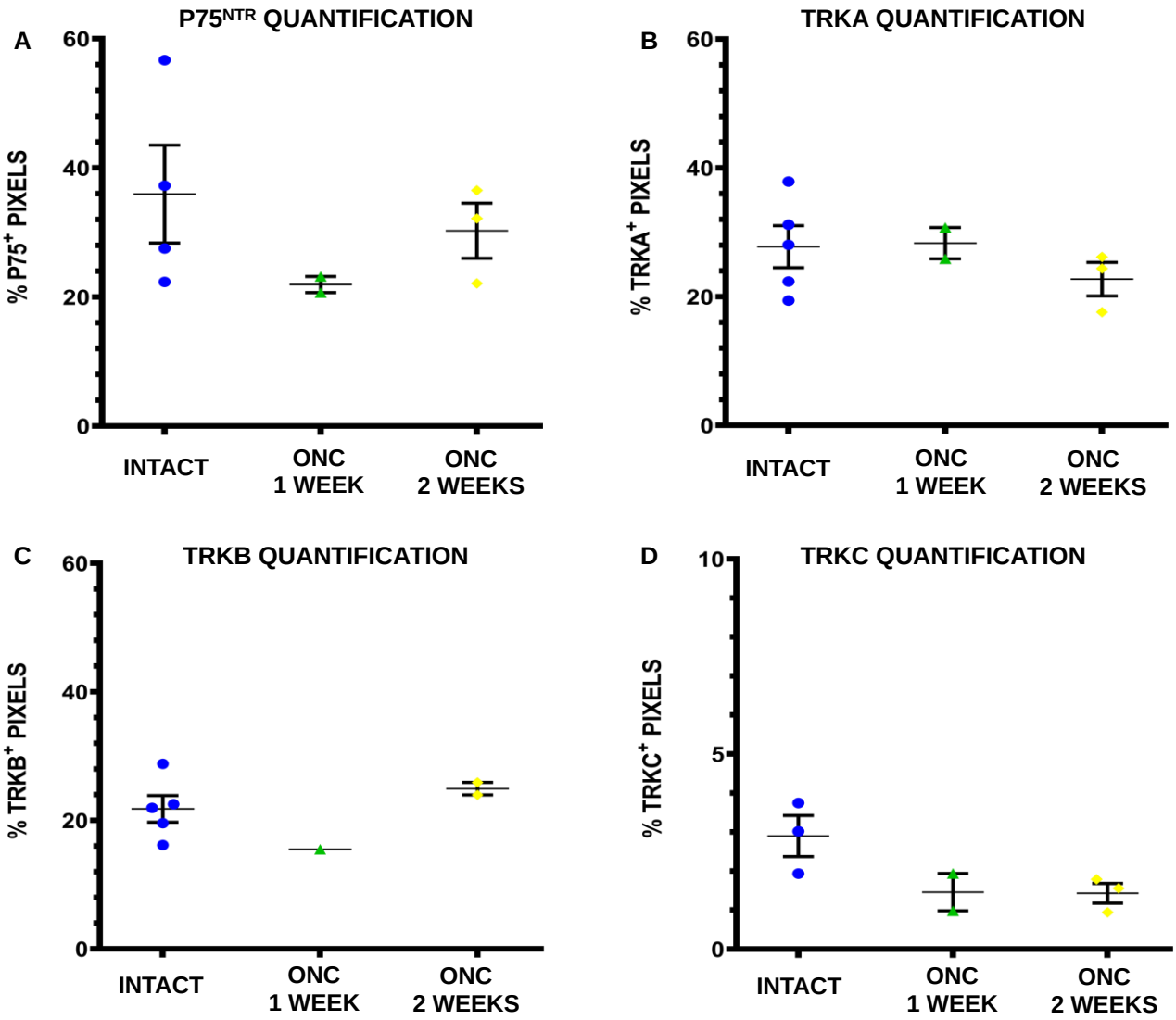

Figure 3-6: Quantification of $p75^{NTR}$ and tyrosine kinase receptors (TrkA; TrkB; TrkC) expression in immunostained mouse retinal sections by image analysis. (A; B; C; D) Percentage (%) of positive pixels for (A) $p75^{NTR}$; (B) TrkA; (C) TrkB; (D) TrkC. Data are presented as mean ± SEM; "INTACT" (A) n=4 | (B) n=5 | (C) n=5 | (D) n=3; "ONC 1 WEEK" (A) n=2 | (B) n=2 | (C) n=1 | (D) n=2; "ONC 2 WEEKS (A) n=3 | (B) n=3 | (C) n=2 | (D) n=3; Tukey's post-hoc pairwise test assuming $P_{1\text{-}way\text{-}Anova} < 0.05$.

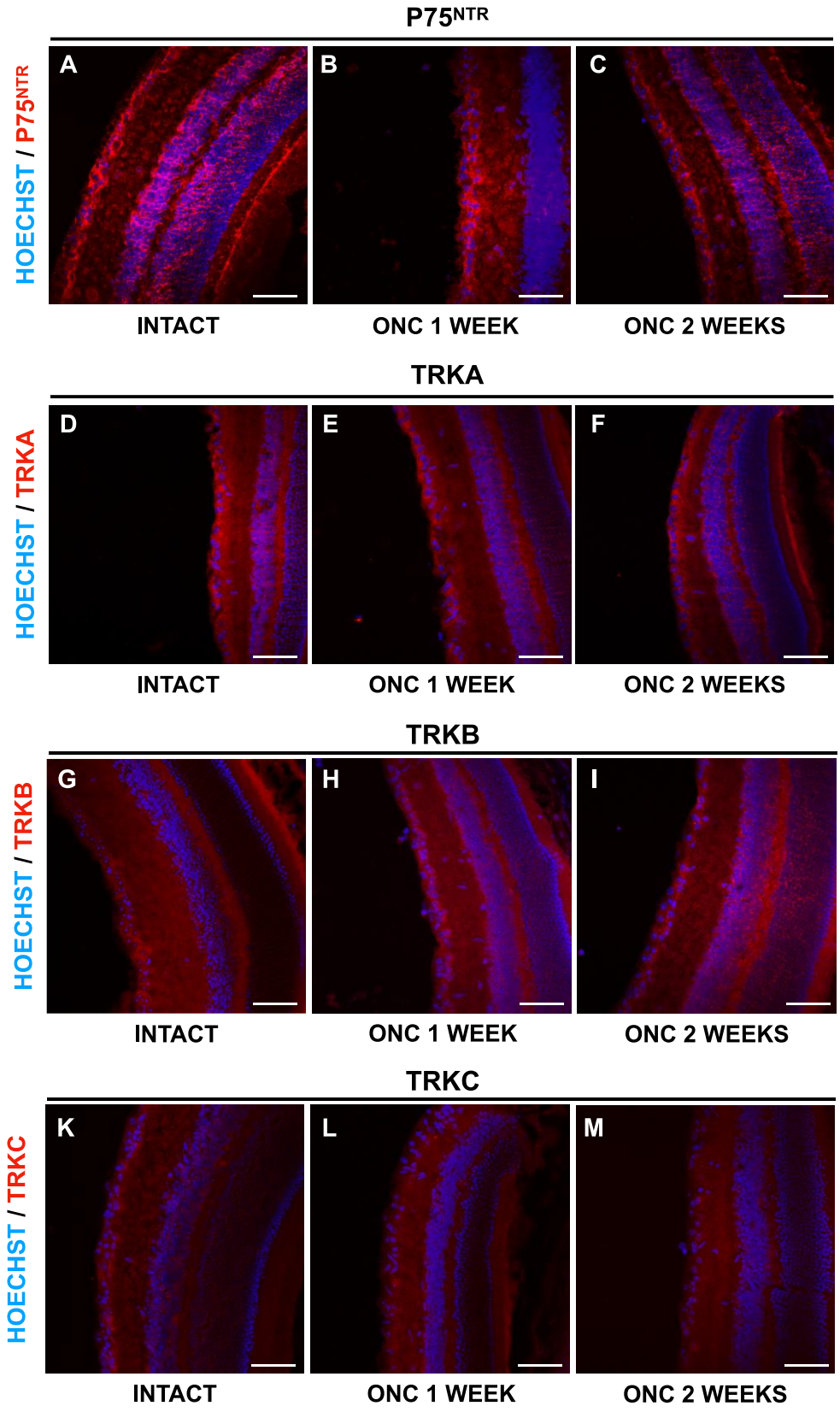

Figure 3-7: Representative confocal fluorescence images of intact (A; D; G; K) and injured eyes, at 1 (B; E; H; L) and 2 (C; F; I; M) weeks post-ONC, acquired from mouse retinal sections immunostained for $p75^{NTR}$, TrkA, TrkB, TrkC. Blue: Hoechst; Red: (A; B; C) $p75^{NTR}$ | (D; E; F) TrkA | (G; H; I) TrkB | (K; L; M) TrkC. Scale bar: 50 µm.

3.2 Effects of BNN27 Delivery via Eye Drops on ONC

BNN27 is a small BBB-permeable, microneurotrophin that can specifically bind and activate the TrkA receptor promoting neuronal survival *(Gravanis, Pediaditakis, and Charalampopoulos 2017, Pediaditakis et al. 2016)*.

In order to investigate the effects of BNN27 on wound healing response after ONC, and specifically evaluate if BNN27 can save RGCs from ONC-induced apoptosis. Mice submitted to ONC injury were divided in three (3) groups. Group A received no treatment, groups B and C were treated daily with one (1) drop of BNN27 10 mM (group B) and 50 mM (group C) for a period of 7 days. BNN27 was delivered in 5 µl DMSO drops.

In order to uncover any possible neuroprotective effects of BNN27 on RGCs, RGC survival was the first parameter to be evaluated [*Figure 3-8*]. *Figure 3-8* shows that RGC density is reduced by approximately 50% in injured mice receiving no treatment. Moreover, in mice that received one drop of BNN27 10 mM daily, a trend (P = 0.33) for RGC protection from ONC-induced apoptosis was detected 1 week post-ONC. Likewise, with the previous experiment, the number of animals used is small and therefore that is probably the cause for the lack of statistical significance in the case of BNN27 (10 mM) treatment.

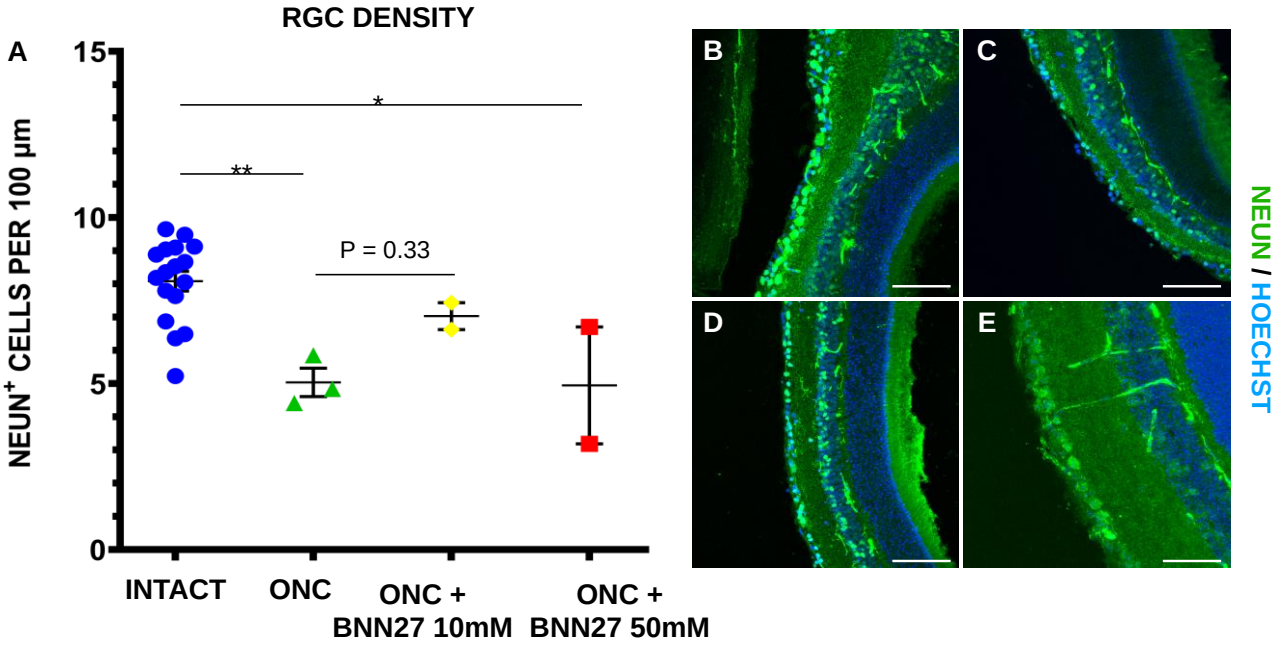

*Figure 3-8: Quantification of RGC survival in mouse retinal sections immunostained for NeuN by image analysis. (A) NeuN⁺ cells (RGCs) per 100 µm. Data are presented as mean ± SEM; "INTACT" n=17; "ONC" n=3; "ONC+BNN27 10mM" n=4; "ONC+BNN27 50mM" n=5; *P < 0.05; **P < 0.01; Tukey's post-hoc pairwise test assuming $P_{1\text{-way-Anova}} < 0.05$. (B; C; D; E) Representative confocal fluorescence images of intact and injured eyes 7 days post-ONC, acquired from immunostained mouse retinal sections; (B) "INTACT"; (C) "ONC"; (D) "ONC+BNN27 10mM"; (E) "ONC+BNN27 50mM". Blue: Hoechst; Green: NeuN. Scale bar: 50 µm.*

RGC survival was evaluated via an additional method in order to verify the aforementioned results, specifically the number of nuclei in GCL was counted via Hematoxylin-Eosin staining. As seen in *Figure 3-9* the number of nuclei counted in the GCL in intact or injured retinas, receiving some or no treatment, presented no significant differences. This demonstrates that H&E staining is not

appropriate for calculating RGC survival because it lacks RGC specificity. Additionally, the number of nuclei counted in GCL of intact eyes using H&E staining was almost 2 times larger than the number of RGCs counted by immunostaining for NeuN, a specific RGC marker. This can be explained when considered that Hematoxylin stains nucleic acids, therefore every nucleus located in the GCL will be stained *(Chlipala et al. 2020, Fischer et al. 2008)*, whereas NeuN specifically stains RGCs. Given the fact that RGCs consist 50-65% of the cells located in GCL in mice depending on the labelling and counting method *(Schlamp et al. 2013)*, it is reasonable to count almost twice the number of cells when counting nuclei using H&E staining compared to when counting $NeuN^+$ cells (RGCs) using IHC for staining.

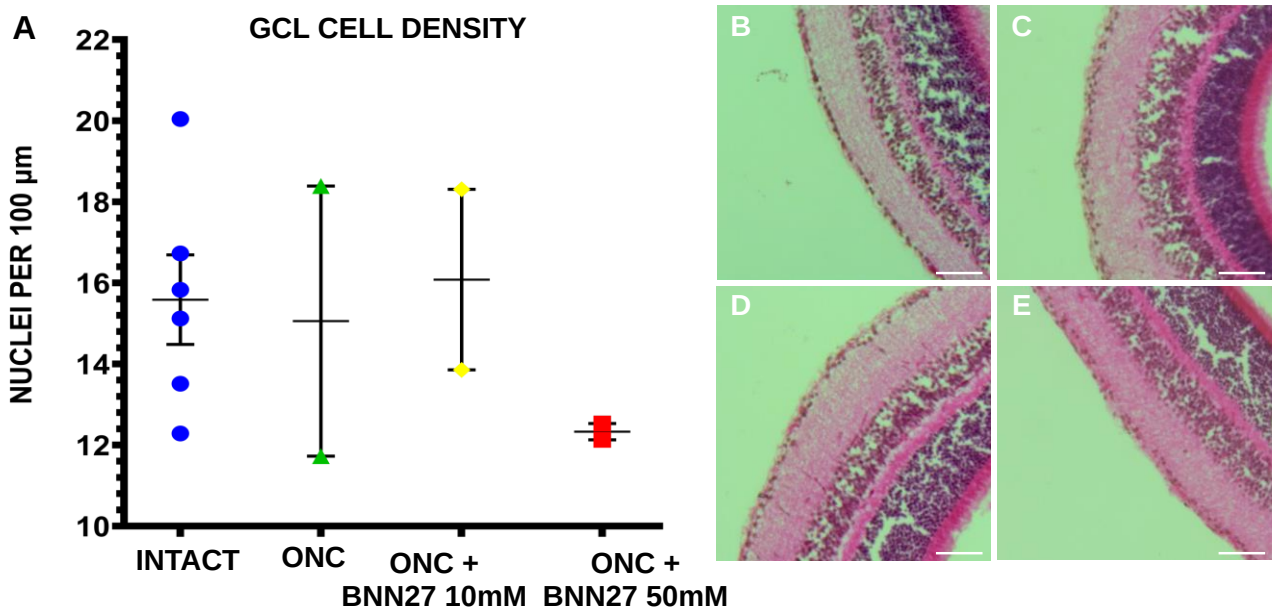

Figure 3-9: Quantification of GCL cell density Hematoxylin-Eosin stained mouse retinal sections by image analysis. (A) Cell nuclei per 100 µm. Data are presented as mean ± SEM; "INTACT" n=6; "ONC" n=2; "ONC+BNN27 10mM" n=2; "ONC+BNN27 50mM" n=2; Tukey's post-hoc pairwise test assuming $P_{1\text{-way-Anova}} < 0.05$. (B; C; D; E) Representative images of intact and injured eyes 7 days post-ONC, acquired from Hematoxylin-Eosin stained mouse retinal sections; (B) "INTACT"; (C) "ONC"; (D) "ONC+BNN27 10mM"; (E) "ONC+BNN27 50mM". Blue: Nuclei; Pink: Extracellular matrix / Cytoplasm. Scale bar: 50 µm.

Next, we focused on evaluating the ability of BNN27 to prevent astroglial activation. To assess the activation levels of astroglial cells in mouse retina, $GFAP^+$ astrocyte and Müller cell processes were measured in all retinal layers and their number per 100 µm was calculated. *Figure 3-10* shows that the number of $GFAP^+$ processes presents a 12-fold increase in all injured groups, receiving treatment or not, when compared to intact eyes (1) week after ONC. These results suggest that BNN27 did not affect astroglial activation one week after injury in mouse retina given the dose and administration chosen.

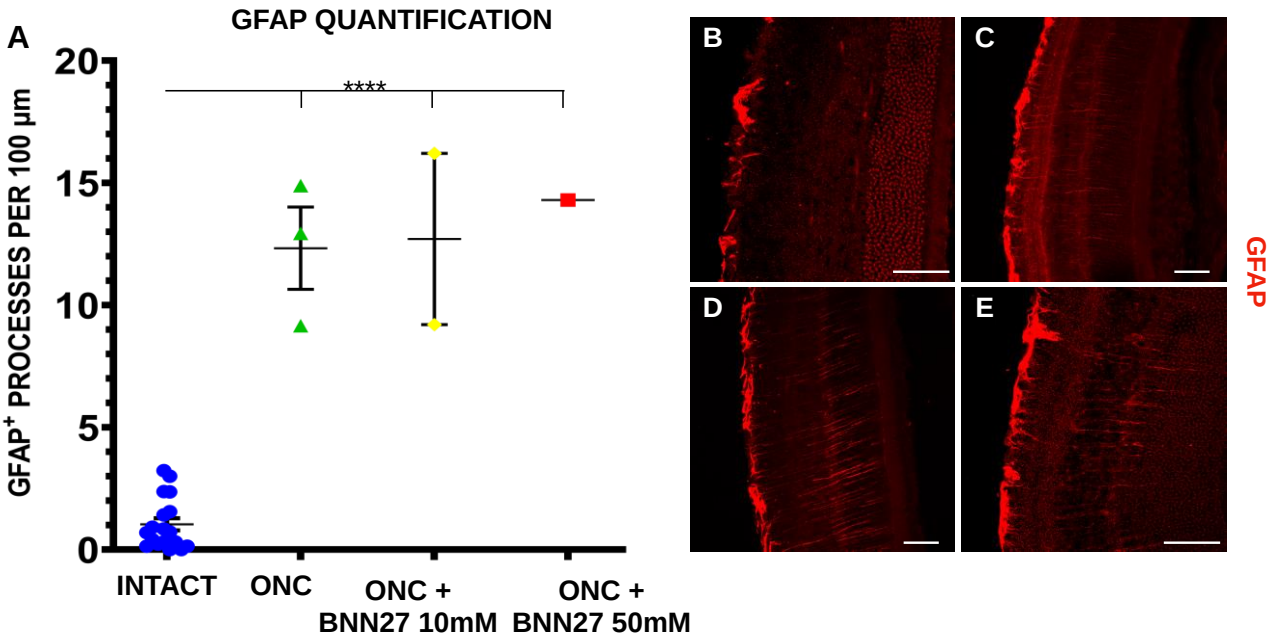

*Figure 3-10: Quantification of GFAP expression in mouse retinal sections immunostained for GFAP by image analysis. (A) GFAP$^+$ (astroglial) cell processes per 100 µm. Data are presented as mean ± SEM; "INTACT" n=18; "ONC" n=3; "ONC+BNN27 10mM" n=2; "ONC+BNN27 50mM" n=1; ****P < 0.0001; Tukey's post-hoc pairwise test assuming $P_{1\text{-way-Anova}} < 0.05$. (B; C; D; E) Representative images of intact and injured eyes 7 days post-ONC, acquired from immunostained mouse retinal sections; (B) "INTACT"; (C) "ONC"; (D) "ONC+BNN27 10mM"; (E) "ONC+BNN27 50mM"; Red: GFAP. Scale bar: 50 µm.*

In order to study an alternative drug dosing strategy for BNN27 drops, it became of interest to investigate the effects of BNN27 delivery for a longer period of treatment. Specifically, mice were submitted to ONC injury and treated with one drop of BNN27 every two (2) days for a period of 2 weeks. Mice were divided in three (3) groups namely, i) group A, which received no treatment, ii) group B, which received one 5 µl drop of 10 mM BNN27 and iii) group C, which received one 5 µl drop of 50 mM BNN27 every second day for fourteen (14) days. Again, BNN27 was dissolved in DMSO. Assessing the state of RGCs [*Figure 3-11*] it became clear that 2 weeks post-ONC, RGC number decreased in injured eyes that received no treatment by almost 70% compared to control eyes. Both doses of BNN27 presented a trend (BNN27 10 mM: P = 0.21; BNN27 50 mM: P = 0.11) to rescue RGCs from injury-induced apoptosis 2 weeks post-ONC. Again, due to the small number of animals used, this effect did not achieve statistical significance.

Next, the effect of BNN27 on astroglial activation was evaluated. *Figure 3-12* shows that the number of GFAP$^+$ processes in injured retinas was almost 11 times higher compared to intact retinas 2 weeks post-ONC. On the contrary, when comparing the groups bearing ONC injury with each other, no significant differences on retinal GFAP levels were found, regardless of receiving any treatment or not. As a consequence, it is concluded that BNN27 has no effect on the activation of retinal astroglial cells in mice, when treated with one drop of BNN27 every two days over two weeks. These results are consistent with the previous experiment where mice were treated with BNN27 for 1 week, where again BNN27 treatment had no effect on astroglial activation.

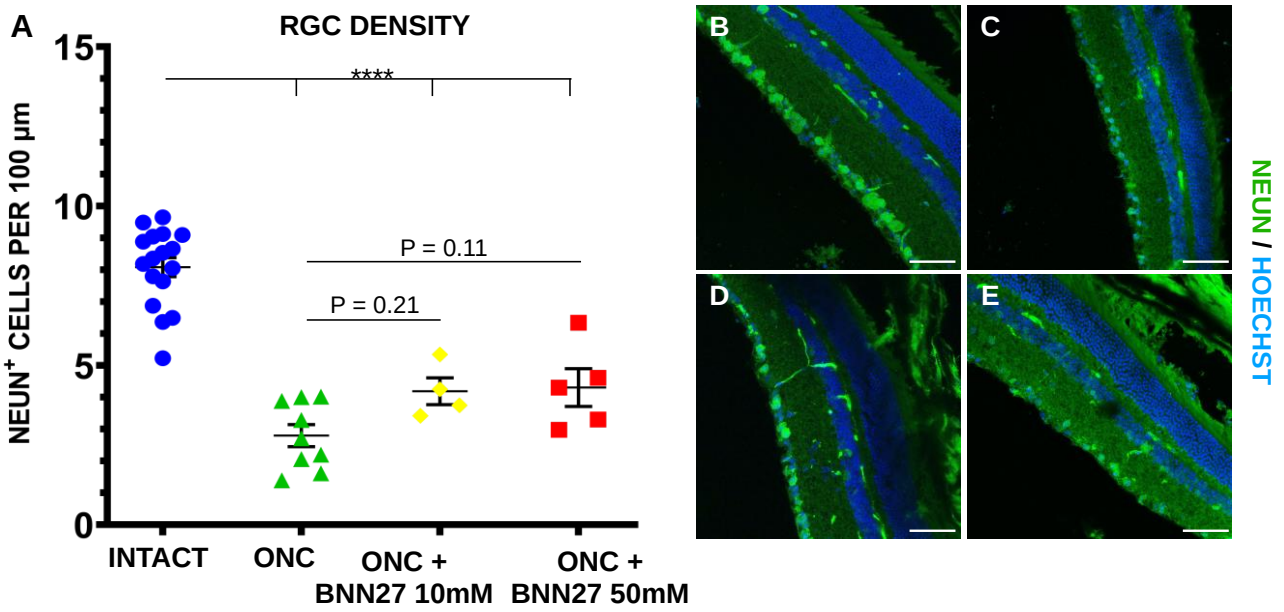

*Figure 3-11: Quantification of RGC survival in immunostained mouse retinal sections by image analysis. (A) NeuN$^+$ cells (RGCs) per 100 µm. Data are presented as mean ± SEM; "INTACT" n=17; "ONC" n=9; "ONC+BNN27 10mM" n=4; "ONC+BNN27 50mM" n=5; ****P < 0.0001; Tukey's post-hoc pairwise test assuming $P_{1\text{-way-Anova}} < 0.05$. (B; C; D; E) Representative confocal fluorescence images of intact and injured eyes 14 days post-ONC, acquired from immunostained mouse retinal sections; (B) "INTACT"; (C) "ONC"; (D) "ONC+BNN27 10mM"; (E) "ONC+BNN27 50mM". Blue: Hoechst; Green: NeuN. Scale bar: 50 µm.*

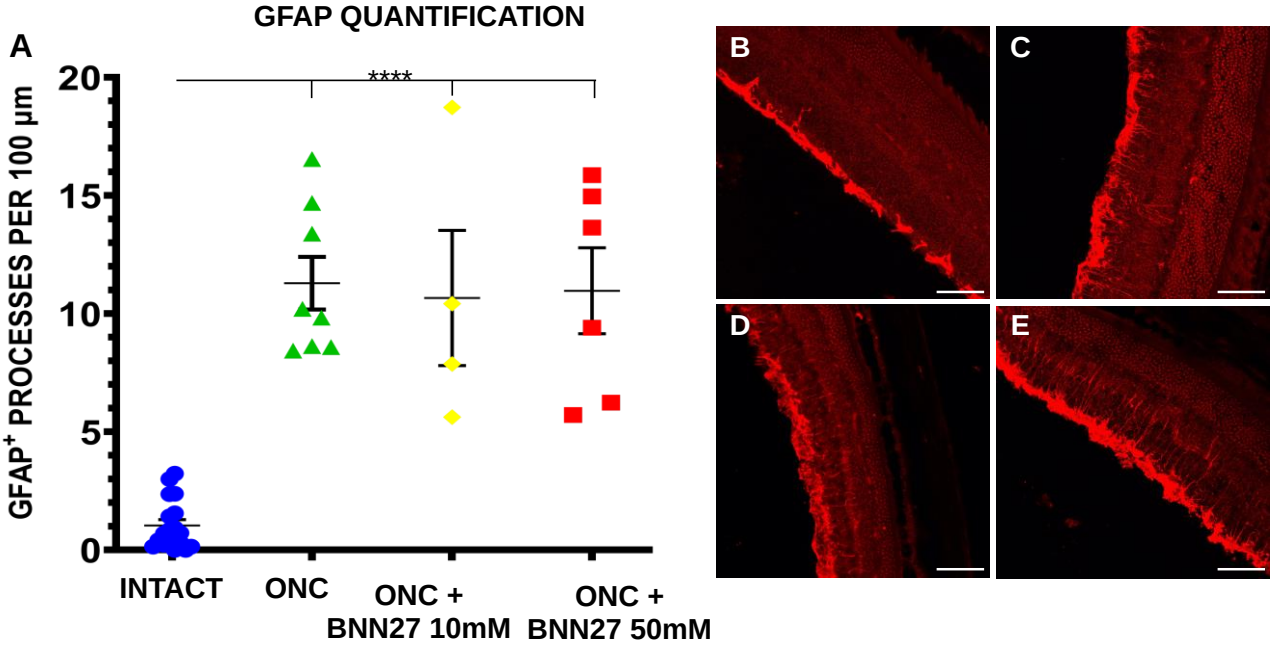

*Figure 3-12: Quantification of GFAP expression in immunostained mouse retinal sections by image analysis. (A) GFAP$^+$ (astroglial) cell processes per 100 µm. Data are presented as mean ± SEM; "INTACT" n=18; "ONC" n=7; "ONC+BNN27 10mM" n=4; "ONC+BNN27 50mM" n=6; ****P < 0.0001; Tukey's post-hoc pairwise test assuming $P_{1\text{-way-Anova}} < 0.05$. (B; C; D; E) Representative confocal fluorescence images of intact and injured eyes 14 days post-ONC, acquired from immunostained mouse retinal sections; (B) "INTACT"; (C) "ONC"; (D) "ONC+BNN27 10mM"; (E) "ONC+BNN27 50mM"; Red: GFAP. Scale bar: 50 µm.*

3.3 Effects of BNN27 Delivery via Biomaterials on ONC

Despite the fact that conventional eye drops may be an easy way for drug delivery to the eye, the intraocular bioavailability of the drug may be reduced due to various factors (such as nasolachrymal drainage, drug dilution with tears, etc.) causing only small amounts of the drug (1-3%) to penetrate the cornea and reach the intraocular tissue *(Urtti 2006, Kulkarni et al. 2016)*. In order to overcome such issues, this work evaluates biomaterials as a means to achieve a more targeted and efficient delivery of BNN27 in the injured retina and the optic nerve. Towards this direction, two strategies were pursued. Firstly, BNN27 was encapsulated in a peptide gel that is formed inside a porous collagen scaffold. This approach utilizes the small pores of the gel in order to delay BNN27 diffusion out of the graft. Secondly, BNN27 was covalently attached on the porous scaffold itself.

3.3.1 BNN27 Delivery via Encapsulation in a Peptide Gel Formed Inside a Porous Collagen-GAG Scaffold

In this study drug delivery via biomaterials was pursued using two different approaches. For the first approach, a porous collagen-GAG scaffold (4x3x1.5 mm) was soaked in BNN27 50 μM solution while for the second, BNN27 50μM was entrapped in a peptide (Fmoc-FF) gel which was formed inside the aforementioned porous collagen-GAG scaffold in order to prolong the drug release period. Scaffolds were soaked in 6 μl of the appropriate solution. For the purpose of this experiment, mice were submitted to ONC and divided in five (5) groups. Group A received no treatment, group B received a scaffold containing peptide gel without BNN27, group C received a scaffold soaked in BNN27 50 μM and group D received a scaffold containing a peptide gel with BNN27 50 μM. All groups were sacrificed fourteen (14) days after ONC injury. The collagen-scaffolds used for this experiment.

Figure 3-13 & Figure 3-14 show that RGC number was decreased by almost 70% 2 weeks post-ONC compared to intact eyes. No significant differences were observed in RGC numbers among injured groups. Therefore, it can be concluded that delivery of 6 μl 50 μM BNN27 via a peptide gel inside a porous scaffold did not protect RGCs from ONC injury induced death two weeks post-injury, neither when it was administered via a collagen scaffold soaked in BNN27 solution nor when it was entrapped in a peptide gel formed inside the collagen scaffold.

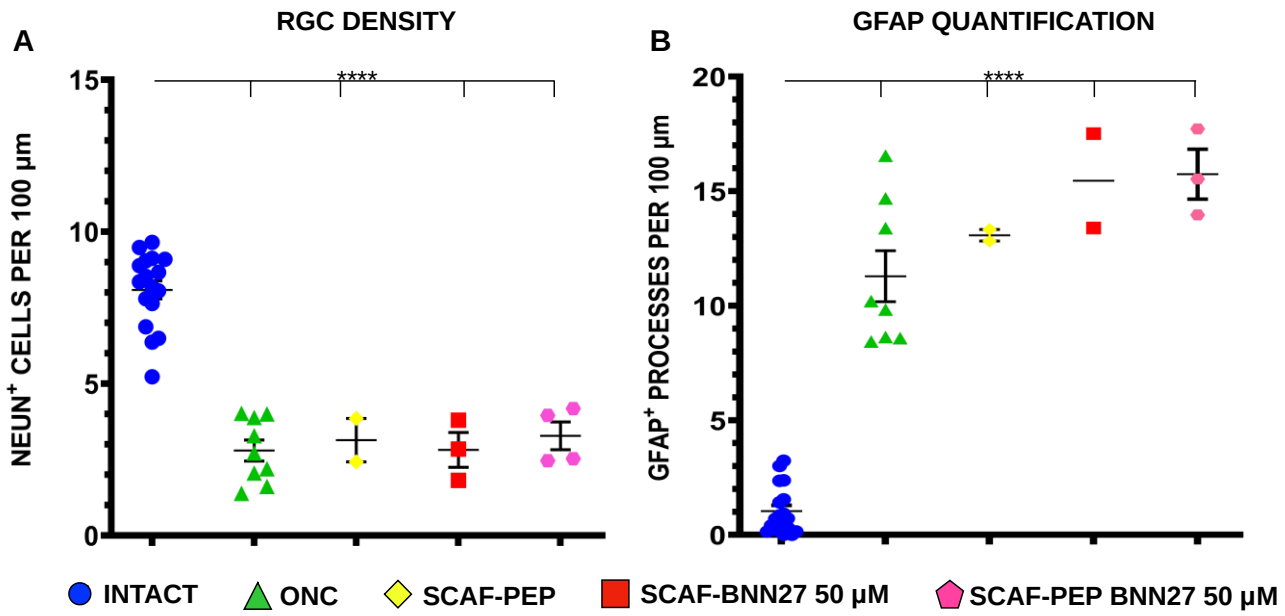

*Figure 3-13: Effects of BNN27 delivery by encapsulation inside a peptide gel on RGC survival and astrogliosis 2 weeks after ONC. (A) Quantification of RGC survival in immunostained mouse retinal sections by image analysis 14 days post-ONC; NeuN+ cells (RGCs) per 100 µm. (B) Quantification of GFAP expression in immunostained mouse retinal sections by image analysis 14 days post-ONC; GFAP$^+$ (astroglial) cell processes per 100 µm. Data are presented as mean ± SEM; (A) "INTACT" n=17; "ONC" n=9; "SCAF-PEP" n=2; "SCAF-BNN27 (50µM)" n=3; "SCAF-PEP-BNN27 (50µM)" n=4 | (B) "INTACT" n=18; "ONC" n=7; "SCAF-PEP" n=2; "SCAF-BNN27 (50µM)" n=2; "SCAF-PEP-BNN27 (50µM)" n=3 ****P < 0.0001; Tukey's post-hoc pairwise test assuming $P_{1\text{-way-Anova}} < 0.05$.*

Furthermore, GFAP quantification [*Figure 3-13 & Figure 3-14*] demonstrated that ONC increased by at least 11 folds the amount of GFAP$^+$ processes in mouse retina of injured compared to intact eyes. However, no significant differences were detected concerning the number of GFAP$^+$ processes among groups with injured eyes. Consequently, it is safe to conclude that BNN27 50 µM did not prevent the activation of astrocytes and Müller cells in mouse retina two weeks post-injury, regardless of the administration approach (collagen scaffold soaked in BNN27 solution; entrapment of BNN27 in peptide gel formed inside collagen scaffold). Additionally, both RGC analysis and GFAP quantification indicate that collagen scaffold in combination with the peptide gel did not present any adverse effects regarding RGC survival and astroglial activation.

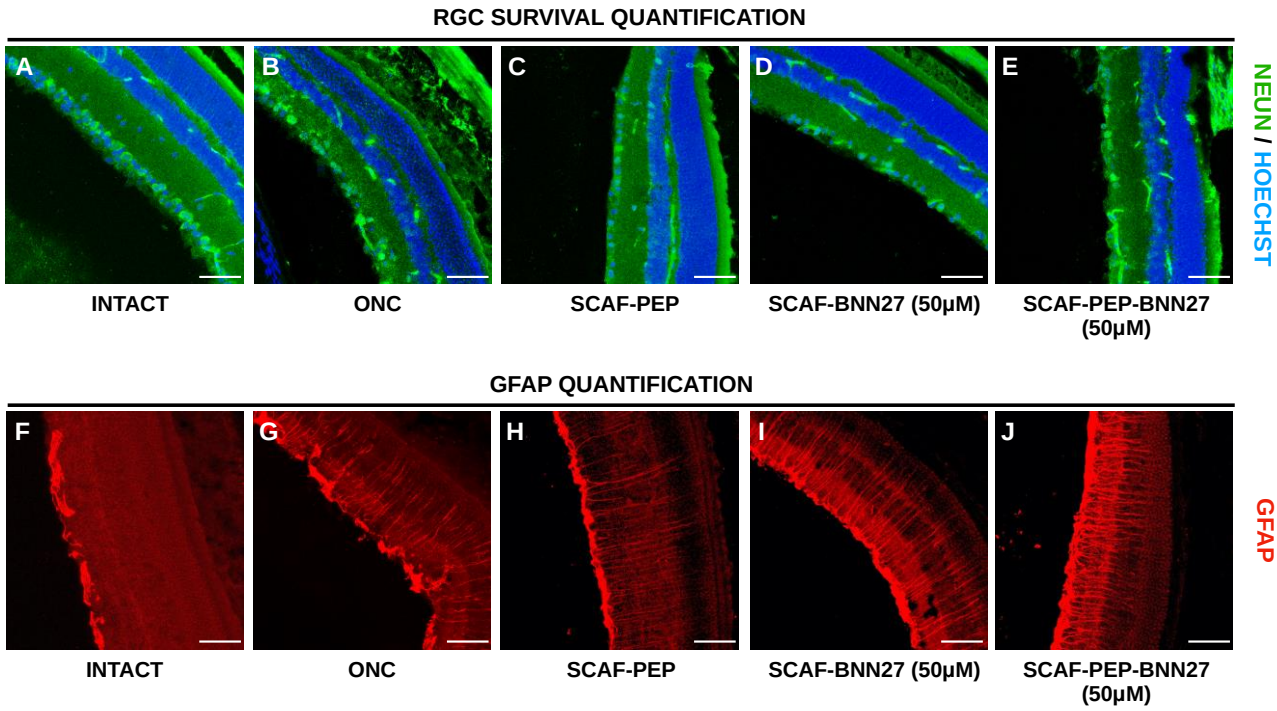

Figure 3-14: Representative confocal fluorescence images of intact and injured eyes 14 days post-ONC, acquired from immunostained mouse retinal sections; (A;F) "INTACT"; (B;G) "ONC"; (C;H) "SCAF-PEP"; (D;I) "SCAF-BNN27 (50µM)"; (E;J) "SCAF-PEP-BNN27 (50µM)". Blue: Hoechst; Green: NeuN; Red: GFAP. Scale bar: 50 µm.

In order to estimate the rate of BNN27 delivery when delivered by encapsulation inside a peptide gel, it was decided to evaluate the ability of the peptide gel to prolong the release of BNN27. Due to the lack of an easy direct method for quantifying BNN27, it was decided to quantify the diffusion of fluorescein out of the peptide gel instead of BNN27. Fluorescein is widely used as fluorescent tracer for many applications *(Gessner and Mayer 2000)*. This experiment consisted of three (3) groups: A) the "Steady State" group which is a fluorescein solution whose concentration equals the expected one when all fluorescein is released from the gel into the surrounding solution; B) the "Scaffold+Fluorescein" group, where the scaffold is soaked in fluorescein solution in water; C) the "Scaffold+Peptide+Fluorescein" group, where fluorescein is entrapped in the peptide gel which is formed inside the scaffold. Results [*Figure 3-15*] show that fluorescein released from group C reaches a plateau between 52 h and 100 h, which is maintained until 124 h. However, results do not support that the presence of the peptide gel delays the diffusion of fluorescein out of the porous scaffold.

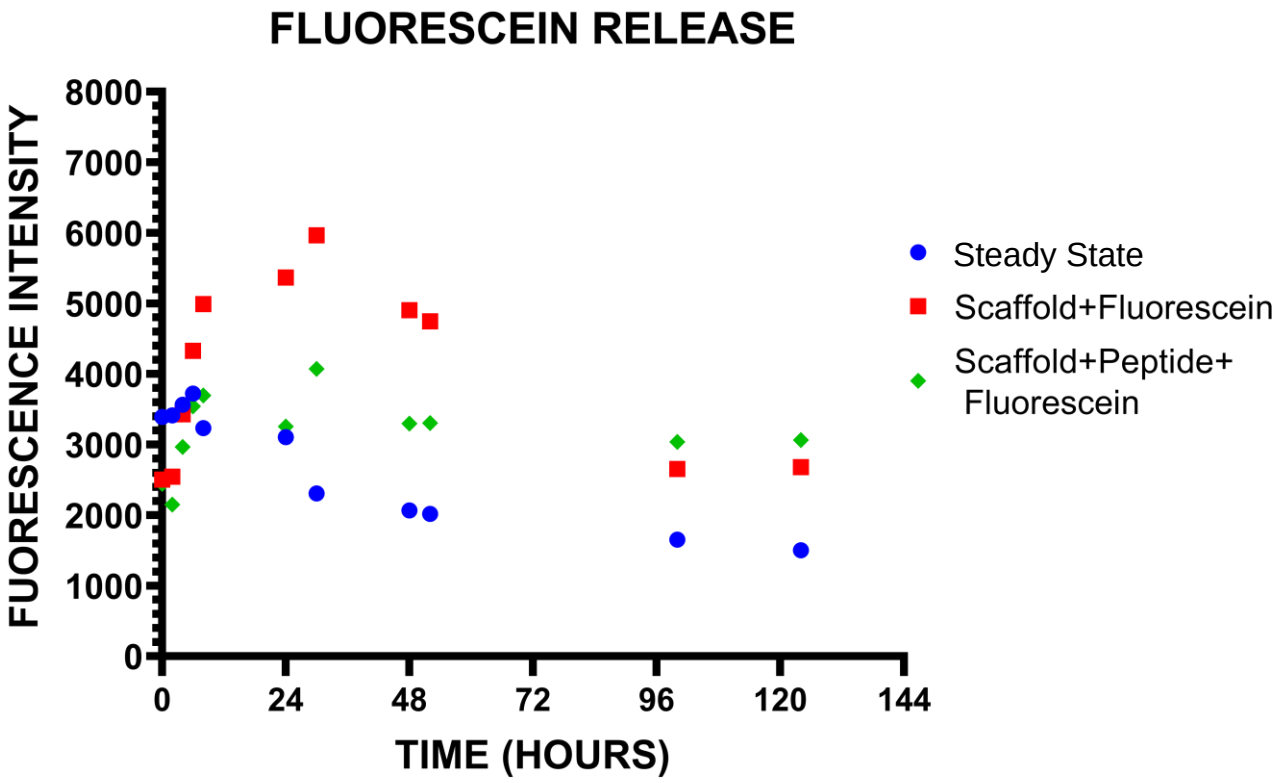

Figure 3-15: Quantification of the release rate of fluorescein from porous collagen-GAG scaffold with or without peptide gel. Data are expressed as fluorescence intensity (y-axis) per time (x-axis). The term "Steady State" is used to describe the state where the total amount of fluorescein has been released from the scaffold in the solution.

3.3.2 BNN27 Delivery via Covalent Conjugation on Collagen-GAG Scaffold

In order to further prolong BNN27 release from the porous collagen-GAG scaffold, a procedure was developed in order to covalently attach BNN27 on the porous collagen-GAG scaffold. The procedure development was based on the Bachelor's thesis of Marileta Tsakanika *(Tsakanika 2019)*. The first step [*Figure 3-16*] was to activate a fraction of the amine (-NH2) groups available on the scaffold using 3-(2-Pyridyldithio)propionic acid *N*-hydroxysuccinimide ester (SPDP), a heterobifunctional cross-linking reagent with amine and sulfhydryl reactivity. Next, a synthetic substance named 'TC447' developed by Dr. T. Callogeropoulou (NHRF, Athens) was used as of the intermediate linker for BNN27 on the scaffold. TC447 can react via its sulfhydryl (-SH) domain with SPDP-activated amines, leading to a TC447-conjugated scaffold. Finally, the last step would be to create a chemical bond between TC447 and BNN27 in order to generate a scaffold covalently connected with BNN27 and achieve a specific BNN27 delivery to the mouse ON and retina that lasts for an adequate amount of time to rescue injured RGCs from ONC-induced cell death.

In order to measure the efficiency of SPDP activation of collagen scaffold amines (the fraction $f_{activated}$ of amine groups activated by SPDP), scaffolds (1x1x1.5 mm) were activated with 500 μM SPDP and then treated with 25 mM dithiothreitol (DTT), a reducing agent, in order to react with SPDP and produce pyridine 2-thione (P2T). The released P2T was collected in the reaction volume.

Absorption measurements of the produced pyridine 2-thione at 343 nm can be utilized to calculate the moles of released P2T ($n_{P2T} = n_{SPDP}$) in the solution via the Beer-Lambert Law:

$$A = \varepsilon \cdot c \cdot l$$

$f_{activated}$ was calculated (detailed description in Materials & Methods section "*SPDP-activated Amine Group Quantification*") using the following equation:

$$f_{activated} = \frac{n_{SPDP}}{n_{NH2,collagen}}$$

Where $n_{H2,collagen}$ is the total amount in moles of the amine groups included in the porous collagen-GAG scaffold.

***Table 3-1:* Absorbance measurements and calculations for the determination of $f_{activated}$**

Replicate Number	Sample ID	$V_{reaction}$ [µl]	l [cm]	A_{343}	ΔA_{343}	n_{SPDP} [nmol]	$n_{NH2,collagen}$ [nmol]	$f_{activated}$ [%]
1	Scaf. #1	100	0.35	0,104	0.0085	0.3	7.02	4.25
	Blank #1	100	0.35	0,094	-	-	7.02	-
	Blank #2	100	0.35	0,097	-	-	7.02	-
2	Scaf. #1	100	0.35	0,106	0.0085	0.3	7.02	4.25
	Blank #1	100	0.35	0,097	-	-	7.02	-
	Blank #2	100	0.35	0,097	-	-	7.02	-

Calculations [*Table 3-1*] suggest that approximately $f_{activated} = 4.25$ % of the amine groups included in the collagen-GAG scaffold were activated via treatment with 500 µM SPDP for 1 h.

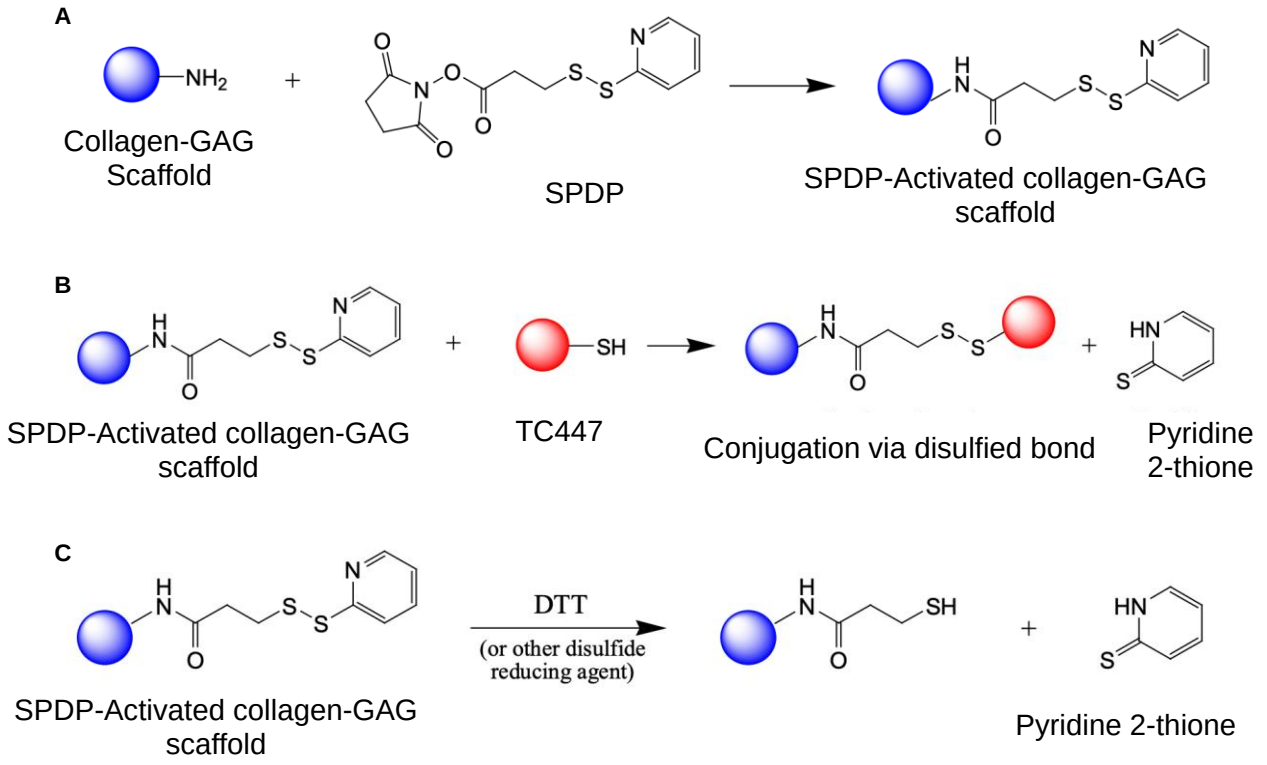

Figure 3-16: A) Reaction between porous collagen-GAG scaffold and SPDP. B) Reaction between SPDP-activated collagen-GAG scaffold and TC447. C) Reaction between SPDP-activated collagen-GAG scaffold and DTT [Modified from (Thermo_Scientific)].

After verifying that SPDP can successfully activates amine groups on the scaffold, the ability of TC447 to conjugate with the SPDP-activated amines was next to be tested. For this purpose, an experiment was conducted [*Figure 3-17 & Figure 3-18*], having three different groups. In the first group (group A), scaffolds were treated with 50 µM TC447 without being activated with SPDP. In the second group (group B), scaffolds were activated with 500 µM SPDP and then treated with 50 µM TC447. In the third group (group C), scaffolds were activated with 500 µM SPDP, treated with 25 mM DTT and then treated with 50 µM TC447. Taking advantage of the collagen autofluorescence when excited by UVlight, scaffold struts were visualized via confocal microscopy using 405 nm laser for excitation. Additionally, TC447 is connected to a BODIPY group, which emits fluorescence when excited by a 488 nm laser line. All scaffolds were imaged i) immediately after TC447 conjugation (day 0), ii) after a rigorous overnight wash (day 1) and iii) two days after TC447 conjugation following a treatment with 25 mM DTT and (day 2). This experiment was conducted three times, results from each experiment are presented in *Figure 3-17 & Figure 3-18*.

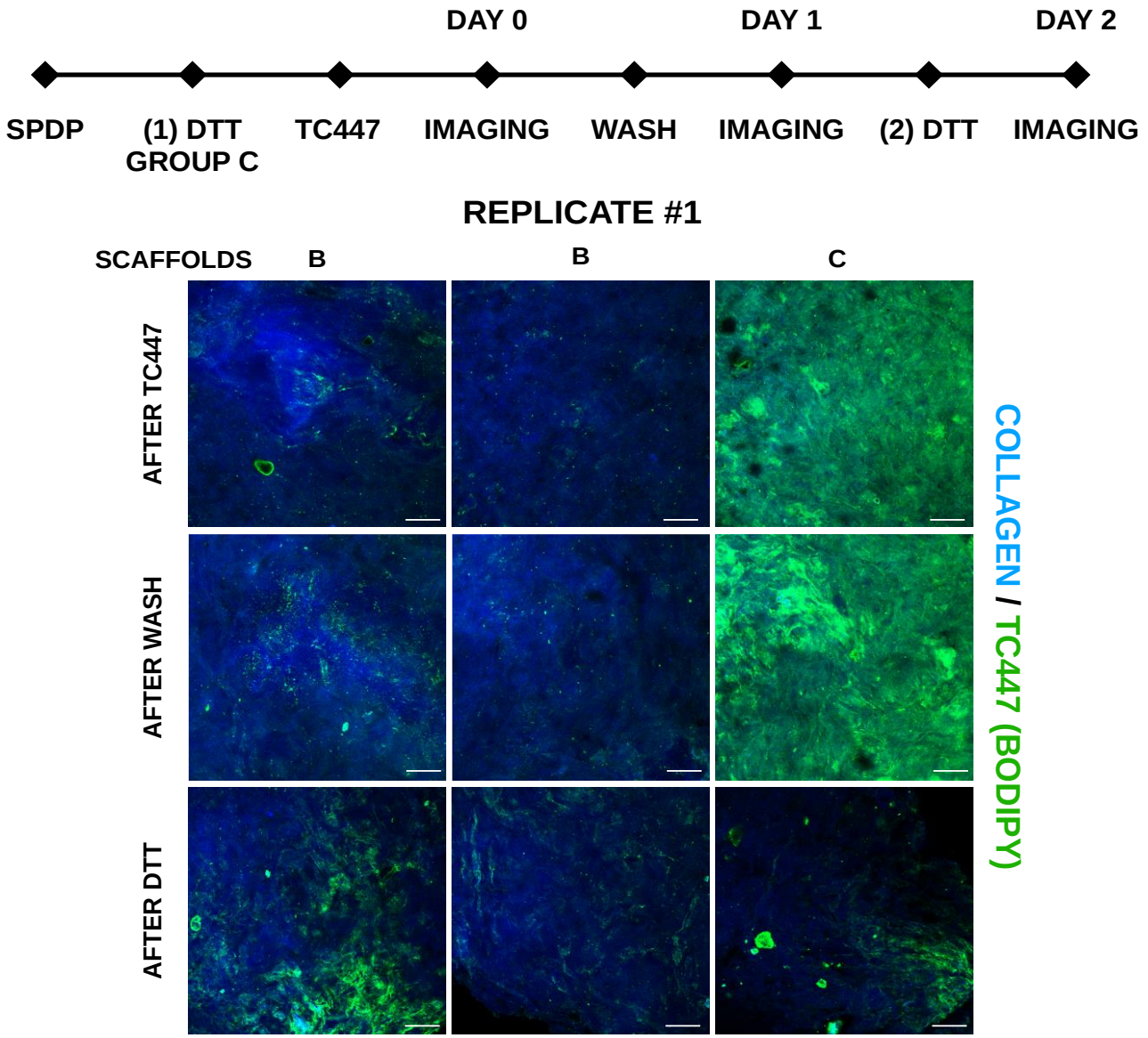

Figure 3-17: Timeline and representative confocal fluorescence images from the first replicate of the TC447 covalent conjugation on collagen-GAG scaffold. Top: Timeline of the experiment with the stages used to treat the collagen-GAG scaffolds. Bottom: Representative confocal fluorescence images of collagen-GAG scaffolds from the first replicate of the experiment. Blue: Collagen; Green: TC447 (Fluorescence due to BODIPY group); Scale Bar: 50 µm.

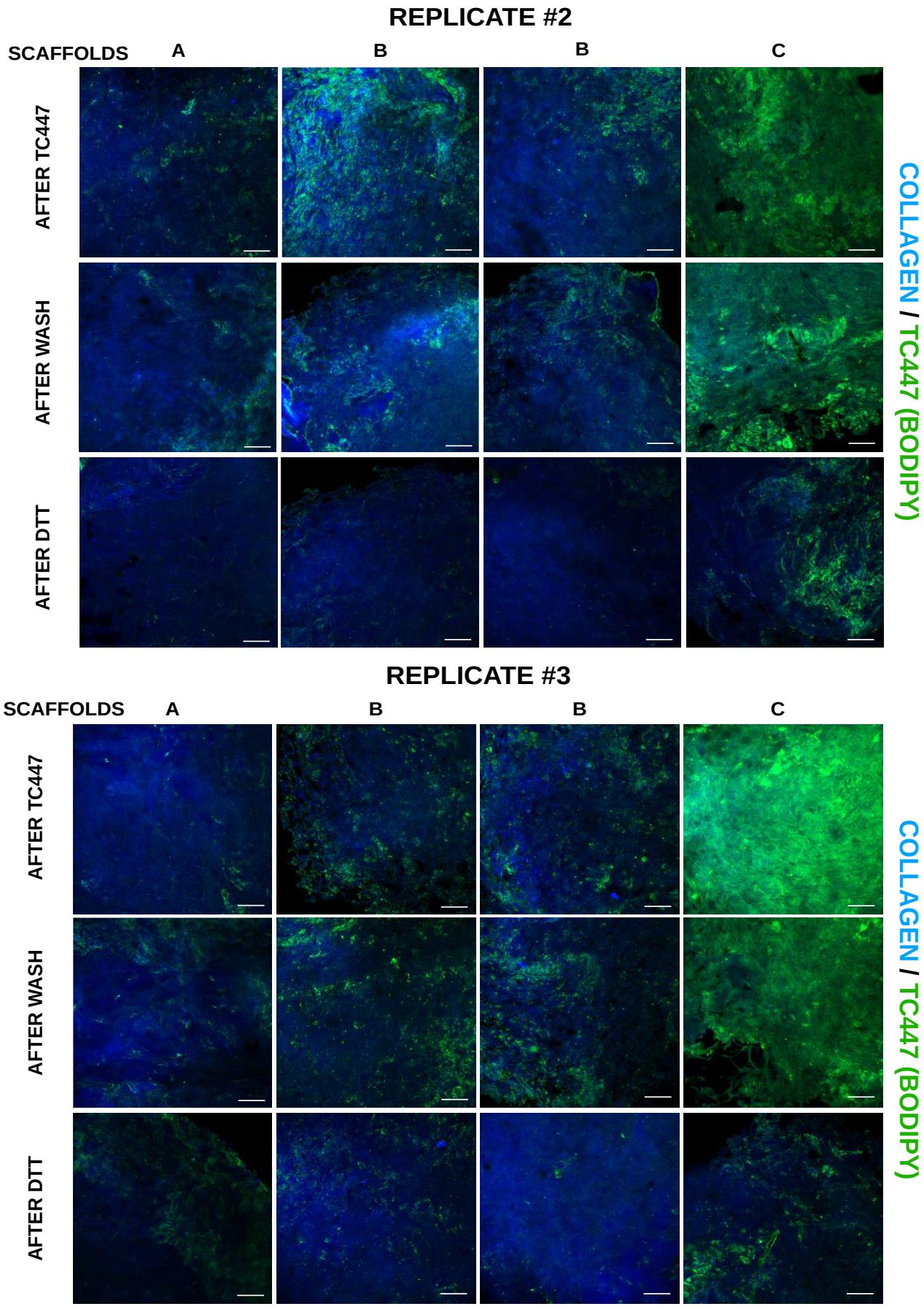

Figure 3-18: Representative confocal fluorescence images of collagen-GAG scaffolds from the second and third replicate of the TC447 covalent conjugation on collagen-GAG scaffold. Top: Second

replicate. Bottom: Third replicate. Blue: Collagen; Green: TC447 (Fluorescence due to BODIPY group); Scale Bar: 50 µm.

Imaging results on day 0 show that TC447 is successfully conjugated on SPDP-activated scaffolds. Day 1 imaging shows that the attached TC447 was not detached by washing overnight, further suggesting that TC447 is covalently attached on the scaffold. After treating TC447-conjugated scaffolds with 25 mM DTT the detected TC447 emission is reduced significantly. This can be explained by the fact that DTT cleaves the disulfide bond connecting TC447 to the scaffold, causing TC447 to be successfully washed away. These findings suggest that TC447 is indeed conjugated via a covalent bond on the collagen-GAG scaffold which can be reduced using DTT.

Results show that some amount of TC447 was not conjugated evenly on porous scaffolds. Such TC447 hot spots could occur due to unspecific interactions of TC447 with GAG or because of imperfect solubilization of TC447.

Lastly, an important finding of this experiment is that TC447 conjugation is highly enhanced on SPDP-activated scaffolds that were treated with DTT prior to TC447. This result indicates that the microenvironment created as an outcome of chemical interactions among SPDP, collagen-GAG and DTT, favors the conjugation of TC447 on the scaffold in a more efficient manner compared to TC447 conjugation on SPDP-activated scaffold alone.

Chapter 4: Discussion & Conclusions

TON is a condition characterized by the occurrence of an optic nerve injury caused by direct or indirect head and/or facial trauma *(Jang 2018)*. Depending of the intensity of the damage caused by the injury, this condition may lead to vision impairment or permanent vision loss *(Li, Schlamp, and Nickells 1999, McKinnon, Schlamp, and Nickells 2009, Yin et al. 2019)*. Current clinical treatments are limited to the administration of corticosteroids and surgical decompression of the optic canal, presenting low efficiency and several side effects *(Chaon and Lee 2015, Pula and MacDonald 2012, Honda et al. 2011)*. Our vision relies upon high-quality signal conduction from the retina to subcortical target areas of the brain, via the optic nerve, which consists of RGC axon bundles *(Li, Schlamp, and Nickells 1999, McKinnon, Schlamp, and Nickells 2009, Yin et al. 2019)*. None of the available treatments so far can prevent injury-induced RGC apoptosis or induce the regeneration of RGCs in order to restore vision *(Chaon and Lee 2015)*.

The objective of this study was to quantify the effects of the BNN27 microneurotrophin on key cell phenotypes after ONC injury in mice, using two different delivery strategies. Firstly, BNN27 was administrated via eye drops for 7 and 14 days after injury. Secondly, BNN27 was entrapped in a peptide gel formed inside a porous collagen-GAG scaffold and then was released to the neighboring optic nerve at the injury site.

4.1 Characterization of ONC Model

The first experiments of this work aim to characterize the ONC model used for this study. The objective was to confirm that ONC was successful and reproducible as well as to evaluate the histopathology that is induced by injury. For this purpose, i) RGC survival; ii) astroglial activation; iii) microglial activation; iv) expression of NT receptors ($p75^{NTR}$, TrkA, TrkB, TrkC) were assessed in the retinal tissue.

Analysis of RGC survival showed that RGC density is significantly decreased by 50% at 7 days post-ONC and by 70% at 14 days post-ONC as a result of the injury. Literature reports RGC loss ranging from approximately 50-70% for the first week and 68-90% for the second week in ONC mice or rats *(Feng et al. 2017, Takeuchi et al. 2018, Sánchez-Migallón et al. 2018, Grinblat et al. 2018, Laughter et al. 2018, Sánchez-Migallón et al. 2015, Mesentier-louro et al. 2017, Mesentier-Louro et al. 2019, Kole et al. 2020, Levkovitch-Verbin et al. 2000, Agudo et al. 2008, Agudo et al. 2009, Nadal-Nicolas et al. 2009, Parrilla-Reverter et al. 2009, Kim et al. 2015, Li et al. 2020)* which agree with the findings of this study and therefore confirm that ONC was inflicted successfully in our study. It is worth to note that some studies report much lower rates of RGC loss, such as 20% at 7 fays post-*ONC (Agudo et al. 2008, Parrilla-Reverter et al. 2009)* while other report much higher, such as 99% at 14 days post-ONC (*Kitamura et al. 2019)*. Critical parameters in this obvious variability, observed in injury-induced RGC apoptosis, are the distance of the injury from the eye *(Agudo et al. 2008, Agudo et al. 2009, Nadal-Nicolas et al. 2009, Sánchez-Migallón et al. 2018, Villegas-Perez 1992)* as well as the method of inflicting the injury such as (i) the choice of tool and ii) the duration of applied pressure for injury infliction). Even though most published studies use forceps for optic nerve crushing, the amount of force applied to inflict the injury cannot be exactly the same among individuals, due its

elegant and manual nature. Moreover, the fact that in this study 12 out of 14 mice submitted to surgery were successfully injured suggests that induced ONC injury was reproducible.

Quantification of astroglial activation clearly indicated that ONC induced increase in the number of $GFAP^+$ processes of astrocytes and Müller cells 7 and 14 days after injury. These findings are directly in line with previous studies that also report increased $GFAP^+$ processes and upregulation of GFAP in rodent retina (mouse/rat) 7 and 14 days after ONC *(Tang et al. 2020, Nascimento-Dos-Santos et al. 2020, Mesentier-Louro et al. 2019, Mesentier-louro et al. 2017, Huang et al. 2018, Wang et al. 2016)*. Moreover, our findings regarding microglial activation show no clear effect of ONC on IBA1 staining both at 1 and 2 weeks post-injury on mouse retinal sections. This is in contrast to previous studies that reported significantly IBA1 upregulation in injured retinas 7 and 14 days after crush *(Tang et al. 2020, Nascimento-Dos-Santos et al. 2020, Huang et al. 2018, Wang et al. 2016, Bohm et al. 2012)*. Yet, one study reported no significant alteration on retinal microglia (IBA1) 3 days after crush *(Morzaev et al. 2015)*.

Moving further with the characterization of our ONC model, we examined the expression of neurotrophin receptors $p75^{NTR}$, TrkA, TrkB and TrkC. No statistically significant alterations were observed in the expression of $p75^{NTR}$, TrkA, and TrkB at 1 and 2 weeks post-ONC. However, a trend for TrkC downregulation, although not statistically significant yet, was detected for the same period. It is important to highlight the fact that for this experiment the number of animals used were small (n=2 for 7 days; n=3 for 14 days), therefore if more animals were to be used, this trend will probably become a statistically significant difference. Comparing our results with previous studies, it should be noted that few previous studies report ONC effects on the expression of NT receptors. Contrary to our findings, a study reports significantly increased expression for $p75^{NTR}$ 1 and 2 weeks after ONC in rats *(Mesentier-louro et al. 2017, Mesentier-Louro et al. 2019)*. Furthermore, in line with our findings, the same research group reports no significant change in the expression of TrkA 1 week post-ONC *(Mesentier-louro et al. 2017, Mesentier-Louro et al. 2019)*. Results for TrkA expression 2 weeks post-injury are not clear, because in the first study the aforementioned research group reports a slight decrease *(Mesentier-louro et al. 2017)* whereas in the following study this decrease is absent *(Mesentier-Louro et al. 2019)*. Regarding TrkB expression after ONC, a previous study demonstrated, in agreement with our results, no significant alterations 7 days after ONC, while for the second week they report a significant decrease which we did not observe. No prior studies have reported the effects of ONC on the expression of TrkC.

Taking all the above into consideration, this experiment demonstrated that ONC induced RGC apoptosis in an effective and reproducible way. Additionally, ONC induced astroglial activation and a trend for TrkC downregulation 7 and 14 days after crush. Lastly, no significant alterations were observed in the expression of $p75^{NTR}$, TrkA and TrkB, while no clear effect of ONC was observed on IBA1 expression 1 and 2 weeks post-ONC.

4.2 Effects of BNN27 Delivery via Eye Drops on ONC

After characterizing our ONC model, our next goal was to evaluate the effects of BNN27 when administered via eye drops daily for 7 days. For this purpose, the survival of RGCs and the level of astroglial activation were assessed in the retinal tissue 7 days after injury. Our results demonstrated a trend for BNN27 to rescue RGC from ONC-induced apoptosis when administered at a concentration of 10 mM. Although currently not statistically significant due to the use of small number of animals (n=2), this trend has potential to become significant if the number of animals is increased. Concerning astroglial activation, in agreement with our previous experiment, GFAP increased in injured retinas. BNN27 did not manage to decrease the number of $GFAP^+$ processes 7 days after crush, when administered daily via eye drops. A review of the literature reveals conflicting results regarding BNN27 effect on GFAP. To be more specific, a previous study reports reduction of GFAP in rat retina when BNN27 is administered intraperitoneally for 7 days at a concentration of 10 mg/kg and 50 mg/kg in a rat streptozotocin (STZ) model of diabetic retinopathy *(Ibán-Arias et al. 2019)*. On the contrary, another study reports that BNN27 administration increased gliosis (GFAP) 24 hours post injury, in a mouse model of retinal detachment, when BNN27 was administered intraperitoneally in a concentration of 200 mg/kg *(Tsoka et al. 2018)*. It is worth noting that the doses of BNN27 used in the aforementioned studies, 10 mg/kg; 50 mg/kg; 200 mg/kg *(Ibán-Arias et al. 2019) (Tsoka et al. 2018)*, are significantly (10-200 times) higher compared to BNN27 doses used in our study (0.66 mg/kg or 10 mM; 3.3 mg/kg or 50 mM).

Having some positive results from BNN27 administration, we decided to conduct another experiment, administrating BNN27 eye drops once every 2 days for 2 weeks. In agreement with the previous 1-week experiment, RGC survival and the level of astroglial activation were evaluated. Another promising result was demonstrated this time by both BNN27 concentrations administrated (10 mM; 50 mM). BNN27 administration presented a trend for RGC protection 14 days post injury. At this point, regarding the lack of statistical significance of the detected trend, it is interesting to note that aside from the small number of animals used, another reason may be the increased interval time among BNN27 dose administration. Specifically, in the 1-week experiment mice received treatment daily, whereas in this experiment (2-week) mice were treated every 48 h. It is possible then, that BNN27 had already been cleared from the injury site, via diffusing in the surrounding tissue, before the next dose was administrated, leading to reduced efficacy of the treatment. Moreover, in line with the results from previous experiments, BNN27 administration failed to attenuate the increased activation levels of astroglial cells in injured retinas 14 days after crush.

Summarizing the findings of this section, BNN27 administration demonstrated a trend for RGC protection against ONC-induced apoptosis when administered via eye drops, either daily for 1 week or once every 2 days for 2 weeks. However, no significant alteration was observed in the amount of $GFAP^+$ astroglial cell processes in injured retinas treated with BNN27 eye drops for the same periods.

4.3 Effects of BNN27 Delivery via Biomaterials on ONC

Since BNN27 administration via eye drops yielded some promising findings regarding the survival of RGCs, we then decided to follow a biomaterial-based delivery approach. An additional reason for pursuing a biomaterial delivery approach is that when using eye drop delivery, the intraocular bioavailability of the drug is rather poor due to various factors such as nasolachrymal drainage, drug dilution with tears, conjunctival absorption, etc. Otherwise stated, only a small portion of the substance meant to be delivered, actually reaches the intended target when using eye drops. For this purpose, BNN27 was entrapped in a peptide gel formed inside a porous collagen-GAG scaffold. Once the scaffold was placed at the injury site, BNN27 would be gradually released to the animal tissue, achieving targeted delivery to the injury site. Another reason for selecting this strategy was that the route through which target cells uptake BNN27 is of importance. For instance, if RGCs uptake BNN27 through their axons (when BNN27 is delivered to the ON via scaffold), or through other receptors facing the retina (when BNN27 is delivered via eye drops), may be of importance for the end-result of BNN27 course of action.

Our findings from this experiment demonstrated that BNN27 was unable to rescue injured RGCs from ONC-induced apoptosis as well as to reduce the activation of astrocytes and Müller cells 2 weeks after injury. Moreover, concerning the use of the peptide gel, no adverse effects were observed on the survival of RGCs and the activation of astroglial cells as a consequence of using the peptide gel. Although, BNN27 effect on astroglial activation was anticipated based on the results of our previous experiments using BNN27 eye drops, the observed lack of effect on RGC survival was unexpected. This outcome can be explained due to the use of very low BNN27 dose (50 μM) utilized in this experiment in comparison with the previously described eye drop experiments (BNN27 doses: 10 mM, 50 mM). It should be noted that this low BNN27 dose (50 μM) was chosen based on BNN27 solubility, in order to keep BNN27 entirely soluble in the solution used to form the peptide gel. Feedback from Dr. Theodora Callogeropoulou suggested that we should use the same BNN27 concentration as used in previous experiments (10 mM; 50 mM). Moreover, another explanation would be that BNN27 was released from the peptide gel and diffused to the animal tissue much faster than we expected, due to inability of the peptide gel to sufficiently delay the release of BNN27.

To conclude, findings from this first experiment on biomaterial-based BNN27 delivery suggest that BNN27 did not achieve to maintain RGC density or reduce astroglial activation in injured retinas 14 days after crush when delivered via a peptide gel formed inside a porous collagen-GAG scaffold. Even though some of these results may seem unexpected, the reasons for this outcome are illuminated and therefore this experiment has true potential for improvement.

Aiming to further prolong the delivery of BNN27 from the porous collagen-GAG scaffold we decided to develop a procedure where BNN27 is covalently conjugated on our scaffold. During this process, the scaffold is originally activated using a cross-linking agent, SPDP, and then treated with TC447, a synthetic compound created to link BNN27 with the collagen-GAG scaffold. After TC447 is conjugated on the SPDP-activated scaffold, BNN27 is chemically linked on TC447 completing the procedure. In this study, due to certain time limits, we focused our work on activating the collagen-GAG scaffold using SPDP and then covalently conjugating TC447 on the scaffold.

Our results demonstrate that TC447 is successfully conjugated on SPDP-activated scaffolds whereas it does not detach after being washed overnight, indicating that TC447 is conjugated via a covalent

bond. Additionally, when TC447-conjugated scaffolds are treated with 25 mM DTT, the detected emission resulting from TC447 is significantly reduced. This finding can be explained by the fact that DTT cleaves the disulfide bond connecting TC447 to the scaffold, enabling the successful removal of TC447 and further supporting that TC447 conjugation on the scaffold is covalent.

Moreover, some amount of TC447 is observed to be conjugated on porous collagen-GAG scaffolds in an uneven manner. This event may occur due to unspecific interactions of TC447 with GAG or due to inadequate solubilization of TC447.

Finally, an important result yielded from this experiment is that TC447 conjugation is significantly augmented in SPDP-activated scaffolds that were first treated with DTT and then with TC447. This finding suggests that the microenvironment created as an outcome of chemical interactions among SPDP, collagen-GAG and DTT, favors the conjugation of TC447 on the scaffold in a more efficient manner compared to TC447 conjugation on SPDP-activated scaffold alone.

Collectively, the results from this experiment suggest that TC447 conjugation on SPDP-activated porous collagen-GAG scaffolds occurs via a covalent bond, whereas some amount of TC447 may be conjugated on scaffolds due to unspecific interactions of TC447 with GAG or due to inadequate TC447 solubilization. Importantly, it was observed that TC447 conjugation is highly enhanced on SPDP-activated scaffolds treated with DTT prior to TC447. This finding indicates that chemical interactions among SPDP, collagen-GAG and DTT lead to the generation of a microenvironment that promotes TC447 conjugation on this scaffold more efficiently compared to TC447 conjugation on SPDP-activated scaffold alone.

In conclusion, the results from this section demonstrated that BNN27 did not present any neuroprotective effects on RGC survival and astroglial activation 14 days after crush when delivered via a peptide gel formed inside a porous collagen-GAG scaffold. However, the reasons underlying these results are recognized giving this experiment potential for improvement. Furthermore, TC447 is successfully conjugated on SPDP-activated collagen-GAG scaffolds in a covalent manner, although some amount of unspecific TC447 conjugation is observed. Last but not least, TC447 conjugation on SPDP-activated scaffolds treated first with DTT and then with TC447 is significantly increased, indicating that the microenvironment generated as an outcome of chemical interactions among SPDP, collagen-GAG and DTT, favors the conjugation of TC447 on the scaffold in a more efficient manner compared to TC447 conjugation on SPDP-activated scaffold alone.

4.4 Concluding Remarks

This study focused on quantifying the effects of microneurotrophin BNN27 on key cell phenotypes after optic nerve crush (ONC) injury in mice. BNN27 was delivered by two strategies: i) BNN27 administration via eye drops and ii) BNN27 delivery using biomaterials. Biomaterial delivery of BNN27 was pursued via two approaches. In the first approach, BNN27 was entrapped in a gel formed by self-assembled peptides inside a porous collagen-GAG scaffold, which afterwards was placed directly around a crushed ON injury site. During the second approach, BNN27 was covalently conjugated on porous collagen-GAG scaffolds.

In this study we presented a successful and reproducible ONC injury which induces RGC apoptosis, astroglial activation and a trend for TrkC downregulation 1 and 2 weeks after crush. Furthermore, no significant alterations were observed in the expression of $p75^{NTR}$, TrkA, TrkB, and no clear effect of ONC was detected on IBA1 7 and 14 days post injury. Regarding our first strategy BNN27 administration demonstrated a trend for RGC protection against ONC-induced apoptosis when administered via eye drops, either daily for 1 week or once every 2 days for 2 weeks. However, no significant alteration was observed in the amount of $GFAP^{+}$ astroglial cell processes in injured retinas treated with BNN27 eye drops for the same periods. Concerning our second strategy, delivery of BNN27 via a peptide gel formed inside a porous collagen-GAG scaffold did not present any neuroprotective effects on RGC survival and astroglial activation 14 days after crush, yet this method is characterized by potential for improvement. In addition, TC447 is covalently conjugated on a porous collagen-GAG scaffold in successful way, although some non-specific TC447 conjugation was observed. Importantly, TC447 conjugation is significantly augmented on SPDP-activated scaffolds treated with DTT prior to TC447, suggesting that chemical interactions among SPDP, collagen-GAG and DTT lead to the generation of a microenvironment that favors the conjugation of TC447 on this scaffold in a more efficient manner compared to TC447 conjugation on SPDP-activated scaffold alone.

The results of this study can shed light in the field of tissue regeneration after optic nerve injury producing valuable information about BNN27 effects on retinal tissue regeneration in mice. Lastly, this study generates new knowledge on the field of research treatments for TON, providing data on novel drug delivery strategies, facilitating the development of innovative TON treatments.

Appendix

A1. SPDP Functionalization of a Porous Collagen Scaffold Sample

Xenofon Mallios, July 2020
Based on Tsakanika, 2019

Reagents

- SPDP 20 mM stock solution | Sigma-Aldrich (P3415)
- EDTA 0.5M | Thermo Fisher Scientific (15575020)
- PBS
- Porous collagen scaffold sample (1 mm x 1 mm x 1.5 mm)

Equipment

- 1.5ml eppendorf tubes
- 50 ml Falcon tube
- Shaker
- Forceps
- Pipettes

Procedure

1. Prepare 1 mM EDTA in PBS inside a 50 ml falcon tube.
   - Recipe for 40 ml: Add 80µl EDTA 0.5 M to 40 ml PBS, mix well.
2. Prepare 500 µM SPDP working solution in PBS-EDTA 1mM.
   - Recipe for 200 µl (~ 4 reactions $V_{REACTION}$ = 50µl): add 5 µl 20 mM SPDP to 195 µl 1 mM EDTA in PBS.
3. Use a pipette to add 50 µl 500 µM SPDP in an eppendorf tube.
4. Use forceps to transfer a scaffold inside a 1.5 ml eppendorf tube.
   - Make sure the scaffold is completely immersed in the SPDP working solution.
5. Incubate for 1 hour at room temperature (RT).
   - Pipette briefly (4-6 times) up to 150-200 µl every 15 min.
   - Be careful not to draw / damage scaffold with tip.
6. Use a pipette to carefully remove the 50 µl SPDP working solution from the eppendorf tube.
7. Wash 3 times in 1 ml 1 mM PBS-EDTA solution.
   - Add 1 ml 1 mM EDTA-PBS in the eppendorf tube.
   - Incubate for 10 min at room temperature (RT).
   - Pipette briefly (4-6 times) up to 150-200 µl every 5 min.
   - Be careful not to draw / damage scaffold with tip.
8. Discard 1 mM EDTA-PBS solution.
9. Place scaffold in 1 ml PBS overnight at 4°C.
   - For better washing efficiency place at eppendorf rotator.
10. Store scaffold in 1ml PBS at 4°C.

A2. TC447 Conjugation With an SPDP-Activated Porous Collagen Scaffold

Xenofon Mallios, July 2020
Based on Tsakanika, 2019

Reagents

- TC447 10mM stock solution. TC447 is **sensitive to light**, it must be protected at all times. It must be stored at **-20°C wrapped in aluminium foil**.
- DMSO Sigma-Aldrich (D6879)
- PBS

Equipment

- Eppendorf tubes
- Forceps
- Pipette
- Aluminium foil
- SPDP-activated porous scaffold sample (1mm x 1mm x 1.5mm)

Procedure

1. Prepare 100 μM TC447 (intermediate dilution) in DMSO.
   - Recipe for 1 ml: Add 10 μl 10 mM TC447 stock solution to 990 μl DMSO, mix well.
   - Store at -20°C, protect from light.
2. Prepare 5 μM TC447 (working solution) in DMSO.
   - The reaction volume required per scaffold is 50 μl.
   - Recipe for 500 μl: Add 25 μl 100 μM TC447 to 975 μl DMSO, mix well.
   - Store at -20°C, protect from light.
3. Close lights before proceeding to the next steps.
4. Use a pipette to remove PBS solution from 1.5 ml eppendorf tube that contains the SPDP-activated scaffold.
5. Use a pipette to add 50 μl 5 μM TC447 in the eppendorf tube.
   - Make sure the SPDP-activated scaffold is totally immersed in 5 μM TC447 solution.
6. Wrap eppendorf tube with aluminium foil to protect from light.
7. Incubate 24 h (overnight) at 4°C.
8. Wash 3 times in 1 ml PBS.
   - Add 1 ml PBS in the eppendorf tube.
   - Incubate for 10 min at room temperature (RT).
   - Pipette briefly (4-6 times) up to 150-200 μl every 5 min.
   - Be careful not to draw / damage scaffold with tip.
9. Discard PBS.
10. Place scaffold in 1 ml PBS overnight at 4°C.
    - For better washing efficiency place at eppendorf rotator.
11. Store in PBS at 4°C for up to 24 h.

Recipe for TC447 Solution				
TC447 Concentration [µM]	**TC447 10 mM Volume [µl]**	**TC447 100 µM Volume [µl]**	**DMSO Volume [µl]**	**Final Solution Volume [µl]**
50	1	-	199	200
5	-	10	190	200
0.5	-	1	199	200

A3. Quantification of SPDP-Activated Amine Groups in Porous Collagen Scaffold

Xenofon Mallios, July 2020
Based on Tsakanika, 2019

Reagents

- 1M DTT (Minotech, K09-1)
- PBS 1x

Equipment

- Synergy™ HTX Multi-Mode Reader (Biotek)
- 96-well-plate (Thermo Fisher, 167008)
- Pipette
- SPDP-activated porous scaffold sample (1 mm x 1 mm x 1.5 mm)

Procedure

1. Prepare 25 mM DTT in PBS
   - Recipe for 500 µl: Add 12.5 µl 1 M DTT (stock solution) to 487.5 µl PBS, mix well. Prepare always fresh.
2. Add 100 µl 25 mM DTT in eppendorf tube and carefully place SPDP-activated scaffold inside using forceps.
3. Incubate for 1 h at RT.
   - Pipette briefly (4-6 times) up to 30-40 µl every 15 min.
   - Be careful not to draw / damage scaffold with tip.
4. Transfer supernatant (V = 100 µl) in 96-well-plate and measure absorbance of pyridine 2-thione (product of SPDP reduction via DTT) at 343 nm in Synergy™ HTX Multi-Mode Reader (Biotek).
5. The quantity (moles) of activated amine groups are equal to the moles of pyridine 2-thione released by DTT.

Based on Beer-Lampert Law:

$$A = \varepsilon \cdot c \cdot l$$

the absorbance A of the solution depends on the molar attenuation coefficient ε (in M^{-1} cm^{-1}) of the absorbing molecule, the concentration c of the absorbing molecule, and the optical path length (unit: cm) where absorbance takes place. Finally, the concentration c can be expressed as $c = n/V$ (where n is in units of moles and V in units of L) therefore:

$$A = \varepsilon \cdot \frac{n}{V} \cdot l$$

The optical length (in cm) can be expressed as a function of the solution volume (in L) and the well radium (in mm) as:

$$V = 10^{-5}\pi r^2 l$$

Combining the previous three equations, and correcting for appropriate units, n can be estimated based on absorbance A measurements as:

$$n = 10^{-5}\pi \frac{A}{\varepsilon} r^2$$

Where ε is in units $M^{-1}\,cm^{-1}$ and r is in units mm. In the case of pyridine 2-thione (ε = 8080 $M^{-1}cm^{-1}$) measurements in a 96-well plate (r = 3 mm), the quantity of released (by DTT) pyridine 2-thione can be estimated as:

$$n_{P2T} = 10^{-5}\pi \frac{A}{8080} 3^2 = 3.5 \cdot 10^{-8} \cdot A$$

Since the quantity n_{p2t} of released pyridine 2-thione equals the quantity n_{SPDP} of SPDP-activated -NH_2 in the scaffold, the fraction of SPDP-activated -NH_2 in the scaffold equals:

$$f_{activated} = \frac{n_{SPDP}}{n_{NH2,collagen}}$$

References

Abdesselem, Houari, Aleksandra Shypitsyna, Gonzalo P. Solis, Vsevolod Bodrikov, and Claudia A. O. Stuermer. 2009. "No Nogo66- and NgR-mediated inhibition of regenerating axons in the zebrafish optic nerve." *Journal of Neuroscience*. doi: 10.1523/JNEUROSCI.3561-09.2009.

Agudo, M., M. C. Perez-Marin, U. Lonngren, P. Sobrado, A. Conesa, I. Canovas, M. Salinas-Navarro, J. Miralles-Imperial, F. Hallbook, and M. Vidal-Sanz. 2008. "Time course profiling of the retinal transcriptome after optic nerve transection and optic nerve crush." *Mol Vis* no. 14:1050-63.

Agudo, Marta, Maria C. Pérez-Marín, Paloma Sobrado-Calvo, Ulrika Lönngren, Manuel Salinas-Navarro, Isabel Cánovas, Francisco M. Nadal-Nicolás, Jaime Miralles-Imperial, Finn Hallböök, and Manuel Vidal-Sanz. 2009. "Immediate upregulation of proteins belonging to different branches of the apoptotic cascade in the retina after optic nerve transection and optic nerve crush." *Investigative Ophthalmology and Visual Science* no. 50 (1):424-431. doi: 10.1167/iovs.08-2404.

Ahmad, Syed Shoeb. 2017. An introduction to DARC technology. Elsevier B.V.

Ahmed, Nuzhat. 2006. "15 Role of Integrins in Ovarian Cancer." In, 425-439. Elsevier Inc.

Akaike, Akinori, Yukihiro Ohno, Masashi Sasa, and Shuji Takaori. 1987. "Excitatory and inhibitory effects of dopamine on neuronal activity of the caudate nucleus neurons in vitro." *Brain Research* no. 418 (2):262-272. doi: 10.1016/0006-8993(87)90094-1.

Allen, Shelley J., David Dawbarn, Maria G. Spillantini, Michel Goedert, Gordon K. Wilcock, Timothy H. Moss, and Frances M. Semenenko. 1989. "Distribution of β-nerve growth factor receptors in the human basal forebrain." *Journal of Comparative Neurology* no. 289 (4):626-640. doi: 10.1002/cne.902890408.

Almasieh, Mohammadali, Ariel M. Wilson, Barbara Morquette, Jorge Luis Cueva Vargas, and Adriana Di Polo. 2012. The molecular basis of retinal ganglion cell death in glaucoma. Prog Retin Eye Res.

Anatomyczar. Optic nerve parts.

Ankerhold, Richard, Christian A. Leppert, Martin Bastmeyer, and Claudia A. O. Stuermer. 1998. "E587 antigen is upregulated by goldfish oligodendrocytes after optic nerve lesion and supports retinal axon regeneration." *GLIA*. doi: 10.1002/(SICI)1098-1136(199807)23:3<257::AID-GLIA8>3.0.CO;2-1.

Anthony Altar, C., Ning Cai, Tricia Bliven, Melissa Juhasz, James M. Conner, Ann L. Acheson, Ronald M. Lindsay, and Stanley J. Wiegand. 1997. "Anterograde transport of brain-derived neurotrophic factor and its role in the brain." *Nature* no. 389 (6653):856-860. doi: 10.1038/39885.

Asher, Richard A., Daniel A. Morgenstern, Penny S. Fidler, Kathryn H. Adcock, Atsuhiko Oohira, Janet E. Braistead, Joel M. Levine, Richard U. Margolis, John H. Rogers, and James W. Fawcett. 2000. "Neurocan is upregulated in injured brain and in cytokine-treated astrocytes." *Journal of Neuroscience* no. 20 (7):2427-2438. doi: 10.1523/jneurosci.20-07-02427.2000.

Badea, Tudor C., Hugh Cahill, Jen Ecker, Samer Hattar, and Jeremy Nathans. 2009. "Distinct Roles of Transcription Factors Brn3a and Brn3b in Controlling the Development, Morphology, and Function of Retinal Ganglion Cells." *Neuron*. doi: 10.1016/j.neuron.2009.01.020.

Bähr, Mathias. 2000. Live or let die - Retinal ganglion cell death and survival during development and in the lesioned adult CNS. Trends Neurosci.

Barres, B. A., M. C. Raff, F. Gaese, I. Bartke, G. Dechant, and Y. A. Barde. 1994. "A crucial role for neurotrophin-3 in oligodendrocyte development." *Nature* no. 367 (6461):371-375. doi: 10.1038/367371a0.

Bastakis, G. G., N. Ktena, D. Karagogeos, and M. Savvaki. 2019. "Models and treatments for traumatic optic neuropathy and demyelinating optic neuritis." *Dev Neurobiol* no. 79 (8):819-836. doi: 10.1002/dneu.22710.

Becker, Catherina G., and Thomas Becker. 2002. "Repellent guidance of regenerating optic axons by chondroitin sulfate glycosaminoglycans in zebrafish." *Journal of Neuroscience*. doi: 10.1523/jneurosci.22-03-00842.2002.

Becker, Thomas, and Catherina G. Becker. 2014. Axonal regeneration in zebrafish.

Benevento, J. D., J. P. S. Garcia, A. B. Baxter, P. M. T. Garcia, R. A. Holliday, and R. B. Rosen. 2004. "Optic Nerve Measurements in Normal Human Eyes by MRI." *Investigative Ophthalmology & Visual Science* no. 45 (13):2398-2398.

Benfey, Martin, and Albert J. Aguayo. 1982. "Extensive elongation of axons from rat brain into peripheral nerve grafts." *Nature* no. 296 (5853):150-152. doi: 10.1038/296150a0.

Bennett, J. L., S. R. Zeiler, and K. R. Jones. 1999. "Patterned expression of BDNF and NT-3 in the retina and anterior segment of the developing mammalian eye." *Investigative ophthalmology & visual science* no. 40 (12):2996-3005.

Benowitz, L. I., V. E. Shashoua, and M. G. Yoon. 1981. "Specific changes in rapidly transported proteins during regeneration of the goldfish optic nerve." *Journal of Neuroscience*. doi: 10.1523/jneurosci.01-03-00300.1981.

Benson, M. Douglas, Mario I. Romero, Mark E. Lush, Q. Richard Lu, Mark Henkemeyer, and Luis F. Parada. 2005. "Ephrin-B3 is a myelin-based inhibitor of neurite outgrowth." *Proceedings of the National Academy of Sciences of the United States of America* no. 102 (30):10694-10699. doi: 10.1073/pnas.0504021102.

Berkelaar, M., D. B. Clarke, Y. C. Wang, G. M. Bray, and A. J. Aguayo. 1994. "Axotomy results in delayed death and apoptosis of retinal ganglion cells in adult rats." *Journal of Neuroscience* no. 14 (7):4368-4374. doi: 10.1523/jneurosci.14-07-04368.1994.

Bilsland, L. G., and G. Schiavo. 2009. "Axonal Transport Tracers." In, 1209-1216. Elsevier Ltd.

Bohm, M. R., S. Pfrommer, C. Chiwitt, M. Bruckner, H. Melkonyan, and S. Thanos. 2012. "Crystallin-beta-b2-overexpressing NPCs support the survival of injured retinal ganglion cells and photoreceptors in rats." *Invest Ophthalmol Vis Sci* no. 53 (13):8265-79. doi: 10.1167/iovs.12-10334.

Bomze, Howard M., Ketan R. Bulsara, Bermans J. Iskandar, Pico Caroni, and J. H. Pate Skene. 2001. "Spinal axon regeneration evoked by replacing two growth cone proteins in adult neurons." *Nature Neuroscience* no. 4 (1):38-43. doi: 10.1038/82881.

Bonilla, Iris E., Katsuhisa Tanabe, and Stephen M. Strittmatter. 2002. "Small proline-rich repeat protein 1A is expressed by axotomized neurons and promotes axonal outgrowth." *Journal of Neuroscience* no. 22 (4):1303-1315. doi: 10.1523/JNEUROSCI.22-04-01303.2002.

Bothwell, M. 1995. "Functional Interactions of Neurotrophins and Neurotrophin Receptors." *Annual Review of Neuroscience* no. 18 (1):223-253. doi: 10.1146/annurev.ne.18.030195.001255.

Brady, Roseann, Syed Ishrat All Zaidi, Catherine Mayer, and David M. Katz. 1999. "BDNF is a target-derived survival factor for arterial baroreceptor and chemoafferent primary sensory neurons." *Journal of Neuroscience* no. 19 (6):2131-2142. doi: 10.1523/JNEUROSCI.19-06-02131.1999.

Bringmann, Andreas, Ianors Iandiev, Thomas Pannicke, Antje Wurm, Margrit Hollborn, Peter Wiedemann, Neville N. Osborne, and Andreas Reichenbach. 2009. Cellular signaling and factors involved in Müller cell gliosis: Neuroprotective and detrimental effects.

Bringmann, Andreas, Thomas Pannicke, Jens Grosche, Mike Francke, Peter Wiedemann, Serguei N. Skatchkov, Neville N. Osborne, and Andreas Reichenbach. 2006. Müller cells in the healthy and diseased retina. Prog Retin Eye Res.

Brockerhoff, Susan E. 2006. "Measuring the optokinetic response of zebrafish larvae." *Nature Protocols* no. 1 (5):2448-2451. doi: 10.1038/nprot.2006.255.

Brown, Richard E., and Sarah Bolivar. 2018. "The importance of behavioural bioassays in neuroscience." *Journal of Neuroscience Methods* no. 300:68-76. doi: 10.1016/j.jneumeth.2017.05.022.

Bruce-Gregorios, Jocelyn H. 2006. *Histopathologic Techniques*. Second edi ed: Goodwill Trading Co.,Inc.

Bruno, V., U. Scapagnini, and P. L. Canonico. 1993. "Excitatory amino acids and neurotoxicity." *Functional neurology* no. 8 (4):279-292.

Buccafusco, Jerry J. 2009. "Methods of Behavior Analysis in Neuroscience. 2nd edition. Boca Raton (FL): CRC Press." In, 247-258. CRC Press/Taylor & Francis.

Budak, Yasemin, and Akdoğan Müberra. 2010. "Retinal ganglion cell death in glaucoma. Chapter 2." *Ocular Disease: Mechanisms and Management*:207-213. doi: 10.1016/B978-0-7020-2983-7.00027-9.

Butt, Arthur M., M. Pugh, P. Hubbard, and G. James. 2004. Functions of optic nerve glia: Axoglial signalling in physiology and pathology. Nature Publishing Group.

Butt, Arthur M., and Bruce R. Ransom. 1989. "Visualization of oligodendrocytes and astrocytes in the intact rat optic nerve by intracellular injection of lucifer yellow and horseradish peroxidase." *Glia* no. 2 (6):470-475. doi: 10.1002/glia.440020609.

Butt, Arthur M., and Bruce R. Ransom. 1993. "Morphology of astrocytes and oligodendrocytes during development in the intact rat optic nerve." *Journal of Comparative Neurology* no. 338 (1):141-158. doi: 10.1002/cne.903380110.

Calkins, David J. 2012. Critical pathogenic events underlying progression of neurodegeneration in glaucoma. Prog Retin Eye Res.

Cantley, Lewis C. 2002. The phosphoinositide 3-kinase pathway. American Association for the Advancement of Science.

Ceccatelli, S., P. Ernfors, M. J. Villar, H. Persson, and T. Hökfelt. 1991. "Expanded distribution of mRNA for nerve growth factor, brain-derived neurotrophic factor, and neurotrophin 3 in the rat brain after colchicine treatment." *Proceedings of the National Academy of Sciences of the United States of America* no. 88 (22):10352-10356. doi: 10.1073/pnas.88.22.10352.

Chang, Min Lin, Ching Hsiang Wu, Ya Fen Jiang-shieh, Jeng Yung Shieh, and Chen Yuan Wen. 2007. "Reactive changes of retinal astrocytes and Müller glial cells in kainate-induced neuroexcitotoxicity." *Journal of Anatomy* no. 210 (1):54-65. doi: 10.1111/j.1469-7580.2006.00671.x.

Chao, Moses V. 2003. "Neurotrophins and their receptors: A convergence point for many signalling pathways." *Nature Reviews Neuroscience* no. 4 (4):299-309. doi: 10.1038/nrn1078.

Chao, Moses V., and Mark Bothwell. 2002. Neurotrophins: To cleave or not to cleave. Cell Press.

Chaon, Benjamin C., and Michael S. Lee. 2015. "Is there treatment for traumatic optic neuropathy?" *Current Opinion in Ophthalmology* no. 26 (6):445-449. doi: 10.1097/ICU.0000000000000198.

Checa-Casalengua, Patricia, Caihui Jiang, Irene Bravo-Osuna, Budd A. Tucker, Irene T. Molina-Martínez, Michael J. Young, and Rocío Herrero-Vanrell. 2011. "Retinal ganglion cells survival in a glaucoma model by GDNF/Vit e PLGA microspheres prepared according to a novel microencapsulation procedure." *Journal of Controlled Release* no. 156 (1):92-100. doi: 10.1016/j.jconrel.2011.06.023.

Chen, H., and A. J. Weber. 2004. "Brain-derived neurotrophic factor reduces TrkB protein and mRNA in the normal retina and following optic nerve crush in adult rats." *Brain Res* no. 1011 (1):99-106. doi: 10.1016/j.brainres.2004.03.024.

Chen, Malo S., Andrea B. Huber, Marjan E. D. Van Der Haar, Marcus Frank, Lisa Schnell, Adrian A. Spillmann, Franziska Christ, and Martin E. Schwab. 2000. "Nogo-A is a myelin-associated neurite outgrowth inhibitor and an antigen for monoclonal antibody IN-1." *Nature* no. 403 (6768):434-439. doi: 10.1038/35000219.

Chierzi, Sabrina, Enrica Strettoi, Maria Cristina Cenni, and Lamberto Maffei. 1999. "Optic nerve crush: Axonal responses in wild-type and bcl-2 transgenic mice." *Journal of Neuroscience* no. 19 (19):8367-8376. doi: 10.1523/jneurosci.19-19-08367.1999.

Chlipala, Elizabeth, Christine M. Bendzinski, Kevin Chu, Joshua I. Johnson, Miles Brous, Karen Copeland, and Brad Bolon. 2020. "Optical density-based image analysis method for the evaluation of hematoxylin and eosin staining precision." *Journal of Histotechnology* no. 43 (1):29-37. doi: 10.1080/01478885.2019.1708611.

ClinSciences. Luxol fast blue (LBF) stain Clinisciences.

Cockerham, Glenn C., Gregory L. Goodrich, Eric D. Weichel, James C. Orcutt, Joseph F. Rizzo, Kraig S. Bower, and Ronald A. Schuchard. 2009. "Eye and visual function in traumatic brain injury." *Journal of Rehabilitation Research and Development* no. 46 (6):811-818. doi: 10.1682/JRRD.2008.08.0109.

Cockerham, Glenn C., Thomas A. Rice, Eva H. Hewes, Kimberly P. Cockerham, Sonne Lemke, Gloria Wang, Richard C. Lin, Catherine Glynn-Milley, and Lars Zumhagen. 2011. Closed-eye ocular injuries in the Iraq and Afghanistan wars. Massachussetts Medical Society.

Condorelli, Daniele F., Tuija Salin, Paola Dell'Albani, Giuseppa Mudò, Massimo Corsaro, Tonis Timmusk, Madis Metsis, and Natale Belluardo. 1995. "Neurotrophins and theirtrk receptors in cultured cells of the glial lineage and in white matter of the central nervous system." *Journal of Molecular Neuroscience* no. 6 (4):237-248. doi: 10.1007/BF02736783.

Connor, B., and M. Dragunow. 1998. The role of neuronal growth factors in neurodegenerative disorders of the human brain. Brain Res Brain Res Rev.

Crawley, Jacqueline N. 2007. *What's Wrong With My Mouse?* Hoboken, NJ, USA: John Wiley & Sons, Inc.

Cui, Qi. 2006. Actions of neurotrophic factors and their signaling pathways in neuronal survival and axonal regeneration. Humana Press.

D'Amelio, Marcello, Morgan Sheng, and Francesco Cecconi. 2012. Caspase-3 in the central nervous system: Beyond apoptosis. Trends Neurosci.

David, S., and A. Aguayo. 1981. "Axonal elongation into peripheral nervous system "bridges" after central nervous system injury in adult rats." *Science* no. 214 (4523):931-933. doi: 10.1126/science.6171034.

Dawbarn, D., S. J. Allen, and F. M. Semenenko. 1988a. "Coexistence of choline acetyltransferase and nerve growth factor receptors in the rat basal forebrain." *Neuroscience Letters* no. 94 (1-2):138-144. doi: 10.1016/0304-3940(88)90284-4.

Dawbarn, D., S. J. Allen, and F. M. Semenenko. 1988b. "Immunohistochemical localization of β-nerve growth factor receptors in the forebrain of the rat." *Brain Research* no. 440 (1):185-189. doi: 10.1016/0006-8993(88)91175-4.

Dawson, Valina L. 2005. Molecular mechanisms in neuronal and axonal apoptosis and necrosis.

de Hoz, Rosa, Beatriz I. Gallego, Ana I. Ramírez, Blanca Rojas, Juan J. Salazar, Francisco J. Valiente-Soriano, Marcelino Avilés-Trigueros, Maria P. Villegas-Perez, Manuel Vidal-Sanz, Alberto Triviño, and José M. Ramírez. 2013. "Rod-Like Microglia Are Restricted to Eyes with Laser-Induced Ocular Hypertension but Absent from the Microglial Changes in the Contralateral Untreated Eye." *PLoS ONE* no. 8 (12):e83733-e83733. doi: 10.1371/journal.pone.0083733.

De Lima, Silmara, Yoshiki Koriyama, Takuji Kurimoto, Julia Teixeira Oliveira, Yuqin Yin, Yiqing Li, Hui Ya Gilbert, Michela Fagiolini, Ana Maria Blanco Martinez, and Larry Benowitz. 2012. "Erratum: Full-length axon regeneration in the adult mouse optic nerve and partial recovery of simple visual behaviors (Proceedings of the National Academy of Sciences of the United States of America (2012) 109, 23, (9149-9154) doi:10.1073/pnas.1119449109)." *Proceedings of the National Academy of Sciences of the United States of America* no. 109 (33):13465-13465. doi: 10.1073/pnas.1211885109.

Dechant, Georg, and Yves Alain Barde. 2002. The neurotrophin receptor p75NTR: Novel functions and implications for diseases of the nervous system. Nat Neurosci.

Deinhardt, Katrin, Taeho Kim, Daniel S. Spellman, Richard E. Mains, Betty A. Eipper, Thomas A. Neubert, Moses V. Chao, and Barbara L. Hempstead. 2011. "Neuronal growth cone retraction relies on proneurotrophin receptor signaling through rac." *Science Signaling* no. 4 (202). doi: 10.1126/scisignal.2002060.

Di Polo, Adriana, Ludwig J. Aigner, Robert J. Dunn, Garth M. Bray, and Albert J. Aguayo. 1998. "Prolonged delivery of brain-derived neurotrophic factor by adenovirus-infected Müller cells temporarily rescues injured retinal ganglion cells." *Proceedings of the National Academy of Sciences of the United States of America* no. 95 (7):3978-3983. doi: 10.1073/pnas.95.7.3978.

Dou, Chang Lin, and Joel M. Levine. 1994. "Inhibition of neurite growth by the NG2 chondroitin sulfate proteoglycan." *Journal of Neuroscience* no. 14 (12):7616-7628. doi: 10.1523/jneurosci.14-12-07616.1994.

Drew, Clifton P., and Wun Ju Shieh. 2015. "Immunohistochemistry." In, 109-115. Elsevier Inc.

Dreyer, Evan B., David Zurakowski, Robert A. Schumer, Steven M. Podos, and Stuart A. Lipton. 1996. "Elevated glutamate levels in the vitreous body of humans and monkeys with glaucoma." *Archives of Ophthalmology* no. 114 (3):299-305. doi: 10.1001/archopht.1996.01100130295012.

Duvdevani, R., M. Rosner, M. Belkin, J. Sautter, B. A. Sabel, and M. Schwartz. 1990. "Graded crush of the rat optic nerve as a brain injury model: Combining electrophysiological and behavioral outcome." *Restorative Neurology and Neuroscience* no. 2 (1):31-38. doi: 10.3233/RNN-1990-2104.

Edmund, Jens, and Erik Godtfredsen. 1963. "UNILATERAL OPTIC ATROPHY FOLLOWING HEAD INJURY." *Acta Ophthalmologica* no. 41 (6):693-697. doi: 10.1111/j.1755-3768.1963.tb03588.x.

Eggen, B. J. L., D. Raj, U. K. Hanisch, and H. W. G. M. Boddeke. 2013. Microglial phenotype and adaptation.

Eitan, Shoshana, Arieh Solomon, Vered Lavie, Eti Yoles, David L. Hirschberg, Michael Belkin, and Michal Schwartz. 1994. "Recovery of visual response of injured adult rat optic nerves treated with transglutaminase." *Science* no. 264 (5166):1764-1768. doi: 10.1126/science.7911602.

Elkabes. 1995. "DEVELOPMENTAL REGULATION OF NEUROTROPHIN-3
AND TRK C SPLICE VARIANTS IN OPTIC NERVE GLIA
IN VIVO."

Emran, Farida, Jason Rihel, and John E. Dowling. 2008. "A behavioral assay to measure responsiveness of zebrafish to changes in light intensities." *Journal of visualized experiments : JoVE* (20). doi: 10.3791/923.

Fagan, Anne M., Hong Zhang, Story Landis, Richard J. Smeyne, Inmaculada Silos-Santiago, and Mariano Barbacid. 1996. "TrkA, but not TrkC, receptors are essential for survival of sympathetic neurons in vivo." *Journal of Neuroscience* no. 16 (19):6208-6218. doi: 10.1523/JNEUROSCI.16-19-06208.1996.

Fain, Gordon, and Alapakkam P. Sampath. 2018. "Rod and cone interactions in the retina." *F1000Research*. doi: 10.12688/f1000research.14412.1.

Fang, Yuan, Xiaofen Mo, Wenyi Guo, Meng Zhang, Peihua Zhang, Yan Wang, Xianfang Rong, Jie Tian, and Xinghuai Sun. 2010. "A new type of Schwann cell graft transplantation to promote optic nerve regeneration in adult rats." *Journal of Tissue Engineering and Regenerative Medicine* no. 4 (8):581-589. doi: 10.1002/term.264.

Fariñas, Isabel, George A. Wilkinson, Carey Backus, Louis F. Reichardt, and Ardem Patapoutian. 1998. "Characterization of neurotrophin and Trk receptor functions in developing sensory ganglia: Direct NT-3 activation of TrkB neurons in vivo." *Neuron* no. 21 (2):325-334. doi: 10.1016/S0896-6273(00)80542-5.

Feng, Liang, Zhen Puyang, Hui Chen, Peiji Liang, John B. Troy, and Xiaorong Liu. 2017. "Overexpression of brain-derived neurotrophic factor protects large retinal ganglion cells after optic nerve crush in mice." *eNeuro* no. 4 (1):1-8. doi: 10.1523/ENEURO.0331-16.2016.

Fischer, Andrew H., Kenneth A. Jacobson, Jack Rose, and Rolf Zeller. 2008. "Hematoxylin and eosin staining of tissueand cell sections." *Cold Spring Harbor Protocols* no. 3 (5):4986-4988. doi: 10.1101/pdb.prot4986.

Flachsbarth, Kai, Katharina Kruszewski, Gila Jung, Wanda Jankowiak, Kristoffer Riecken, Lars Wagenfeld, Gisbert Richard, Boris Fehse, and Udo Bartsch. 2014. "Neural stem cell–based intraocular administration of ciliary neurotrophic factor attenuates the loss of axotomized ganglion cells in adult mice." *Investigative Ophthalmology and Visual Science* no. 55 (11):7029-7039. doi: 10.1167/iovs.14-15266.

Ford, Rebecca L., Vickie Lee, Wen Xing, and Catey Bunce. 2012. "A 2-year prospective surveillance of pediatric traumatic optic neuropathy in the United Kingdom." *Journal of AAPOS* no. 16 (5):413-417. doi: 10.1016/j.jaapos.2012.04.009.

Forrester, John V., Andrew D. Dick, Paul G. McMenamin, Fiona Roberts, and Eric Pearlman. 2015. *The eye: Basic sciences in practice*: Elsevier Inc.

Frade, J. M., A. Rodriguez-Tebar, and Y. A. Barde. 1996. "Induction of cell death by endogenous nerve growth factor through its p75 receptor." *Nature* no. 383 (6596):166-168. doi: 10.1038/383166a0.

Friedman, Neil J., Peter K. Kaiser, and William B. Trattler. 2016. *Review of Ophthalmology: Expert Consult*: Elsevier Health Sciences.

Galindo-Romero, Caridad, F. Javier Valiente-Soriano, M. Jiménez-López, Diego García-Ayuso, Maria P. Villegas-Pérez, Manuel Vidal-Sanz, and Marta Agudo-Barriuso. 2013. "Effect of brain-derived neurotrophic factor on mouse axotomized retinal ganglion cells and phagocytic microglia." *Investigative Ophthalmology and Visual Science* no. 54 (2):974-985. doi: 10.1167/iovs.12-11207.

Gallego, Beatriz I., Juan J. Salazar, Rosa de Hoz, Blanca Rojas, Ana I. Ramírez, Manuel Salinas-Navarro, Arturo Ortín-Martínez, Francisco J. Valiente-Soriano, Marcelino Avilés-Trigueros, Maria P. Villegas-Perez, Manuel Vidal-Sanz, Alberto Triviño, and Jose M. Ramírez. 2012. "IOP induces upregulation of GFAP and MHC-II and microglia reactivity in mice retina contralateral to experimental glaucoma." *Journal of Neuroinflammation* no. 9. doi: 10.1186/1742-2094-9-92.

Gao, Hua, Xiaoxi Qiao, Franz Hefti, Joe G. Hollyfield, and Beat Knusel. 1997. "Elevated mRNA expression of brain-derived neurotrophic factor in retinal ganglion cell layer after optic nerve injury." *Investigative Ophthalmology and Visual Science* no. 38 (9):1840-1847.

García-Caballero, Cristina, Esther Prieto-Calvo, Patricia Checa-Casalengua, Elena García-Martín, Vicente Polo-Llorens, Julián García-Feijoo, Irene Teresa Molina-Martínez, Irene Bravo-Osuna, and Rocío Herrero-Vanrell. 2017. "Six month delivery of GDNF from PLGA/vitamin E biodegradable microspheres after intravitreal injection in rabbits." *European Journal of Pharmaceutical Sciences* no. 103:19-26. doi: 10.1016/j.ejps.2017.02.037.

Garcia, Tarcyane Barata, Margrit Hollborn, and Andreas Bringmann. 2017. "Expression and signaling of NGF in the healthy and injured retina." *Cytokine and Growth Factor Reviews* no. 34:43-57. doi: 10.1016/j.cytogfr.2016.11.005.

George, Edwin B., Jonathan D. Glass, and John W. Griffin. 1995. "Axotomy-induced axonal degeneration is mediated by calcium influx through ion-specific channels." *Journal of Neuroscience* no. 15 (10):6445-6452. doi: 10.1523/jneurosci.15-10-06445.1995.

Gessner, Thomas, and Udo Mayer. 2000. Triarylmethane and Diarylmethane Dyes.

Giannaccini, Martina, Alice Usai, Federica Chiellini, Viviana Guadagni, Massimiliano Andreazzoli, Michela Ori, Massimo Pasqualetti, Luciana Dente, and Vittoria Raffa. 2018. "Neurotrophin-conjugated nanoparticles prevent retina damage induced by oxidative stress." *Cellular and Molecular Life Sciences* no. 75 (7):1255-1267. doi: 10.1007/s00018-017-2691-x.

Glajch, Kelly E., Laura Ferraiuolo, Kaly A. Mueller, Matthew J. Stopford, Varsha Prabhkar, Achille Gravanis, Pamela J. Shaw, and Ghazaleh Sadri-Vakili. 2016. "MicroNeurotrophins improve survival in motor neuron-astrocyte co-cultures but do not improve disease phenotypes in a mutant SOD1 mouse model of amyotrophic lateral sclerosis." *PLoS ONE* no. 11 (10). doi: 10.1371/journal.pone.0164103.

Glynn, Dervila, Rachel A. Bortnick, and A. Jennifer Morton. 2003. "Complexin II is essential for normal neurological function in mice." *Human molecular genetics* no. 12 (19):2431-2448. doi: 10.1093/hmg/ddg249.

Goedert, M., A. Fine, S. P. Hunt, and A. Ullrich. 1986. "Nerve growth factor mRNA in peripheral and central rat tissues and in the human central nervous system: Lesion effects in the rat brain and levels in

Alzheimer's disease." *Molecular Brain Research* no. 1 (1):85-92. doi: 10.1016/0169-328X(86)90023-9.
Goldman, Daniel. 2014. Müller glial cell reprogramming and retina regeneration.
González-Hoyuela, M., J. A. Barbas, and A. Rodríguez-Tébar. 2001. "The autoregulation of retinal ganglion cell number." *Development (Cambridge, England)* no. 128 (1):117-124.
Grant, S., and M. J. Keating. 1989. "Changing patterns of binocular visual connections in the intertectal system during development of the frog, Xenopus laevis." *Experimental Brain Research* no. 75 (1):117-132. doi: 10.1007/BF00248535.
Gravanis, Achille, Iosif Pediaditakis, and Ioannis Charalampopoulos. 2017. "Synthetic microneurotrophins in therapeutics of neurodegeneration." *Oncotarget* no. 8 (6):9005-9006. doi: 10.18632/oncotarget.14667.
Grinblat, Gabriela A., Reas S. Khan, Kimberly Dine, Howard Wessel, Larry Brown, and Kenneth S. Shindler. 2018. "RGC neuroprotection following optic nerve trauma mediated by intranasal delivery of amnion cell secretome." *Investigative Ophthalmology and Visual Science* no. 59 (6):2470-2477. doi: 10.1167/iovs.18-24096.
Gross, C. E., J. R. DeKock, W. R. Panje, N. Hershkowitz, and J. Newman. 1981. "Evidence for orbital deformation that may contribute to monocular blindness following minor frontal head trauma." *Journal of Neurosurgery* no. 55 (6):963-966. doi: 10.3171/jns.1981.55.6.0963.
Guo, Li, Benjamin M. Davis, Nivedita Ravindran, Joana Galvao, Neel Kapoor, Nasrin Haamedi, Ehtesham Shamsher, Vy Luong, Elena Fico, and M. Francesca Cordeiro. 2020. "Topical recombinant human Nerve growth factor (rh-NGF) is neuroprotective to retinal ganglion cells by targeting secondary degeneration." *Scientific reports* no. 10 (1):3375-3375. doi: 10.1038/s41598-020-60427-2.
Gusel'nikova, V. V., and D. E. Korzhevskiy. 2015. "NeuN as a neuronal nuclear antigen and neuron differentiation marker." *Acta Naturae* no. 7 (2):42-47.
Hajdú, Rozina I., Lenke K. Laurik, Klaudia Szabó, Bulcsú Dékány, Zsuzsanna Almási, Anna Énzsöly, Arnold Szabó, Tamás Radovits, Csaba Mátyás, Attila Oláh, Ágoston Szél, Gábor M. Somfai, Csaba Dávid, and Ákos Lukáts. 2019. "Detailed Evaluation of Possible Ganglion Cell Loss in the Retina of Zucker Diabetic Fatty (ZDF) Rats." *Scientific Reports* no. 9 (1):1-16. doi: 10.1038/s41598-019-46879-1.
Harada, Chikako, Takayuki Harada, Kazuaki Nakamura, Yasuo Sakai, Kohichi Tanaka, and Luis F. Parada. 2006. "Effect of p75NTR on the regulation of naturally occurring cell death and retinal ganglion cell number in the mouse eye." *Developmental biology* no. 290 (1):57-65. doi: 10.1016/j.ydbio.2005.08.051.
Harrington, Anthony W., Ju Young Kim, and Sung Ok Yoon. 2002. "Activation of Rac GTPase by p75 is necessary for c-jun N-terminal kinase-mediated apoptosis." *Journal of Neuroscience* no. 22 (1):156-166. doi: 10.1523/jneurosci.22-01-00156.2002.
Hata, Katsuhiko, Masashi Fujitani, Yuichi Yasuda, Hideo Doya, Tomoko Saito, Satoru Yamagishi, Bernhard K. Mueller, and Toshihide Yamashita. 2006. "RGMa inhibition promotes axonal growth and recovery after spinal cord injury." *Journal of Cell Biology* no. 173 (1):47-58. doi: 10.1083/jcb.200508143.
Hengartner, M. O. 2000. The biochemistry of apoptosis. Nature.
Hernandez, M. Rosario. 2000. The optic nerve head in glaucoma: Role of astrocytes in tissue remodeling. Prog Retin Eye Res.
Heuss, Neal D., Mark J. Pierson, Heidi Roehrich, Scott W. McPherson, Andrea L. Gram, Ling Li, and Dale S. Gregerson. 2018. "Optic nerve as a source of activated retinal microglia post-injury." *Acta neuropathologica communications* no. 6 (1):66-66. doi: 10.1186/s40478-018-0571-8.
Hilber, David J. 2011. "Eye injuries, active component, U.S. Armed Forces, 2000-2010." *MSMR* no. 18 (5):2-7.
Hines-Beard, Jessica, Jeffrey Marchetta, Sarah Gordon, Edward Chaum, Eldon E. Geisert, and Tonia S. Rex. 2012. "A mouse model of ocular blast injury that induces closed globe anterior and posterior pole damage." *Experimental Eye Research* no. 99 (1):63-70. doi: 10.1016/j.exer.2012.03.013.
Hirsch, Sabine, Mary Anne Cahill, and Claudia A. O. Stuermer. 1995. "Fibroblasts at the transection site of the injured goldfish optic nerve and their potential role during retinal axonal regeneration." *Journal of Comparative Neurology*. doi: 10.1002/cne.903600405.
Hofer, M., S. R. Pagliusi, A. Hohn, J. Leibrock, and Y. A. Barde. 1990. "Regional distribution of brain-derived neurotrophic factor mRNA in the adult mouse brain." *The EMBO journal* no. 9 (8):2459-2464.
Holahan, Matthew. 2015. "GAP-43 in synaptic plasticity: molecular perspectives." *Research and Reports in Biochemistry*:137-137. doi: 10.2147/RRBC.S73846.

Honda, Miki, Tomohiro Asai, Takuya Umemoto, Yoshihiko Araki, Naoto Oku, and Minoru Tanaka. 2011. "Suppression of choroidal neovascularization by intravitreal injection of liposomal SU5416." *Archives of Ophthalmology* no. 129 (3):317-321. doi: 10.1001/archophthalmol.2011.12.

Houlton, Josh, Nashat Abumaria, Simon F. R. Hinkley, and Andrew N. Clarkson. 2019. "Therapeutic potential of neurotrophins for repair after brain injury: A helping hand from biomaterials." *Frontiers in Genetics* no. 10 (JUL). doi: 10.3389/fnins.2019.00790.

Hovens, IrisBertha, Csaba Nyakas, and RegienGeertruida Schoemaker. 2014. "A novel method for evaluating microglial activation using ionized calcium-binding adaptor protein-1 staining: cell body to cell size ratio." *Neuroimmunology and Neuroinflammation* no. 1 (2):82-82. doi: 10.4103/2347-8659.139719.

Huang, Eric, and Louis Reichardt. 2001. "Neurotrophins: Roles in Neuronal Development and Function." *Annu Rev Neurosci*. no. 23 (1):1-7. doi: 10.1038/jid.2014.371.

Huang, R., Q. Lan, L. Chen, H. Zhong, L. Cui, L. Jiang, H. Huang, L. Li, S. Zeng, M. Li, X. Zhao, and F. Xu. 2018. "CD200Fc Attenuates Retinal Glial Responses and RGCs Apoptosis After Optic Nerve Crush by Modulating CD200/CD200R1 Interaction." *J Mol Neurosci* no. 64 (2):200-210. doi: 10.1007/s12031-017-1020-z.

Huang, Z. Josh, Alfredo Kirkwood, Tommaso Pizzorusso, Vittorio Porciatti, Bernardo Morales, Mark F. Bear, Lamberto Maffei, and Susumu Tonegawa. 1999. "BDNF regulates the maturation of inhibition and the critical period of plasticity in mouse visual cortex." *Cell* no. 98 (6):739-755. doi: 10.1016/S0092-8674(00)81509-3.

Huebner, Eric A., and Stephen M. Strittmatter. 2009. "Axon Regeneration in the Peripheral and Central Nervous Systems." *Results and Problems in Cell Differentiation. Author Manuscript* no. 48:1-25. doi: 10.1007/400.

Ibán-Arias, Ruth, Silvia Lisa, Smaragda Poulaki, Niki Mastrodimou, Ioannis Charalampopoulos, Achille Gravanis, and Kyriaki Thermos. 2019. "Effect of topical administration of the microneurotrophin BNN27 in the diabetic rat retina." *Graefe's Archive for Clinical and Experimental Ophthalmology* no. 257 (11):2429-2436. doi: 10.1007/s00417-019-04460-6.

Ibrahim, Ahmed S., Khaled Elmasry, Ming Wan, Samer Abdulmoneim, Amber Still, Farid Khan, Abraham Khalil, Alan Saul, Md Nasrul Hoda, and Mohamed Al-Shabrawey. 2018. "A controlled impact of optic nerve as a new model of traumatic optic neuropathy in Mouse." *Investigative Ophthalmology and Visual Science* no. 59 (13):5548-5557. doi: 10.1167/iovs.18-24773.

Inatani, M., M. Honjo, Y. Otori, A. Oohira, N. Kido, Y. Tano, Y. Honda, and H. Tanihara. 2001. "Inhibitory effects of neurocan and phosphacan on neurite outgrowth from retinal ganglion cells in culture." *Investigative ophthalmology & visual science* no. 42 (8):1930-1938.

J. Salazar, Juan, Ana I. Ramírez, Rosa De Hoz, Elena Salobrar-Garcia, Pilar Rojas, José A. Fernández-Albarral, Inés López-Cuenca, Blanca Rojas, Alberto Triviño, and José M. Ramírez. 2019. "Anatomy of the Human Optic Nerve: Structure and Function." In.: IntechOpen.

Jünemann, Anselm Gerhard Maria, Robert Rejdak, Cord Huchzermeyer, Ryszard Maciejewski, Pawel Grieb, Friedrich E. Kruse, Eberhart Zrenner, Konrad Rejdak, and Axel Petzold. 2015. "Elevated vitreous body glial fibrillary acidic protein in retinal diseases." *Graefe's Archive for Clinical and Experimental Ophthalmology*. doi: 10.1007/s00417-015-3127-7.

Jackson, R. 2018. Traumatic Optic Neuropathy: Background, Problem, Epidemiology.

Jang, Sun Young. 2018. "Traumatic optic neuropathy." *Korean Journal of Neurotrauma*. doi: 10.13004/kjnt.2018.14.1.1.

Jansen, Pernille, Klaus Giehl, Jens R. Nyengaard, Kenneth Teng, Oleg Lioubinski, Susanne S. Sjoegaard, Tilman Breiderhoff, Michael Gotthardt, Fuyu Lin, Andreas Eilers, Claus M. Petersen, Gary R. Lewin, Barbara L. Hempstead, Thomas E. Willnow, and Anders Nykjaer. 2007. "Roles for the pro-neurotrophin receptor sortilin in neuronal development, aging and brain injury." *Nature Neuroscience* no. 10 (11):1449-1457. doi: 10.1038/nn2000.

Jelsma, Tony N., Hana Hyman Friedman, Michelle Berkelaar, Garth M. Bray, and Albert J. Aguayo. 1993. "Different forms of the neurotrophin receptor TrkB mRNA predominate in rat retina and optic nerve." *Journal of Neurobiology* no. 24 (9):1207-1214. doi: 10.1002/neu.480240907.

John, S. W., M. G. Anderson, and R. S. Smith. 1999. "Mouse genetics: a tool to help unlock the mechanisms of glaucoma." *Journal of glaucoma* no. 8 (6):400-412.

Jung, Jae Hwan, Patcharin Desit, and Mark R. Prausnitz. 2018. "Targeted drug delivery in the suprachoroidal space by swollen hydrogel pushing." *Investigative Ophthalmology and Visual Science* no. 59 (5):2069-2079. doi: 10.1167/iovs.17-23758.

Kaliyappan, Karunakaran, Murugesan Palanisamy, Jeyapradha Duraiyan, and Rajeshwar Govindarajan. 2012. "Applications of immunohistochemistry." *Journal of Pharmacy and Bioallied Sciences* no. 4 (6):307-307. doi: 10.4103/0975-7406.100281.

Kamiguchi, Yujiroh, Hiroyuki Tateno, and Kazuya Mikamo. 1990. "Types of structural chromosome aberrations and their incidences in human spermatozoa X-irradiated in vitro." *Mutation Research/Fundamental and Molecular Mechanisms of Mutagenesis* no. 228 (2):133-140. doi: https://doi.org/10.1016/0027-5107(90)90069-G.

Kaneko, Shinjiro, Akio Iwanami, Masaya Nakamura, Akiyoshi Kishino, Kaoru Kikuchi, Shinsuke Shibata, Hirotaka J. Okano, Takeshi Ikegami, Ayako Moriya, Osamu Konishi, Chikao Nakayama, Kazuo Kumagai, Toru Kimura, Yasufumi Sato, Yoshio Goshima, Masahiko Taniguchi, Mamoru Ito, Zhigang He, Yoshiaki Toyama, and Hideyuki Okano. 2006. "A selective Sema3A inhibitor enhances regenerative responses and functional recovery of the injured spinal cord." *Nature Medicine* no. 12 (12):1380-1389. doi: 10.1038/nm1505.

Kaplan, David R., and Freda D. Miller. 2000. "Neurotrophin signal transduction in the nervous system." *Current Opinion in Neurobiology* no. 10 (3):381-391. doi: 10.1016/S0959-4388(00)00092-1.

Kerr, J. F. R., A. H. Wyllie, and A. R. Currie. 1972. "Apoptosis: A basic biological phenomenon with wide-ranging implications in tissue kinetics." *British Journal of Cancer* no. 26 (4):239-257. doi: 10.1038/bjc.1972.33.

Kerschensteiner, Martin, Martin E. Schwab, Jeff W. Lichtman, and Thomas Misgeld. 2005. "In vivo imaging of axonal degeneration and regeneration in the injured spinal cord." *Nature Medicine* no. 11 (5):572-577. doi: 10.1038/nm1229.

Khan, Anjum B., Ben Carpenter, Pedro Santos e Sousa, Constandina Pospori, Reema Khorshed, James Griffin, Pedro Velica, Mathias Zech, Sara Ghorashian, Calum Forrest, Sharyn Thomas, Sara Gonzalez Anton, Maryam Ahmadi, Angelika Holler, Barry Flutter, Zaida Ramirez-Ortiz, Terry K. Means, Clare L. Bennett, Hans Stauss, Emma Morris, Cristina Lo Celso, and Ronjon Chakraverty. 2018. "Redirection to the bone marrow improves T cell persistence and antitumor functions." *The Journal of Clinical Investigation* no. 128 (5):2010-2024. doi: 10.1172/JCI97454.

Kim, K. E., I. Jang, H. Moon, Y. J. Kim, J. W. Jeoung, K. H. Park, and H. Kim. 2015. "Neuroprotective Effects of Human Serum Albumin Nanoparticles Loaded With Brimonidine on Retinal Ganglion Cells in Optic Nerve Crush Model." *Invest Ophthalmol Vis Sci* no. 56 (9):5641-9. doi: 10.1167/iovs.15-16538.

Kitamura, Yuta, Guzel Bikbova, Takayuki Baba, Shuichi Yamamoto, and Toshiyuki Oshitari. 2019. "In vivo effects of single or combined topical neuroprotective and regenerative agents on degeneration of retinal ganglion cells in rat optic nerve crush model." *Scientific Reports* no. 9 (1):1-8. doi: 10.1038/s41598-018-36473-2.

Klüver, Heinrich, and Elizabeth Barrera. 1953. "A Method for the Combined Staining of Cells and Fibers in the Nervous System." *Journal of Neuropathology & Experimental Neurology* no. 12 (4):400-403. doi: 10.1097/00005072-195312040-00008.

Kline, Lanning B., and Frank J. Bajandas. 2008. *Neuro-ophthalmology review manual*: SLACK.

Knöferle, Johanna, Jan C. Koch, Thomas Ostendorf, Uwe Michel, Véronique Planchamp, Polya Vutova, Lars Tönges, Christine Stadelmann, Wolfgang Brück, Mathias Bähr, and Paul Lingor. 2010. "Mechanisms of acute axonal degeneration in the optic nerve in vivo." *Proceedings of the National Academy of Sciences* no. 107 (13):6064 LP-6069. doi: 10.1073/pnas.0909794107.

Koch, Jan C., Johanna Knöferle, Lars Tönges, Thomas Ostendorf, Mathias Bähr, and Paul Lingor. 2010. Acute axonal degeneration in vivo is attenuated by inhibition of autophagy in a calcium-dependent manner. Taylor and Francis Inc.

Kolb, Helga. 2011a. Neurotransmitters in the Retina by Helga Kolb – Webvision.

Kolb, Helga. 2011b. Simple Anatomy of the Retina by Helga Kolb – Webvision.

Kole, C., B. Brommer, N. Nakaya, M. Sengupta, L. Bonet-Ponce, T. Zhao, C. Wang, W. Li, Z. He, and S. Tomarev. 2020. "Activating Transcription Factor 3 (ATF3) Protects Retinal Ganglion Cells and Promotes Functional Preservation After Optic Nerve Crush." *Invest Ophthalmol Vis Sci* no. 61 (2):31. doi: 10.1167/iovs.61.2.31.

Korb, Helga. 2013. Glial cells of the Retina by Helga Kolb – Webvision.

Kordower, Jeffrey H., Raymond T. Bartus, Mark Bothwell, Gina Schatteman, and Don M. Gash. 1988. "Nerve growth factor receptor immunoreactivity in the nonhuman primate (Cebus apella): Distribution, morphology, and colocalization with cholinergic enzymes." *Journal of Comparative Neurology* no. 277 (4):465-486. doi: 10.1002/cne.902770402.

Korsching, S. 1993. The neurotrophic factor concept: A reexamination. J Neurosci.

Kottis, Vicky, Pierre Thibault, Daniel Mikol, Zhi Cheng Xiao, Rulin Zhang, Pauline Dergham, and Peter E. Braun. 2002. "Oligodendrocyte-myelin glycoprotein (OMgp) is an inhibitor of neurite outgrowth." *Journal of Neurochemistry* no. 82 (6):1566-1569. doi: 10.1046/j.1471-4159.2002.01146.x.

Kourgiantaki, A., D. S. Tzeranis, K. Karali, K. Georgelou, E. Bampoula, S. Psilodimitrakopoulos, I. V. Yannas, E. Stratakis, K. Sidiropoulou, I. Charalampopoulos, and A. Gravanis. 2020. "Neural stem cell delivery via porous collagen scaffolds promotes neuronal differentiation and locomotion recovery in spinal cord injury." *NPJ Regen Med* no. 5:12. doi: 10.1038/s41536-020-0097-0.

Kreutzberg, Georg W. 1996. Microglia: A sensor for pathological events in the CNS.

Kulkarni, Giriraj T., Nitin Sethi, Rajendra Awasthi, Vivek Kumar Pawar, and Vineet Pahuja. 2016. "Development of Ocular Delivery System for Glaucoma Therapy Using Natural Hydrogel as Film Forming Agent and Release Modifier." *Polimery w medycynie* no. 46 (1):25-33. doi: 10.17219/pim/63750.

Kumaran, ArjunanMuthu, Gangadhara Sundar, and LimThiam Chye. 2015. "Traumatic Optic Neuropathy: A Review." *Craniomaxillofacial Trauma & Reconstruction* no. 8 (1):31-41. doi: 10.1055/s-0034-1393734.

Kumpulainen, T., D. Dahl, L. K. Korhonen, and S. H. Nyström. 1983. "Immunolabeling of carbonic anhydrase isoenzyme C and glial fibrillary acidic protein in paraffin-embedded tissue sections of human brain and retina." *Journal of Histochemistry & Cytochemistry* no. 31 (7):879-886. doi: 10.1177/31.7.6406590.

Kurimoto, Takuji, Yuqin Yin, Kumiko Omura, Hui Ya Gilbert, Daniel Kim, Ling Ping Cen, Lilamarie Moko, Sebastian Kügler, and Larry I. Benowitz. 2010. "Long-distance axon regeneration in the mature optic nerve: Contributions of oncomodulin, cAMP, and pten gene deletion." *Journal of Neuroscience*. doi: 10.1523/JNEUROSCI.4340-10.2010.

Kyrylkova, Kateryna, Sergiy Kyryachenko, Mark Leid, and Chrissa Kioussi. 2012. "Detection of apoptosis by TUNEL assay." *Methods in Molecular Biology* no. 887:41-47. doi: 10.1007/978-1-61779-860-3_5.

Lagenaur, C., and V. Lemmon. 1987. "An L1-like molecule, the 8D9 antigen, is a potent substrate for neurite extension." *Proceedings of the National Academy of Sciences of the United States of America* no. 84 (21):7753-7757. doi: 10.1073/pnas.84.21.7753.

Lai, Bi-Qin, Xue-Chen Qiu, Ke Zhang, Rong-Yi Zhang, Hui Jin, Ge Li, Hui-Yong Shen, Jin-Lang Wu, Eng-Ang Ling, and Yuan-Shan Zeng. 2015. "Cholera Toxin B Subunit Shows Transneuronal Tracing after Injection in an Injured Sciatic Nerve." *PloS one* no. 10 (12):e0144030-e0144030. doi: 10.1371/journal.pone.0144030.

Laughter, Melissa R., James R. Bardill, David A. Ammar, Brisa Pena, David J. Calkins, and Daewon Park. 2018. "Injectable Neurotrophic Factor Delivery System Supporting Retinal Ganglion Cell Survival and Regeneration Following Optic Nerve Crush." *ACS Biomaterials Science and Engineering* no. 4 (9):3374-3383. doi: 10.1021/acsbiomaterials.8b00803.

Lebrun-Julien, Frédéric, Mathieu J. Bertrand, Olivier De Backer, David Stellwagen, Carlos R. Morales, Adriana Di Polo, and Philip A. Barker. 2010. "ProNGF induces TNFα-dependent death of retinal ganglion cells through a p75NTR non-cell-autonomous signaling pathway." *Proceedings of the National Academy of Sciences of the United States of America* no. 107 (8):3817-3822. doi: 10.1073/pnas.0909276107.

Lebrun-Julien, Frédéric, Barbara Morquette, Annie Douillette, H. Uri Saragovi, and Adriana Di Polo. 2009. "Inhibition of p75NTR in glia potentiates TrkA-mediated survival of injured retinal ganglion cells." *Molecular and Cellular Neuroscience* no. 40 (4):410-420. doi: 10.1016/j.mcn.2008.12.005.

Lee-Liu, Dasfne, Emilio E. Méndez-Olivos, Rosana Muñoz, and Juan Larraín. 2017. The African clawed frog Xenopus laevis: A model organism to study regeneration of the central nervous system.

Lee, Jonathan L. C., Barry J. Everitt, and Kerrie L. Thomas. 2004. "Independent Cellular Processes for Hippocampal Memory Consolidation and Reconsolidation." *Science* no. 304 (5672):839-843. doi: 10.1126/science.1095760.

Lee, Junsung, Unbyeol Goh, Ji-Ho Park, Sang-Woo Park, and Hwan Heo. 2018. "Effective Delivery of Exogenous Compounds to the Optic Nerve by Intravitreal Injection of Liposome." *Korean Journal of Ophthalmology* no. 32 (5):417-417. doi: 10.3341/kjo.2017.0128.

Lee, V., R. L. Ford, W. Xing, C. Bunce, and B. Foot. 2010. "Surveillance of traumatic optic neuropathy in the UK." *Eye* no. 24 (2):240-250. doi: 10.1038/eye.2009.79.

Lehmann, Maxine, Alyson Fournier, Immaculada Selles-Navarro, Pauline Dergham, Agnes Sebok, Nicole Leclerc, Gabor Tigyi, and Lisa McKerracher. 1999. "Inactivation of rho signaling pathway promotes

CNS axon regeneration." *Journal of Neuroscience* no. 19 (17):7537-7547. doi: 10.1523/jneurosci.19-17-07537.1999.
Levi-Montalcini, Rita, Stephen D. Skaper, Roberto Dal Toso, Lucia Petrelli, and Alberta Leon. 1996. Nerve growth factor: From neurotrophin to neurokine. Trends Neurosci.
Levkovitch-Verbin, H. 2004. "Animal models of optic nerve diseases." *Eye* no. 18 (11):1066-1074. doi: 10.1038/sj.eye.6701576.
Levkovitch-Verbin, H., C. Harris-Cerruti, Y. Groner, L. A. Wheeler, M. Schwartz, and E. Yoles. 2000. "RGC death in mice after optic nerve crush injury: Oxidative stress and neuroprotection." *Investigative Ophthalmology and Visual Science*.
Lewin, Gary R., and Bruce D. Carter. 2014. Neurotrophic factors. Preface.
Li, Hong-Jiang, Zhao-Liang Sun, Xi-Tao Yang, Liang Zhu, and Dong-Fu Feng. 2017. "Exploring Optic Nerve Axon Regeneration." *Current Neuropharmacology*. doi: 10.2174/1570159x14666161227150250.
Li, L., H. Huang, F. Fang, L. Liu, Y. Sun, and Y. Hu. 2020. "Longitudinal Morphological and Functional Assessment of RGC Neurodegeneration After Optic Nerve Crush in Mouse." *Front Cell Neurosci* no. 14:109. doi: 10.3389/fncel.2020.00109.
Li, Shuang, Jia Hua Fang, and Fa Gang Jiang. 2010. "Histological observation of RGCs and optic nerve injury in acute ocular hypertension rats." *International Journal of Ophthalmology* no. 3 (4):311-315. doi: 10.3980/j.issn.2222-3959.2010.04.08.
Li, Songshan, Qinghai He, Hao Wang, Xuming Tang, Kam Wing Ho, Xin Gao, Qian Zhang, Yang Shen, Annie Cheung, Francis Wong, Yung Hou Wong, Nancy Y. Ip, Liwen Jiang, Wing Ho Yung, and Kai Liu. 2015. "Injured adult retinal axons with Pten and Socs3 co-deletion reform active synapses with suprachiasmatic neurons." *Neurobiology of Disease*. doi: 10.1016/j.nbd.2014.09.019.
Li, Y., C. L. Schlamp, and R. W. Nickells. 1999. "Experimental induction of retinal ganglion cell death in adult mice." *Investigative ophthalmology & visual science* no. 40 (5):1004-1008.
Liorca. 1972. *Anatomía Humana. Tomo II*.
Luo, Xueting, Yadira Salgueiro, Samuel R. Beckerman, Vance P. Lemmon, Pantelis Tsoulfas, and Kevin K. Park. 2013. "Three-dimensional evaluation of retinal ganglion cell axon regeneration and pathfinding in whole mouse tissue after injury." *Experimental Neurology*. doi: 10.1016/j.expneurol.2013.03.001.
Mac Nair, Caitlin E., Cassandra L. Schlamp, Angela D. Montgomery, Valery I. Shestopalov, and Robert W. Nickells. 2016. "Retinal glial responses to optic nerve crush are attenuated in Bax-deficient mice and modulated by purinergic signaling pathways." *Journal of Neuroinflammation* no. 13 (1). doi: 10.1186/s12974-016-0558-y.
Magharious, Mark M., Philippe M. D'Onofrio, and Paulo D. Koeberle. 2011. "Optic nerve transection: A model of adult neuron apoptosis in the central nervous system." *Journal of Visualized Experiments* (51):1-5. doi: 10.3791/2241.
Maisonpierre, Peter C., Leonardo Belluscio, Beth Friedman, Ralph F. Alderson, Stanley J. Wiegand, Mark E. Furth, Ronald M. Lindsay, and George D. Yancopoulos. 1990. "NT-3, BDNF, and NGF in the developing rat nervous system: Parallel as well as reciprocal patterns of expression." *Neuron* no. 5 (4):501-509. doi: 10.1016/0896-6273(90)90089-X.
May, Christian Albrecht. 2008. "Comparative Anatomy of the Optic Nerve Head and Inner Retina in Non-Primate Animal Models Used for Glaucoma Research." *The Open Ophthalmology Journal*. doi: 10.2174/1874364100802010094.
McConnell, P., and M. Berry. 1982. "Regeneration of axons in the mouse retina after injury." *Bibliotheca anatomica* (23):26-37.
McIlwain, David R., Thorsten Berger, and Tak W. Mak. 2013. "Caspase functions in cell death and disease." *Cold Spring Harbor Perspectives in Biology* no. 5 (4):1-28. doi: 10.1101/cshperspect.a008656.
McKerracher, L., S. David, D. L. Jackson, V. Kottis, R. J. Dunn, and P. E. Braun. 1994. "Identification of myelin-associated glycoprotein as a major myelin-derived inhibitor of neurite growth." *Neuron* no. 13 (4):805-811. doi: 10.1016/0896-6273(94)90247-X.
McKinnon, Stuart J., Cassandra L. Schlamp, and Robert W. Nickells. 2009. Mouse models of retinal ganglion cell death and glaucoma. Exp Eye Res.
Mead, B., A. Thompson, B. A. Scheven, A. Logan, M. Berry, and W. Leadbeater. 2014. "Comparative evaluation of methods for estimating retinal ganglion cell loss in retinal sections and wholemounts." *PLoS One* no. 9 (10):e110612. doi: 10.1371/journal.pone.0110612.
Mead, Ben, and Stanislav Tomarev. 2016. Evaluating retinal ganglion cell loss and dysfunction. Academic Press.

Mercer, Aaron J., and Wallace B. Thoreson. 2011. The dynamic architecture of photoreceptor ribbon synapses: Cytoskeletal, extracellular matrix, and intramembrane proteins. NIH Public Access.

Mesentier-louro, Louise A., Sara De Nicolò, Pamela Rosso, Luigi A. De Vitis, Valerio Castoldi, Letizia Leocani, Rosalia Mendez-otero, Marcelo F. Santiago, Paola Tirassa, Paolo Rama, and Alessandro Lambiase. 2017. "Time-Dependent Nerve Growth Factor Signaling Changes in the Rat Retina During Optic Nerve Crush-Induced Degeneration of Retinal Ganglion Cells."1-17. doi: 10.3390/ijms18010098.

Mesentier-Louro, Louise A., Pamela Rosso, Valentina Carito, Rosalia Mendez-Otero, Marcelo F. Santiago, Paolo Rama, Alessandro Lambiase, and Paola Tirassa. 2019. "Nerve Growth Factor Role on Retinal Ganglion Cell Survival and Axon Regrowth: Effects of Ocular Administration in Experimental Model of Optic Nerve Injury." *Molecular Neurobiology* no. 56 (2):1056-1069. doi: 10.1007/s12035-018-1154-1.

Milde, F., S. Lauw, P. Koumoutsakos, and M. L. Iruela-Arispe. 2013. "The mouse retina in 3D: quantification of vascular growth and remodeling." *Integr Biol (Camb)* no. 5 (12):1426-38. doi: 10.1039/c3ib40085a.

Mills, Jason C. 2001. Mechanisms underlying the Hallmark features of the execution-phase of apoptosis.

Moreau-Fauvarque, Caroline, Atsushi Kumanogoh, Emeline Camand, Céline Jaillard, Gilles Barbin, Isabelle Boquet, Christopher Love, E. Yvonne Jones, Hitoshi Kikutani, Catherine Lubetzki, Isabelle Dusart, and Alain Chédotal. 2003. "The transmembrane semaphorin Sema4D/CD100, an inhibitor of axonal growth, is expressed on oligodendrocytes and upregulated after CNS lesion." *Journal of Neuroscience* no. 23 (27):9229-9239. doi: 10.1523/jneurosci.23-27-09229.2003.

Morgenstern, Daniel A., Richard A. Asher, and James W. Fawcett. Chondroitin sulphate proteoglycans in the CNS injury response, 2002.

Morzaev, D., J. D. Nicholson, T. Caspi, S. Weiss, E. Hochhauser, and N. Goldenberg-Cohen. 2015. "Toll-like receptor-4 knockout mice are more resistant to optic nerve crush damage than wild-type mice." (1442-9071 (Electronic)).

Nadal-Nicolas, F. M., M. Jimenez-Lopez, P. Sobrado-Calvo, L. Nieto-Lopez, I. Canovas-Martinez, M. Salinas-Navarro, M. Vidal-Sanz, and M. Agudo. 2009. "Brn3a as a marker of retinal ganglion cells: qualitative and quantitative time course studies in naive and optic nerve-injured retinas." *Invest Ophthalmol Vis Sci* no. 50 (8):3860-8. doi: 10.1167/iovs.08-3267.

Nadal-Nicolás, Francisco M., Manuel Jiménez-López, Manuel Salinas-Navarro, Paloma Sobrado-Calvo, Manuel Vidal-Sanz, and Marta Agudo-Barriuso. 2017. "Microglial dynamics after axotomy-induced retinal ganglion cell death." *Journal of Neuroinflammation* no. 14 (1):1-15. doi: 10.1186/s12974-017-0982-7.

Nag, Sukriti. 2011. Morphology and properties of astrocytes. Methods Mol Biol.

Nascimento-Dos-Santos, G., L. C. Teixeira-Pinheiro, A. J. da Silva-Junior, L. R. P. Carvalho, L. A. Mesentier-Louro, W. W. Hauswirth, R. Mendez-Otero, M. F. Santiago, and H. Petrs-Silva. 2020. "Effects of a combinatorial treatment with gene and cell therapy on retinal ganglion cell survival and axonal outgrowth after optic nerve injury." *Gene Ther* no. 27 (1-2):27-39. doi: 10.1038/s41434-019-0089-0.

Nau, H. E., L. Gerhard, M. Foerster, H. Ch Nahser, V. Reinhardt, and Th Joka. 1987. "Optic nerve trauma: Clinical, electrophysiological and histological remarks." *Acta Neurochirurgica* no. 89 (1-2):16-27. doi: 10.1007/BF01406662.

Negishi. 2001. "Optic nerve regeneration within artificial Schwann cell
graft in the adult rat."

Neufeld, Arthur H. 1999. "Microglia in the optic nerve head and the region of parapapillary chorioretinal atrophy in glaucoma." *Archives of Ophthalmology* no. 117 (8):1050-1056. doi: 10.1001/archopht.117.8.1050.

Nicotera, Pierluigi, Marcel Leist, and Elisa Ferrando-May. Intracellular ATP, a switch in the decision between apoptosis and necrosis, 1998/12//.

Nieto, Miguel Perello. 2015. A simplified schema of the human visual pathway.

Nykjaer, Anders, Ramee Lee, Kenneth K. Teng, Pernille Jansen, Peder Madsen, Morten S. Nielsen, Christian Jacobsen, Marco Kliemannel, Elisabeth Schwarz, Thomas E. Willnow, Barbara L. Hempstead, and Claus M. Petersen. 2004. "Sortilin is essential for proNGF-induced neuronal cell death." *Nature* no. 427 (6977):843-848. doi: 10.1038/nature02319.

O'Brien, F. J., Ioannis V. Harley Ba Fau - Yannas, Lorna Yannas Iv Fau - Gibson, and L. Gibson. "Influence of freezing rate on pore structure in freeze-dried collagen-GAG scaffolds." (0142-9612 (Print)).

Paigen, Kenneth. 1995. A miracle enough: The power of mice. Nat Med.

Paques, Michel, Manuel Simonutti, Sébastien Augustin, Olivier Goupille, Brahim El Mathari, and José Alain Sahel. 2010. "In vivo observation of the locomotion of microglial cells in the retina." *GLIA* no. 58 (14):1663-1668. doi: 10.1002/glia.21037.

Paramitha, D., M. F. Ulum, A. Purnama, D. H. B. Wicaksono, D. Noviana, and H. Hermawan. 2017. "Monitoring degradation products and metal ions in vivo." In, 19-44. Elsevier Inc.

Park, Kevin Kyungsuk, Kai Liu, Yang Hu, Patrice D. Smith, Chen Wang, Bin Cai, Bengang Xu, Lauren Connolly, Ioannis Kramvis, Mustafa Sahin, and Zhigang He. 2008. "Promoting axon regeneration in the adult CNS by modulation of the PTEN/mTOR pathway." *Science*. doi: 10.1126/science.1161566.

Parrilla-Reverter, Guillermo, Marta Agudo, Francisco Nadal-Nicolás, Luis Alarcón-Martínez, Manuel Jiménez-López, Manuel Salinas-Navarro, Paloma Sobrado-Calvo, José M. Bernal-Garro, María P. Villegas-Pérez, and Manuel Vidal-Sanz. 2009. "Time-course of the retinal nerve fibre layer degeneration after complete intra-orbital optic nerve transection or crush: A comparative study." *Vision Research* no. 49 (23):2808-2825. doi: 10.1016/j.visres.2009.08.020.

Pediaditakis, Iosif. 2015. "The neurotrophic effects of endogenous and synthetic Neurosteroids : structure-function analysis of their interactions with neurotrophin receptors and their biological role in neuroprotection."

Pediaditakis, Iosif, Paschalis Efstathopoulos, Kyriakos C. Prousis, Maria Zervou, Juan Carlos Arévalo, Vasileia I. Alexaki, Vassiliki Nikoletopoulou, Efthymia Karagianni, Constantinos Potamitis, Nektarios Tavernarakis, Triantafyllos Chavakis, Andrew N. Margioris, Maria Venihaki, Theodora Calogeropoulou, Ioannis Charalampopoulos, and Achille Gravanis. 2016. "Selective and differential interactions of BNN27, a novel C17-spiroepoxy steroid derivative, with TrkA receptors, regulating neuronal survival and differentiation." *Neuropharmacology* no. 111:266-282. doi: 10.1016/j.neuropharm.2016.09.007.

Pekny, Milos, and Marcela Pekna. 2004. Astrocyte intermediate filaments in CNS pathologies and regeneration.

Pernet, V., S. Joly, N. Jordi, D. Dalkara, A. Guzik-Kornacka, J. G. Flannery, and M. E. Schwab. 2013. "Misguidance and modulation of axonal regeneration by Stat3 and Rho/ROCK signaling in the transparent optic nerve." *Cell Death and Disease*. doi: 10.1038/cddis.2013.266.

Pernet, Vincent, Sandrine Joly, Deniz Dalkara, Noémie Jordi, Olivia Schwarz, Franziska Christ, David V. Schaffer, John G. Flannery, and Martin E. Schwab. 2013. "Long-distance axonal regeneration induced by CNTF gene transfer is impaired by axonal misguidance in the injured adult optic nerve." *Neurobiology of Disease*. doi: 10.1016/j.nbd.2012.11.011.

Pernet, Vincent, and Martin E. Schwab. 2014. Lost in the jungle: New hurdles for optic nerve axon regeneration.

Perry, V. Hugh, Mike D. Bell, Heidi C. Brown, and Malgosia K. Matyszak. 1995. "Inflammation in the nervous system." *Current Opinion in Neurobiology* no. 5 (5):636-641. doi: 10.1016/0959-4388(95)80069-7.

Petzold, Axel. 2015. Glial fibrillary acidic protein is a body fluid biomarker for glial pathology in human disease.

Pirouzmand, Farhad. 2012. "Epidemiological trends of traumatic optic nerve injuries in the largest canadian adult trauma center." *Journal of Craniofacial Surgery* no. 23 (2):516-520. doi: 10.1097/SCS.0b013e31824cd4a7.

Porciatti, Vittorio. 2015. Electrophysiological assessment of retinal ganglion cell function. Academic Press.

Porciatti, Vittorio, Maher Saleh, and Mahesh Nagaraju. 2007. "The pattern electroretinogram as a tool to monitor progressive retinal ganglion cell dysfunction in the DBA/2J mouse model of glaucoma." *Investigative Ophthalmology and Visual Science* no. 48 (2):745-751. doi: 10.1167/iovs.06-0733.

Priscilla, Rupa, and Ben G. Szaro. 2019. "Comparisons of SOCS mRNA and protein levels in Xenopus provide insights into optic nerve regenerative success." *Brain Research*. doi: 10.1016/j.brainres.2018.10.012.

Prusky, Glen T., Nazia M. Alam, Steven Beekman, and Robert M. Douglas. 2004. "Rapid quantification of adult and developing mouse spatial vision using a virtual optomotor system." *Investigative Ophthalmology and Visual Science* no. 45 (12):4611-4616. doi: 10.1167/iovs.04-0541.

Pula, John H., and Christopher J. MacDonald. 2012. Current options for the treatment of optic neuritis. Dove Medical Press Ltd.

Purves, Dale, George J. Augustine, David Fitzpatrick, Lawrence C. Katz, Anthony-Samuel LaMantia, James O. McNamara, and S. Mark Williams. 2001. "The Retina."

Quigley, H. A., R. W. Nickells, L. A. Kerrigan, M. E. Pease, D. J. Thibault, and D. J. Zack. 1995. "Retinal ganglion cell death in experimental glaucoma and after axotomy occurs by apoptosis." *Investigative ophthalmology & visual science* no. 36 (5):774-786.

Raff, Martin C., Barbara A. Barres, Julia F. Burne, Harriet S. Coles, Yasuki Ishizaki, and Michael D. Jacobson. 1993. "Programmed cell death and the control of cell survival: Lessons from the nervous system." *Science* no. 262 (5134):695-700. doi: 10.1126/science.8235590.

Raivich, Gennadij, Marion Bohatschek, Clive Da Costa, Osuke Iwata, Matthias Galiano, Maria Hristova, Abdolrahman S. Nateri, Milan Makwana, Lluís Riera-Sans, David P. Wolfer, Hans Peter Lipp, Adriano Aguzzi, Erwin F. Wagner, and Axel Behrens. 2004. "The AP-1 transcription factor c-Jun is required for efficient axonal regeneration." *Neuron* no. 43 (1):57-67. doi: 10.1016/j.neuron.2004.06.005.

Ramírez, José M., Alberto Triviño, Ana I. Ramírez, Juan J. Salazar, and Julian García-Sanchez. 1996. "Structural specializations of human retinal glial cells." *Vision Research* no. 36 (14):2029-2036. doi: 10.1016/0042-6989(95)00322-3.

Reichardt, Louis F. 2006. Neurotrophin-regulated signalling pathways. Royal Society.

Ribas, Vinicius T., Jan C. Koch, Uwe Michel, Mathias Bähr, and Paul Lingor. 2016. "Attenuation of Axonal Degeneration by Calcium Channel Inhibitors Improves Retinal Ganglion Cell Survival and Regeneration After Optic Nerve Crush." *Molecular Neurobiology* no. 54 (1):72-86. doi: 10.1007/s12035-015-9676-2.

Ribas, Vinicius Toledo, Bianca Schnepf, Malleswari Challagundla, Jan Christoph Koch, Mathias Bähr, and Paul Lingor. 2015. "Early and sustained activation of autophagy in degenerating axons after spinal cord injury." *Brain Pathology* no. 25 (2):157-170. doi: 10.1111/bpa.12170.

Richardson, P. M., V. M. K. Issa, and A. J. Aguayo. 1984. "Regeneration of long spinal axons in the rat." *Journal of Neurocytology* no. 13 (1):165-182. doi: 10.1007/BF01148324.

Richardson, P. M., U. M. McGuinness, and A. J. Aguayo. 1980. "Axons from CNS neurones regenerate into PNS grafts." *Nature* no. 284 (5753):264-265. doi: 10.1038/284264a0.

Riopelle, R. J., P. M. Richardson, and V. M. K. Verge. 1987. "Distribution and characteristics of nerve growth factor binding on cholinergic neurons of rat and monkey forebrain." *Neurochemical Research* no. 12 (10):923-928. doi: 10.1007/BF00966314.

Robinson, Rebecca, Stephen R. Viviano, Jason M. Criscione, Cicely A. Williams, Lin Jun, James C. Tsai, and Erin B. Lavik. 2011. "Nanospheres delivering the EGFR TKI AG1478 promote optic nerve regeneration: The role of size for intraocular drug delivery." *ACS Nano* no. 5 (6):4392-4400. doi: 10.1021/nn103146p.

Robinson, Shenandoah, and Robert Miller. 1996. "Environmental Enhancement of Growth Factor-Mediated Oligodendrocyte Precursor Proliferation." *Molecular and Cellular Neuroscience* no. 8 (1):38-52. doi: https://doi.org/10.1006/mcne.1996.0042.

Rodriguez, Allen R., Luis Pérez de Sevilla Müller, and Nicholas C. Brecha. 2014. *The RNA binding protein RBPMS is a selective marker of ganglion cells in the mammalian retina*. Vol. 522.

Sánchez-Migallón, M. C., F. J. Valiente-Soriano, M. Salinas-Navarro, F. M. Nadal-Nicolás, M. Jiménez-López, M. Vidal-Sanz, and M. Agudo-Barriuso. 2018. "Nerve fibre layer degeneration and retinal ganglion cell loss long term after optic nerve crush or transection in adult mice." *Experimental Eye Research* no. 170:40-50. doi: 10.1016/j.exer.2018.02.010.

Sánchez-Migallón, Maria C., Francisco J. Valiente-Soriano, Francisco M. Nadal-Nicolás, Manuel Vidal-Sanz, and Marta Agudo-Barriuso. 2015. "Apoptotic retinal ganglion cell death after optic nerve transection or crush in mice: Delayed RGC loss with BDNF or a caspase 3 inhibitor." *Investigative Ophthalmology and Visual Science* no. 57 (1):81-93. doi: 10.1167/iovs.15-17841.

Sarkies, Nicholas. 2004. "Traumatic optic neuropathy." *Eye* no. 18 (11):1122-1125. doi: 10.1038/sj.eye.6701571.

Sato, Kota, Yurika Nakagawa, Kazuko Omodaka, Hiroyuki Asada, Shinobu Fujii, Kenji Masaki, and Toru Nakazawa. 2020. "The Sustained Release of Tafluprost with a Drug Delivery System Prevents the Axonal Injury-induced Loss of Retinal Ganglion Cells in Rats." *Current Eye Research* no. 00 (00):1-10. doi: 10.1080/02713683.2020.1715446.

Saxena, Smita, and Pico Caroni. 2007. Mechanisms of axon degeneration: From development to disease. Prog Neurobiol.

Schlamp, Cassandra L., Angela D. Montgomery, Caitlin E. Mac Nair, Claudia Schuart, Daniel J. Willmer, and Robert W. Nickells. 2013. "Evaluation of the percentage of ganglion cells in the ganglion cell layer of the rodent retina." *Molecular Vision*.

Schmalfeldt, M., C. E. Bandtlow, M. T. Dours-Zimmermann, K. H. Winterhalter, and D. R. Zimmermann. 2000. "Brain derived versican V2 is a potent inhibitor of axonal growth." *Journal of Cell Science* no. 113 (5):807.

Schnitzer, Jutta. 1988. *Astrocytes in mammalian retina. Chapter 7*. Vol. 7: Pergamon.
Schwartz, Lawrence M., Sallie W. Smith, Margaret E. E. Jones, and Barbara A. Osborne. 1993. "Do all programmed cell deaths occur via apoptosis?" *Proceedings of the National Academy of Sciences of the United States of America* no. 90 (3):980-984. doi: 10.1073/pnas.90.3.980.
Schwartz, Michal. 2004. "Optic nerve crush : protection and regeneration." no. 62 (February 2003):467-471. doi: 10.1016/S0361-9230(03)00076-5.
Schwartz, Michal, Eti Yoles, and Leonard A. Levin. 1999. "'Axogenic' and 'somagenic' neurodegenerative diseases: definitions and therapeutic implications." *Molecular Medicine Today* no. 5 (11):470-473. doi: 10.1016/S1357-4310(99)01592-0.
Seif, Gamal I., Hiroshi Nomura, and Charles H. Tator. 2007. "Retrograde axonal degeneration ("dieback") in the corticospinal tract after transection injury of the rat spinal cord: A confocal microscopy study." *Journal of Neurotrauma* no. 24 (9):1513-1528. doi: 10.1089/neu.2007.0323.
Seijffers, Rhona, Andrew J. Allchorne, and Clifford J. Woolf. 2006. "The transcription factor ATF-3 promotes neurite outgrowth." *Molecular and Cellular Neuroscience* no. 32 (1-2):143-154. doi: 10.1016/j.mcn.2006.03.005.
Sobrado-Calvo, Paloma, Manuel Vidal-Sanz, and María Villegas-Pérez. 2007. "Rat retinal microglial cells under normal conditions, after optic nerve section, and after optic nerve section and intravitreal injection of trophic factors or macrophage inhibitory factor." *The Journal of comparative neurology* no. 501:866-78. doi: 10.1002/cne.21279.
Sobreviela, Teresa, Douglas O. Clary, Louis F. Reichardt, Melanie M. Brandabur, Jeffrey H. Kordower, and Elliott J. Mufson. 1994. "TrkA-immunoreactive profiles in the central nervous system: Colocalization with neurons containing p75 nerve growth factor receptor, choline acetyltransferase, and serotonin." *Journal of Comparative Neurology* no. 350 (4):587-611. doi: 10.1002/cne.903500407.
Sofroniew, Michael V. 2009. Molecular dissection of reactive astrogliosis and glial scar formation.
Sofroniew, Michael V., Charles L. Howe, and William C. Mobley. 2001. "Nerve Growth Factor Signaling, Neuroprotection, and Neural Repair." *Annual Review of Neuroscience* no. 24 (1):1217-1281. doi: 10.1146/annurev.neuro.24.1.1217.
Souza, Joel G., Karina Dias, Silas A. M. Silva, Lucas C. D. De Rezende, Eduardo M. Rocha, Flavio S. Emery, and Renata F. V. Lopez. 2015. "Transcorneal iontophoresis of dendrimers: PAMAM corneal penetration and dexamethasone delivery." *Journal of Controlled Release* no. 200:115-124. doi: 10.1016/j.jconrel.2014.12.037.
Spalding, Kirsty L., Robert A. Rush, and Alan R. Harvey. 2004. "Target-derived and locally derived neurotrophins support retinal ganglion cell survival in the neonatal rat retina." *Journal of Neurobiology* no. 60 (3):319-327. doi: 10.1002/neu.20028.
Sperry, R. W. 1948. "Patterning of Central Synapses in Regeneration of the Optic Nerve in Teleosts." *Physiological Zoology* no. 21 (4):351-361.
Steininger, Teresa L., Bruce H. Wainer, Rudiger Klein, Mariano Barbacid, and H. Clive Palfrey. 1993. "High-affinity nerve growth factor receptor (Trk) immunoreactivity is localized in cholinergic neurons of the basal forebrain and striatum in the adult rat brain." *Brain Research* no. 612 (1-2):330-335. doi: 10.1016/0006-8993(93)91681-H.
Steinsapir, Kenneth D., and Robert A. Goldberg. 1994. Traumatic optic neuropathy. Surv Ophthalmol.
Streit, Wolfgang J., Sharon A. Walter, and Nathan A. Pennell. 1999. Reactive microgliosis. Prog Neurobiol.
Sun, Ying, Yoon Lim, Fang Li, Shen Liu, Jian-Jun Lu, Rainer Haberberger, Jin-Hua Zhong, and Xin-Fu Zhou. 2012. "ProBDNF Collapses Neurite Outgrowth of Primary Neurons by Activating RhoA." *PLoS ONE* no. 7 (4):e35883-e35883. doi: 10.1371/journal.pone.0035883.
Takeuchi, Hiroto, Satoshi Inagaki, Wataru Morozumi, Yukimichi Nakano, Yuki Inoue, Yoshiki Kuse, Takahiro Mizoguchi, Shinsuke Nakamura, Michinori Funato, Hideo Kaneko, Hideaki Hara, and Masamitsu Shimazawa. 2018. "VGF nerve growth factor inducible is involved in retinal ganglion cells death induced by optic nerve crush." *Scientific Reports* no. 8 (1):1-13. doi: 10.1038/s41598-018-34585-3.
Tang, F., F. Xu, L. Cui, W. Huang, L. Jiang, L. Chen, W. Yan, W. He, C. Shen, H. Huang, J. Lv, X. Zhao, S. Zeng, M. Li, Y. Ouyang, X. Guo, H. Zhong, and M. Zhang. 2020. "The expression and role of PIDD in retina after optic nerve crush." *J Mol Histol* no. 51 (1):89-97. doi: 10.1007/s10735-020-09860-1.
Tang, Maoping, Shi Shi, Yubing Guo, Wangjie Xu, Lianyun Wang, Yi Chen, Zhaoxia Wang, and Zhongdong Qiao. 2014. "GSK-3/CREB pathway involved in the gx-50's effect on Alzheimer's disease." *Neuropharmacology* no. 81:256-266. doi: 10.1016/j.neuropharm.2014.02.008.

Tang, Zhongshu, Shuihua Zhang, Chunsik Lee, Anil Kumar, Pachiappan Arjunan, Yang Li, Fan Zhang, and Xuri Li. 2011. "An optic nerve crush injury murine model to study retinal ganglion cell survival." *Journal of Visualized Experiments* (50):6-8. doi: 10.3791/2685.

Tao, Wensi, Galina Dvoriantchikova, Brian C. Tse, Steven Pappas, Tsung Han Chou, Manuel Tapia, Vittorio Porciatti, Dmitry Ivanov, David T. Tse, and Daniel Pelaez. 2017. "A Novel Mouse Model of Traumatic Optic Neuropathy Using External Ultrasound Energy to Achieve Focal, Indirect Optic Nerve Injury." *Scientific Reports* no. 7 (1):1-14. doi: 10.1038/s41598-017-12225-6.

Tehrani, Shandiz, R. Katherine Delf, William O. Cepurna, Lauren Davis, Elaine C. Johnson, and John C. Morrison. 2018. "In Vivo Small Molecule Delivery to the Optic Nerve in a Rodent Model." *Scientific Reports*. doi: 10.1038/s41598-018-22737-4.

Teng, Henry K., Kenneth K. Teng, Ramee Lee, Saundrene Wright, Seema Tevar, Ramiro D. Almeida, Pouneh Kermani, Risa Torkin, Zhe Yu Chen, Francis S. Lee, Rosemary T. Kraemer, Anders Nykjaer, and Barbara L. Hempstead. 2005. "ProBDNF induces neuronal apoptosis via activation of a receptor complex of p75NTR and sortilin." *Journal of Neuroscience* no. 25 (22):5455-5463. doi: 10.1523/JNEUROSCI.5123-04.2005.

Thach, Allen B., Anthony J. Johnson, Robert B. Carroll, Ava Huchun, Darryl J. Ainbinder, Richard D. Stutzman, Sean M. Blaydon, Sheri L. DeMartelaere, Thomas H. Mader, Clifton S. Slade, Roger K. George, John P. Ritchey, Scott D. Barnes, and Lilia A. Fannin. 2008. "Severe Eye Injuries in the War in Iraq, 2003-2005." *Ophthalmology* no. 115 (2):377-382. doi: 10.1016/j.ophtha.2007.04.032.

Thermo_Scientific. Available from http://tools.thermofisher.com/content/sfs/manuals/MAN0011212_SPDP_CrsLnk_UG.pdf.

Triviño, Alberto, José M. Ramírez, Juan J. Salazar, and Ana I. Ramírez. 1998. "Astroglial Architecture of the Human Optic Nerve: Functional Role of Astrocytes." In, 63-77. Springer US.

Triviño, Alberto, Jose M. Ramírez, Juan J. Salazar, Ana I. Ramírez, and Julian Garcia-Sánchez. 1996. "Immunohistochemical study of human optic nerve head astroglia." *Vision Research* no. 36 (14):2015-2028. doi: 10.1016/0042-6989(95)00317-7.

Tsakanika. 2019. "ADVANCED DEVICE FABRICATION AND DRUG DELIVERY VIA POROUS COLLAGEN SCAFFOLDS."

Tsoka, P., H. Matsumoto, D. E. Maidana, K. Kataoka, I. Naoumidi, A. Gravanis, D. G. Vavvas, and M. K. Tsilimbaris. 2018. "Effects of BNN27, a novel C17-spiroepoxy steroid derivative, on experimental retinal detachment-induced photoreceptor cell death." *Sci Rep* no. 8 (1):10661. doi: 10.1038/s41598-018-28633-1.

Ultsch, Mark H., Christian Wiesmann, Laura C. Simmons, Jill Henrich, Maria Yang, Dorothea Reilly, Steven H. Bass, and Abraham M. De Vos. 1999. "Crystal structures of the neurotrophin-binding domain of TrkA, TrkB and TrkC." *Journal of Molecular Biology* no. 290 (1):149-159. doi: 10.1006/jmbi.1999.2816.

Urfer, Roman, Pantelis Tsoulfas, Lori O'Connell, Jo Anne Hongo, Wei Zhao, and Leonard G. Presta. 1998. "High resolution mapping of the binding site of TrkA for nerve growth factor and TrkC for neurotrophin-3 on the second immunoglobulin-like domain of the TrK receptors." *Journal of Biological Chemistry* no. 273 (10):5829-5840. doi: 10.1074/jbc.273.10.5829.

Urtti, Arto. 2006. Challenges and obstacles of ocular pharmacokinetics and drug delivery. Adv Drug Deliv Rev.

Villegas-Perez. 1992. "Rapid and Protracted Phases of Retinal Ganglion Cell Loss Follow Axotomy in the Optic Nerve of Adult Rats."

Villegas-Pérez, Maria-Paz -P, Manuel Vidal-Sanz, Michael Rasminsky, Garth M. Bray, and Albert J. Aguayo. 1993. "Rapid and protracted phases of retinal ganglion cell loss follow axotomy in the optic nerve of adult rats." *Journal of Neurobiology* no. 24 (1):23-36. doi: 10.1002/neu.480240103.

Von Bartheld, C. S. 1998. Neurotrophins in the developing and regenerating visual system.

Vorobyeva, A. A., V. V. Fominykh, M. V. Onufriev, M. N. Zakharova, and N. V. Gulyaeva. 2014. "Phosphorylated neurofilament heavy subunits as a marker of neurodegeneration in demyelinating diseases of the CNS." *Neurochemical Journal* no. 8 (3):221-225. doi: 10.1134/S1819712414030143.

Wahlsten, Douglas. 2011. *Mouse Behavioral Testing*: Elsevier Inc.

Walsh, F. B. 1966. "Pathological-clinical correlations. I. Indirect trauma to the optic nerves and chiasm. II. Certain cerebral involvements associated with defective blood supply." *Investigative ophthalmology* no. 5 (5):433-449.

Wang, Xingxing, Jun Lin, Alexander Arzeno, Jin Young Choi, Juliann Boccio, Eric Frieden, Ajay Bhargava, George Maynard, James C. Tsai, and Stephen M. Strittmatter. 2015. "Intravitreal delivery of human

ngr-fc decoy protein regenerates axons after optic nerve crush and protects ganglion cells in glaucoma models." *Investigative Ophthalmology and Visual Science* no. 56 (2):1357-1366. doi: 10.1167/iovs.14-15472.

Wang, Xu, Lian Zhao, Jun Zhang, Robert N. Fariss, Wenxin Ma, Friedrich Kretschmer, Minhua Wang, Hao Hua Qian, Tudor C. Badea, Jeffrey S. Diamond, Wen Biao Gan, Jerome E. Roger, and Wai T. Wong. 2016. "Requirement for microglia for the maintenance of synaptic function and integrity in the mature retina." *Journal of Neuroscience* no. 36 (9):2827-2842. doi: 10.1523/JNEUROSCI.3575-15.2016.

Weishaupt, J. H., and M. Bähr. 2001. "Degeneration of axotomized retinal ganglion cells as a model for neuronal apoptosis in the central nervous system - molecular death and survival pathways." *Restorative neurology and neuroscience* no. 19 (1-2):19-27.

Wickham, Louisa, Geoffrey P. Lewis, David G. Charteris, and Steven K. Fisher. 2012. "Cellular Effects of Detachment and Reattachment on the Neural Retina and the Retinal Pigment Epithelium." In.

Winn, P. 2001. *Dictionary of biological psycology*.

Wlesmann, Christian, Mark H. Ultsch, Steven H. Bass, and Abraham M. De Vos. 1999. "Crystal structure of nerve growth factor in complex with the ligand- binding domain of the TrkA receptor." *Nature* no. 401 (6749):184-188. doi: 10.1038/43705.

Wolf, Susanne A., H. W. G. M. Boddeke, and Helmut Kettenmann. 2017. "Microglia in Physiology and Disease." *Annual Review of Physiology* no. 79 (1):619-643. doi: 10.1146/annurev-physiol-022516-034406.

Wong, Wai T. 2013. Microglial aging in the healthy CNS: Phenotypes, drivers, and rejuvenation. Front Cell Neurosci.

Xu, G., Wen-zu Nie Dy Fau - Wang, Pei-hua Wang Wz Fau - Zhang, Jie Zhang Ph Fau - Shen, Beng-ti Shen J Fau - Ang, Guo-hua Ang Bt Fau - Liu, Xue-gang Liu Gh Fau - Luo, Nan-liang Luo Xg Fau - Chen, Zhi-cheng Chen Nl Fau - Xiao, and Z. C. Xiao. 2004. "Optic nerve regeneration in polyglycolic acid-chitosan conduits coated with recombinant L1-Fc." (0959-4965 (Print)).

Yamada, Hidekazu, Barbara Fredette, Kenya Shitara, Kazuki Hagihara, Ryu Miura, Barbara Ranscht, William B. Stallcup, and Yu Yamaguchi. 1997. "The brain chondroitin sulfate proteoglycan brevican associates with astrocytes ensheathing cerebellar glomeruli and inhibits neurite outgrowth from granule neurons." *Journal of Neuroscience* no. 17 (20):7784-7795. doi: 10.1523/jneurosci.17-20-07784.1997.

Yamashita, Toshihide, Kerry Lee Tucker, and Yves Alain Barde. 1999. "Neurotrophin binding to the p75 receptor modulates Rho activity and axonal outgrowth." *Neuron* no. 24 (3):585-593. doi: 10.1016/S0896-6273(00)81114-9.

Yang, Ping, and Zhong Yang. 2012. Enhancing intrinsic growth capacity promotes adult CNS regeneration.

Yao, Kai, Suo Qiu, Yanbin V. Wang, Silvia J. H. Park, Ethan J. Mohns, Bhupesh Mehta, Xinran Liu, Bo Chang, David Zenisek, Michael C. Crair, Jonathan B. Demb, and Bo Chen. 2018. "Restoration of vision after de novo genesis of rod photoreceptors in mammalian retinas." *Nature* no. 560 (7719):484-488. doi: 10.1038/s41586-018-0425-3.

Yin, Yuqin, Silmara De Lima, Hui Ya Gilbert, Nicholas J. Hanovice, Sheri L. Peterson, Rheanna M. Sand, Elena G. Sergeeva, Kimberly A. Wong, Lili Xie, and Larry I. Benowitz. 2019. "Optic nerve regeneration: A long view." *Restorative Neurology and Neuroscience* no. 37 (6):525-544. doi: 10.3233/RNN-190960.

Yoles, E., L. A. Wheeler, and M. Schwartz. 1999. "Alpha2-adrenoreceptor agonists are neuroprotective in a rat model of optic nerve degeneration." *Investigative ophthalmology & visual science* no. 40 (1):65-73.

Yoshii, Akira, and Martha Constantine-Paton. 2010. Postsynaptic BDNF-TrkB signaling in synapse maturation, plasticity, and disease. Dev Neurobiol.

Yu-Wai-Man, Patrick. 2015. Traumatic optic neuropathy-Clinical features and management issues. Elsevier.

Zhang, Shuquan, Minfei Wu, Chuangang Peng, Guanjie Zhao, and Rui Gu. 2017. "GFAP expression in injured astrocytes in rats." *Experimental and Therapeutic Medicine* no. 14 (3):1905-1908. doi: 10.3892/etm.2017.4760.

Zhang, Yushi, Yao Chen, Xiaoxue Yu, Yangjia Qi, Yufeng Chen, Yuxi Liu, Yuntao Hu, and Zhihong Li. 2016. "A flexible device for ocular iontophoretic drug delivery." *Biomicrofluidics* no. 10 (1):11-14. doi: 10.1063/1.4942516.

Zhang, Z. Z., Y. Y. Gong, Y. H. Shi, W. Zhang, X. H. Qin, and X. W. Wu. 2012. "Valproate promotes survival of retinal ganglion cells in a rat model of optic nerve crush." *Neuroscience* no. 224:282-93. doi: 10.1016/j.neuroscience.2012.07.056.